






New Physics at the Pulsar Timing Array (PTA) Frontier

Kai Schmitz
University of Münster, Germany

Astroparticle School 2023
FAU Erlangen-Nürnberg + ECAP + KIT | Obertrubach-Bärnfels | 5,6,7 October 2023

Next milestone in gravitational-wave (GW) astronomy

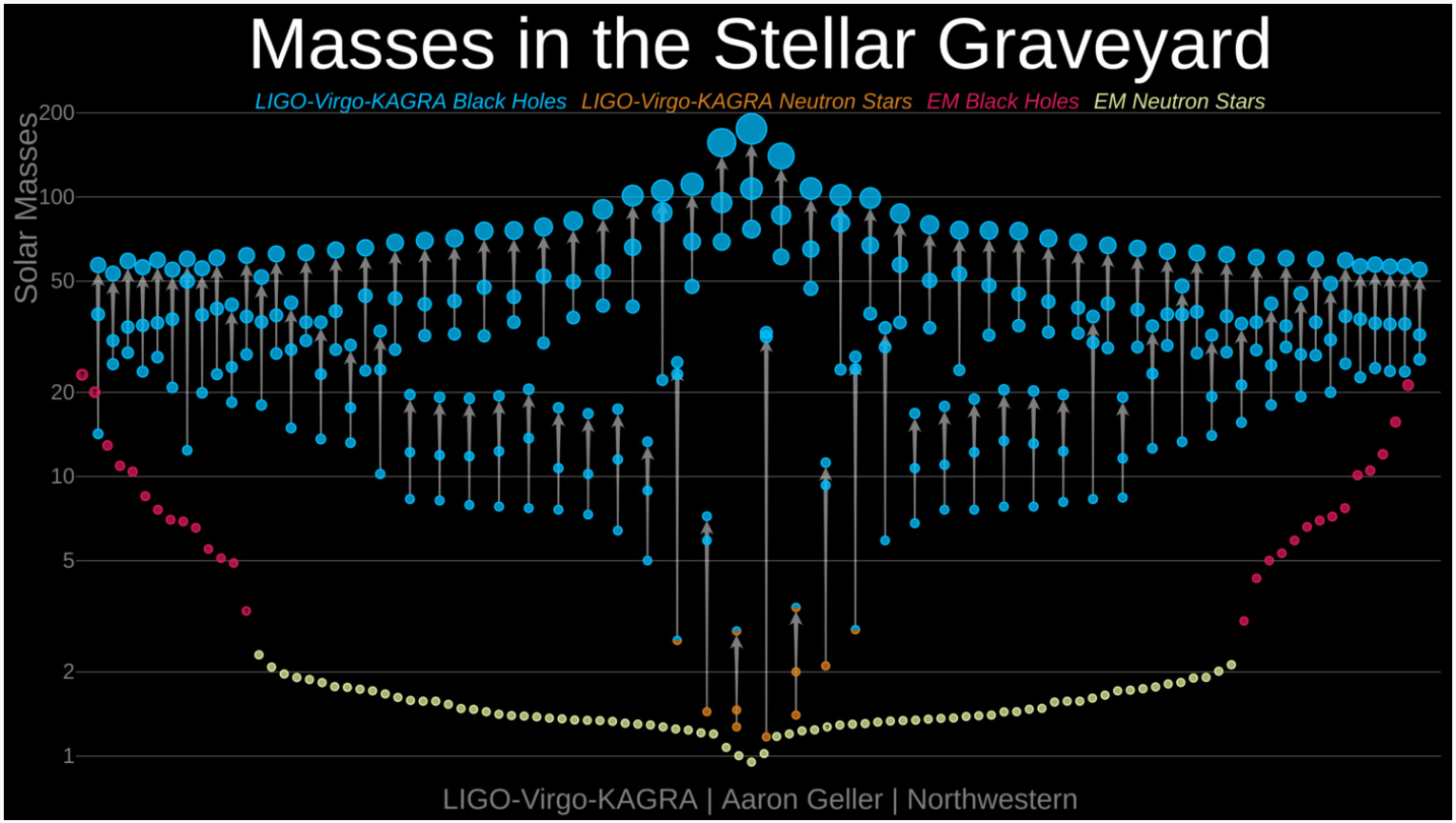

- Status: LVK now routinely observe transient GW signals of astrophysical origin
- Next milestone: Detection of a stochastic GW background (GWB)
- Big news on June 29: **Compelling evidence** for a GWB reported by several teams!

GWB: 21st-century equivalent of the 20th-century discovery of the CMB

20th century

[PLANCK Collaboration]

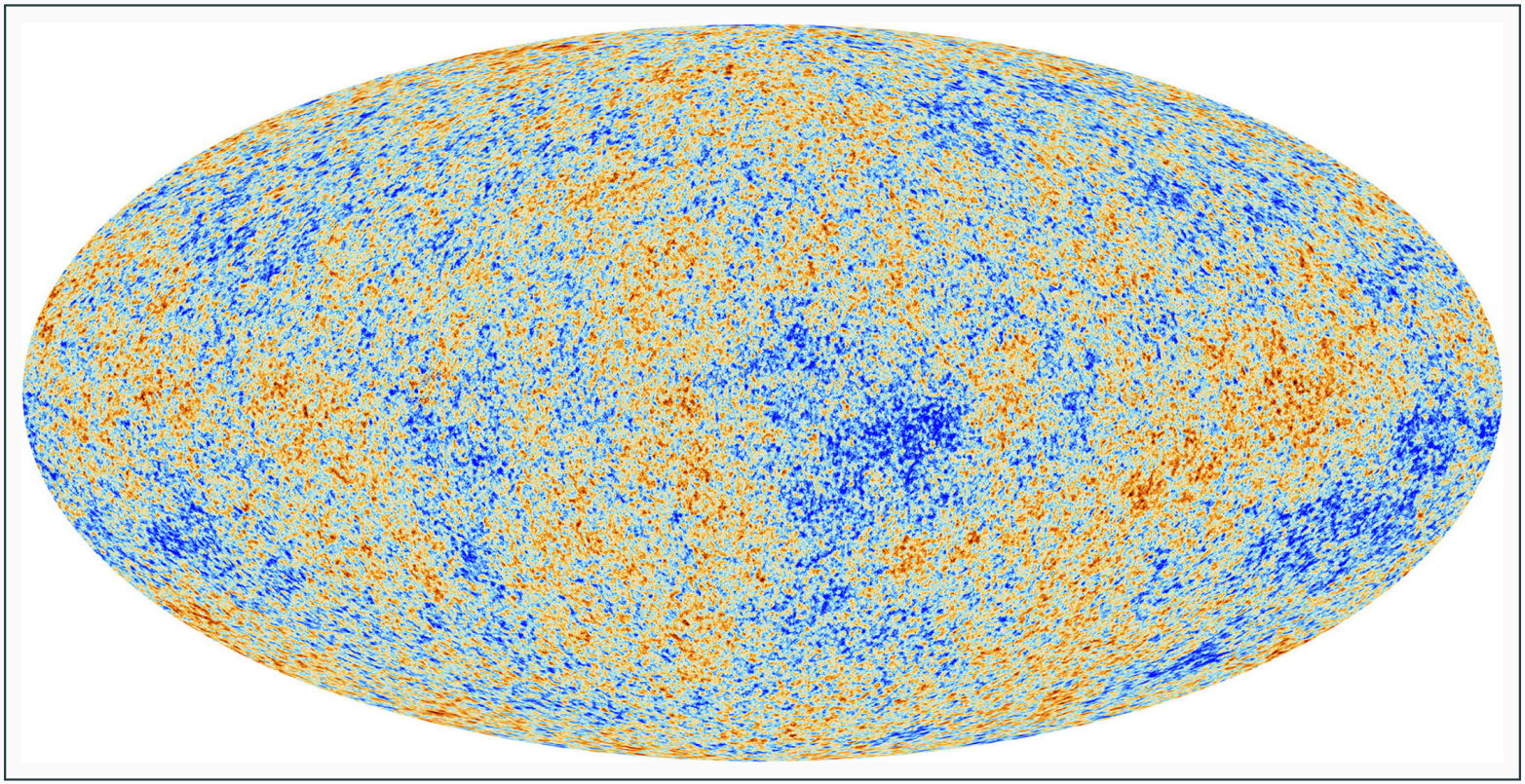

CMB: Cosmic microwave background

Relic photons from the early Universe

GWB: 21st-century equivalent of the 20th-century discovery of the CMB

21th century

[Sato-Polito, Kamionkowski: 2305.05690]

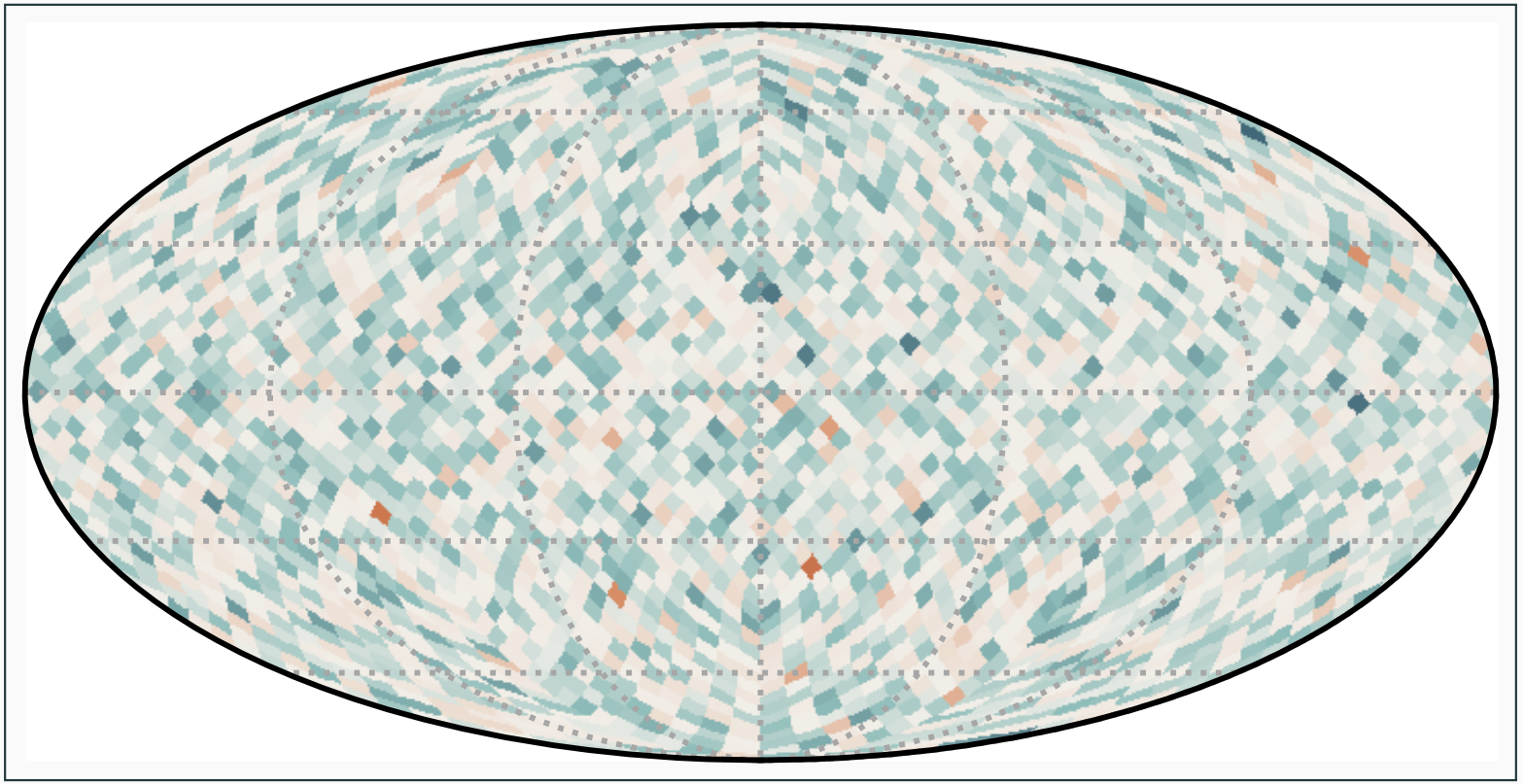

GWB: Gravitational-wave background

Relic gravitational waves from the early Universe $\sim$ *or* $\sim$ **astrophysical signal**

GW spectrum

Just like electromagnetic radiation, GWs reach us across a vast frequency spectrum

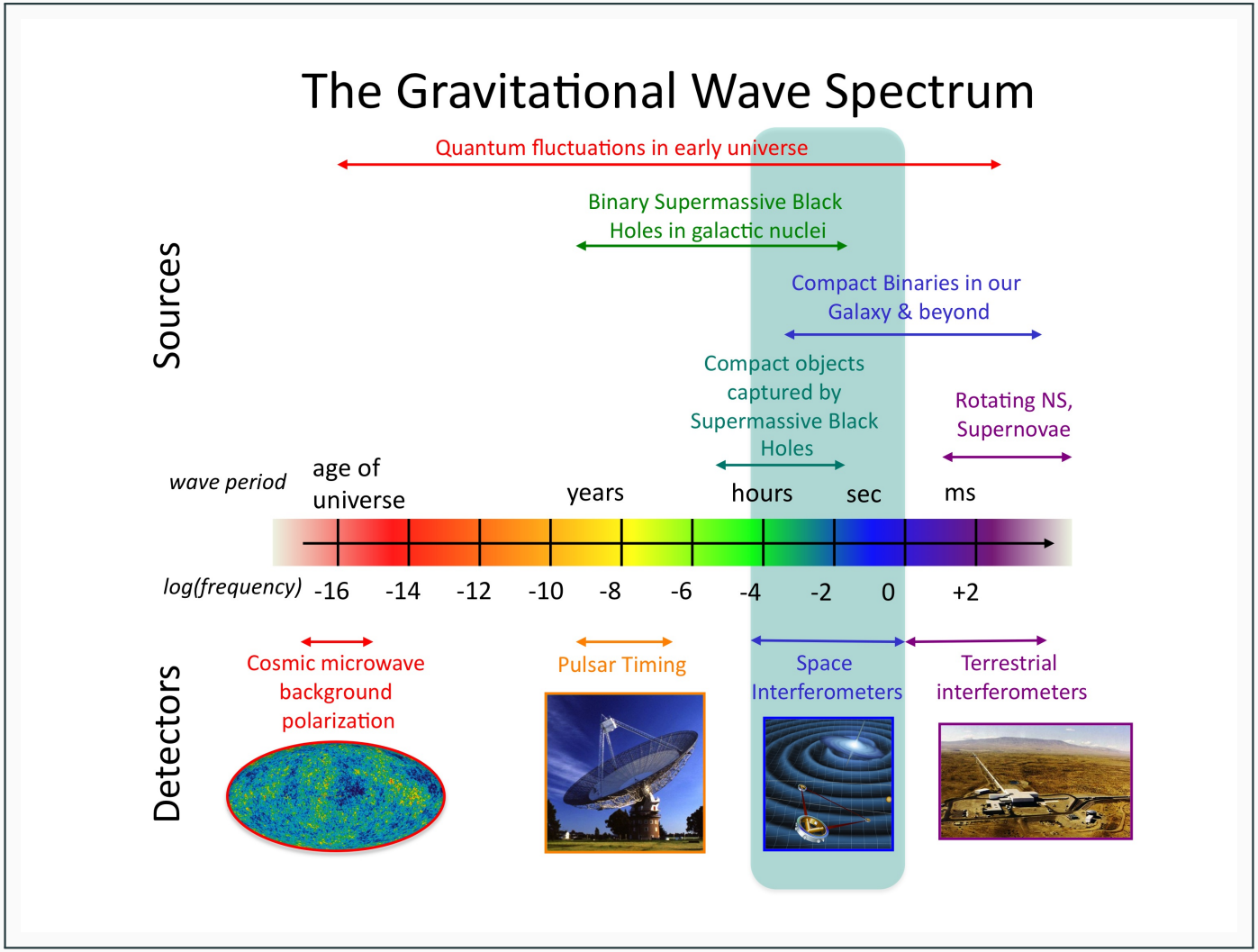

© NASA Goddard Space Flight Center

Multifrequency gravitational-wave astronomy

Ground

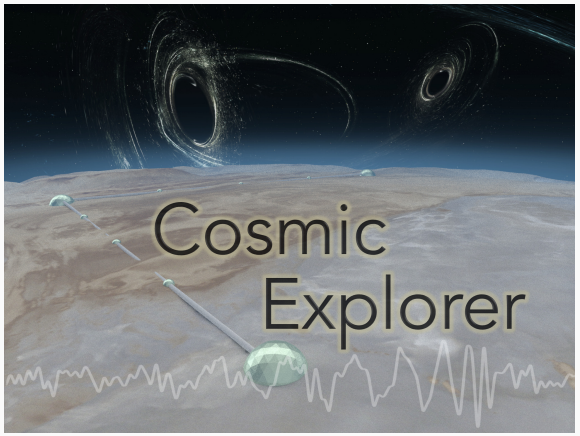

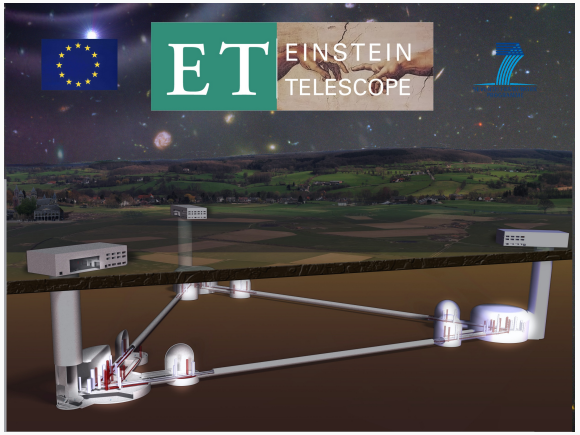

$f \sim 10 \cdots 1000\,\mathrm{Hz}$

Space

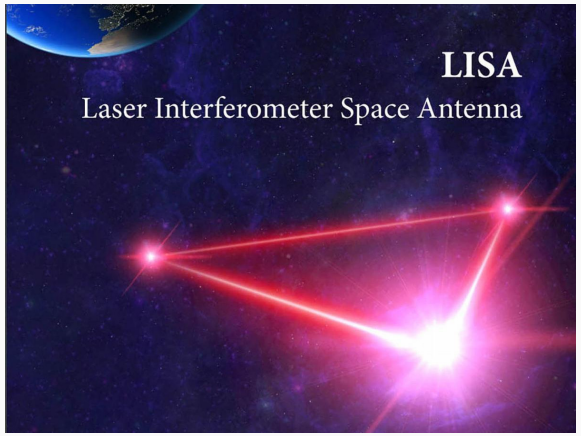

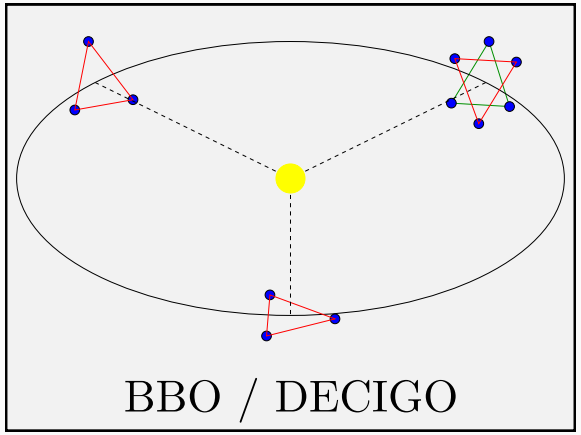

$f \sim 1 \cdots 1000\,\mathrm{mHz}$

Sky

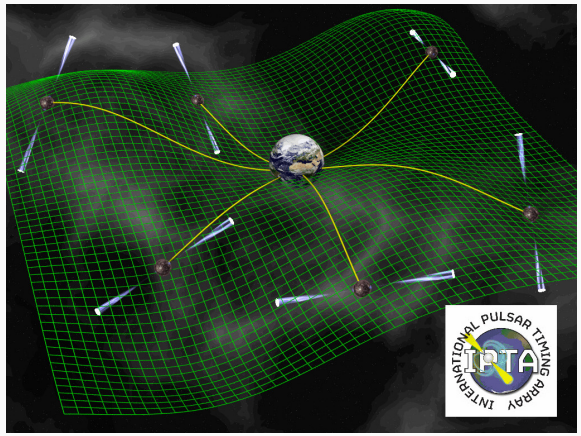

$f \sim 1 \cdots 10\,\mathrm{nHz}$

Characterization of a GWB signal

GWs are tensor perturbations of the metric; specifically, in a flat FLRW universe

$$ds^2 = -dt^2 + a^2(t)\left(\delta_{ij} + h_{ij}\right) dx^i dx^j\,, \qquad \partial_i h_{ij}^{\mathrm{TT}} = 0\,, \quad h_{ii}^{\mathrm{TT}} = 0$$

Characterization of a GWB signal

GWs are tensor perturbations of the metric; specifically, in a flat FLRW universe

$$ds^2 = -dt^2 + a^2(t)\left(\delta_{ij} + h_{ij}\right) dx^i dx^j\,, \qquad \partial_i h_{ij}^{\mathrm{TT}} = 0\,, \quad h_{ii}^{\mathrm{TT}} = 0$$

Strain power spectral density S_h and characteristic strain amplitude $h_c = \sqrt{2fS_h}$

$$\left\langle h_{ij}^{\mathrm{TT}} h_{ij}^{\mathrm{TT}} \right\rangle = 2\left\langle h_+ h_+ \right\rangle + 2\left\langle h_\times h_\times \right\rangle = 4\int_0^\infty df\, S_h(f) = 2\int_0^\infty \frac{df}{f}\, h_c^2(f)$$

Characterization of a GWB signal

GWs are tensor perturbations of the metric; specifically, in a flat FLRW universe

$$ds^2 = -dt^2 + a^2(t)\left(\delta_{ij} + h_{ij}\right) dx^i dx^j\,, \qquad \partial_i h_{ij}^{\mathrm{TT}} = 0\,, \quad h_{ii}^{\mathrm{TT}} = 0$$

Strain power spectral density S_h and characteristic strain amplitude $h_c = \sqrt{2fS_h}$

$$\left\langle h_{ij}^{\mathrm{TT}} h_{ij}^{\mathrm{TT}} \right\rangle = 2\left\langle h_+ h_+ \right\rangle + 2\left\langle h_\times h_\times \right\rangle = 4\int_0^\infty df\, S_h(f) = 2\int_0^\infty \frac{df}{f}\, h_c^2(f)$$

Energy density power spectrum on a logarithmic frequency scale, in units of ρ_{crit}

$$\Omega_{\mathrm{gw}}^{\mathrm{tot}} = \frac{\rho_{\mathrm{gw}}^{\mathrm{tot}}}{\rho_{\mathrm{crit}}} = \int_0^\infty \frac{df}{f}\,\Omega_{\mathrm{gw}}(f)\,, \qquad \Omega_{\mathrm{gw}}(f) = \frac{1}{\rho_{\mathrm{crit}}}\frac{d\rho_{\mathrm{gw}}(f)}{d\ln f} = \frac{4\pi^2 f^3}{3H_0^2}\, S_h(f)$$

Multiply by h^2, where $H_0 = 100\,h\,\mathrm{km/s/Mpc}$, so that $h^2\Omega_{\mathrm{gw}}$ is independent of H_0

GWB treasure map

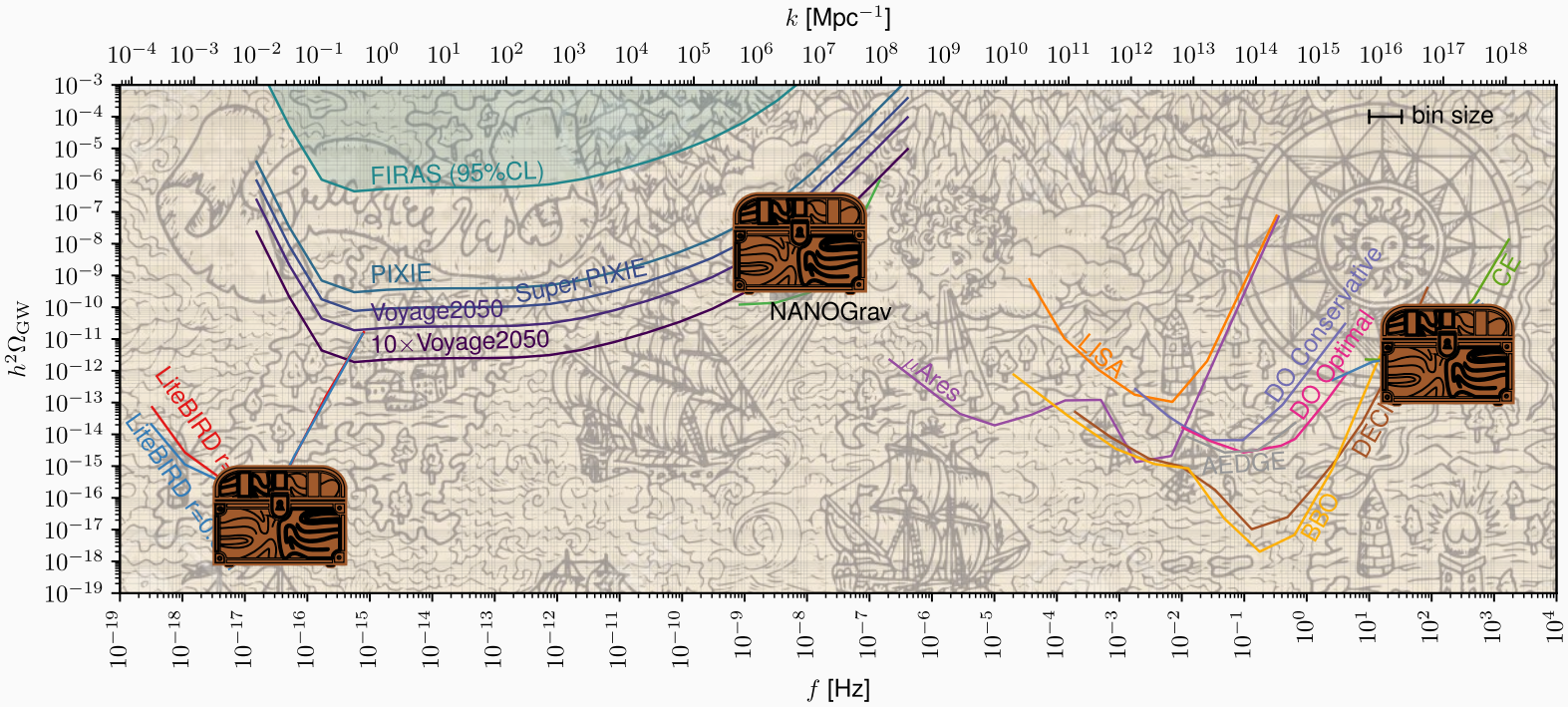

GWB treasure map

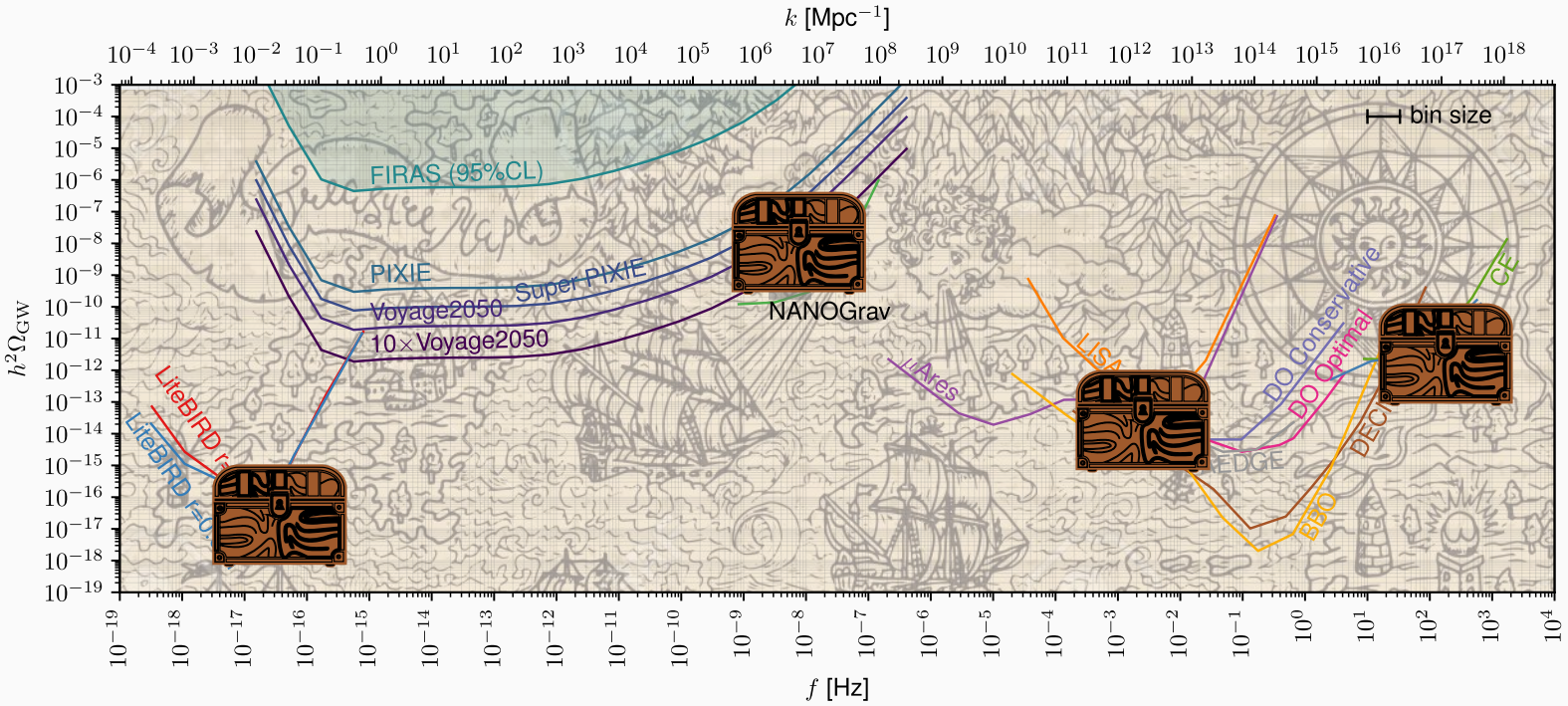

GWB treasure map

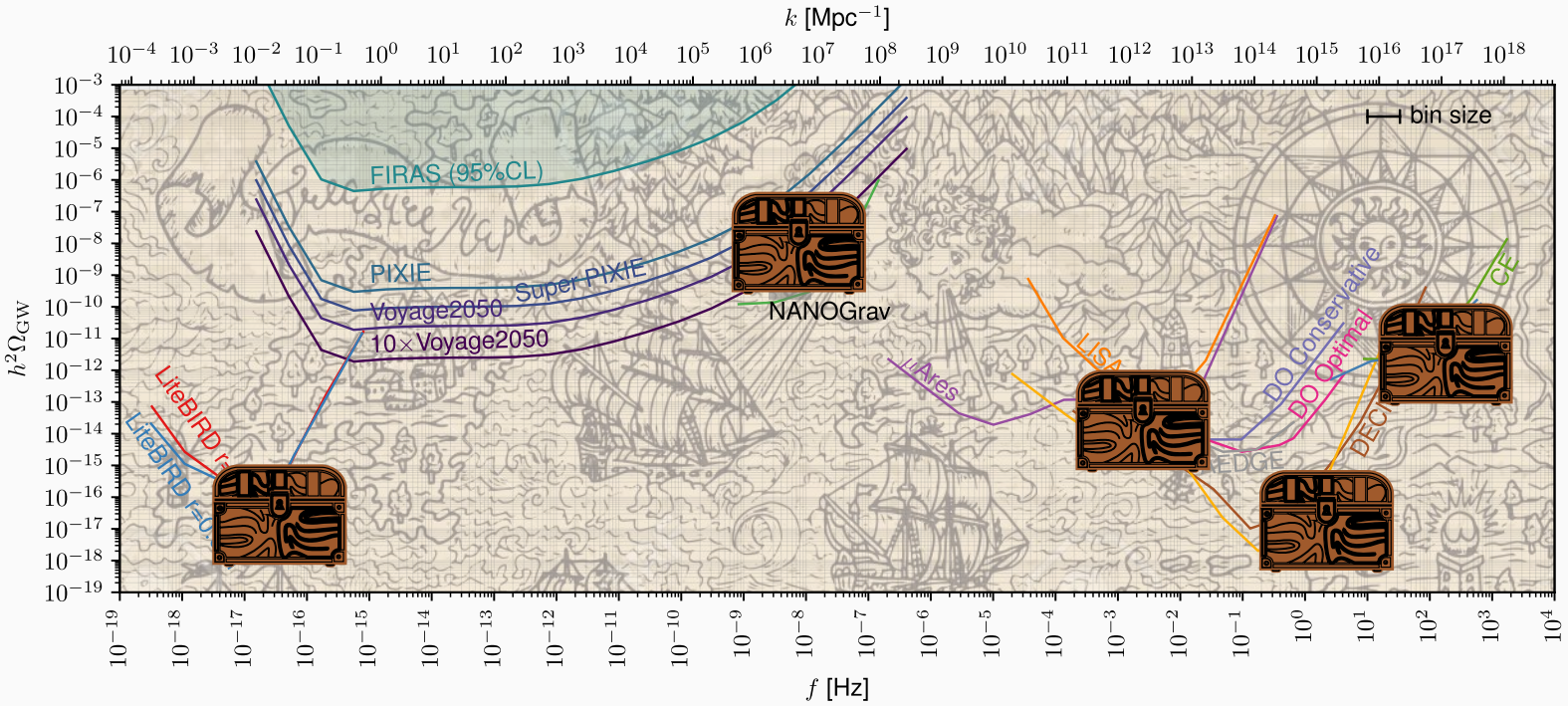

GWB treasure map

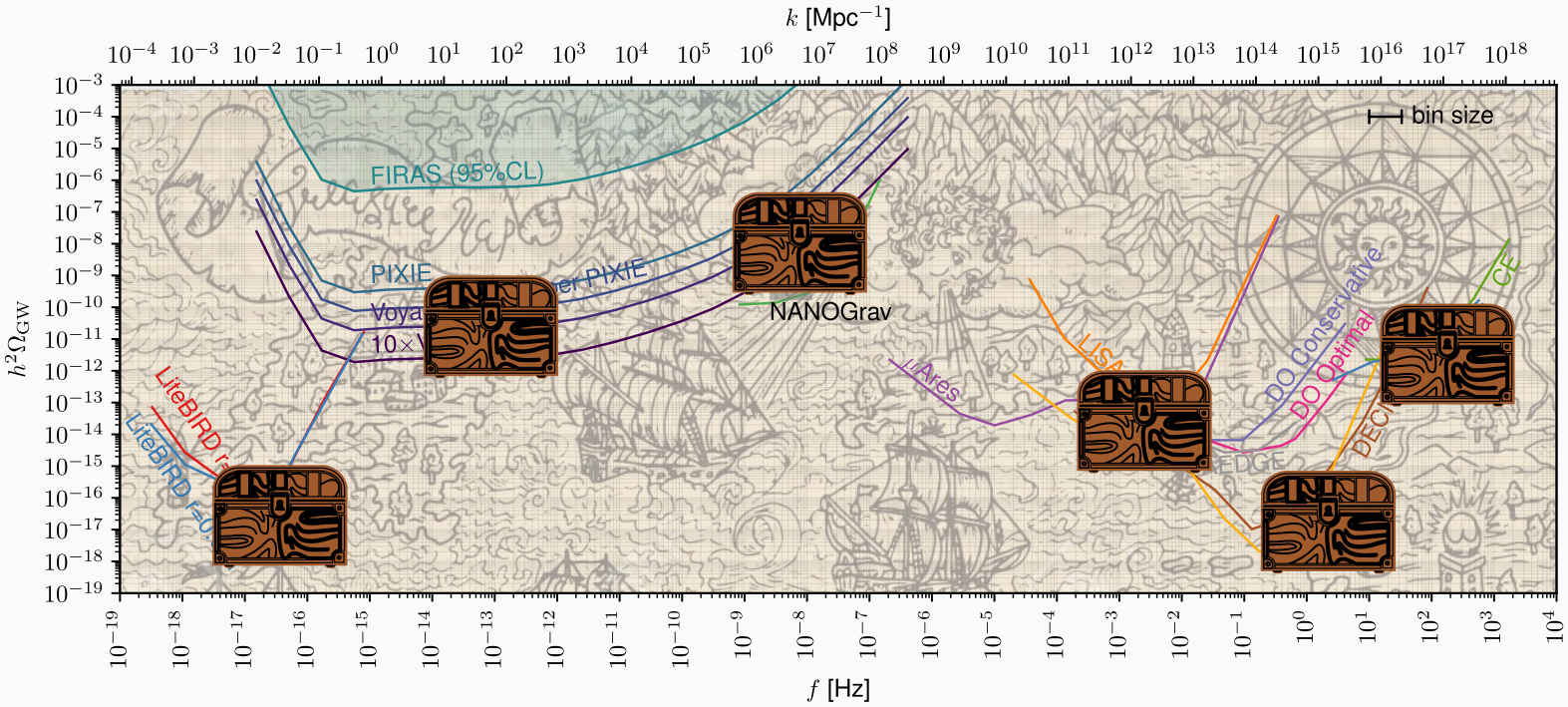

GWB treasure map

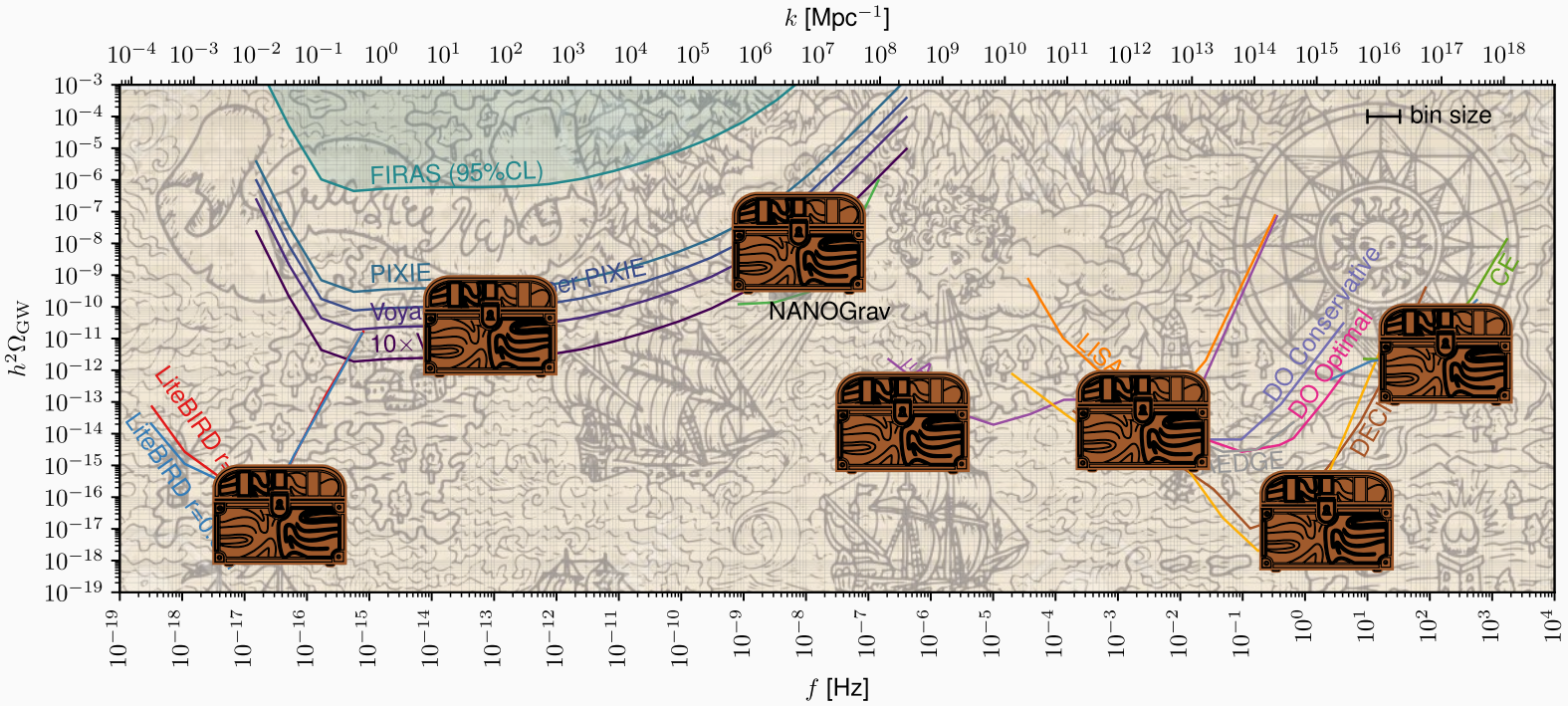

Possible GWB signals across vast frequency range

Galactic and extragalactic astrophysics + **particle physics in the early Universe**

Large arsenal of GW observations and experiments

Cosmic microwave background + **pulsar timing arrays** + interferometers + ...

Outline

I) The pular timing array signal: Compelling evidence for a GWB

II) Astrophysical interpretation: Supermassive black-hole binaries

III) Cosmological interpretations: New physics in the early Universe

IV) Conclusions and outlook: Summary, dark matter, next steps

Along the way: Pulsars, PTAs, statistics, GW physics, BSM in the early Universe, ...

I) The pular timing array signal: Compelling evidence for a GWB

Pulsars

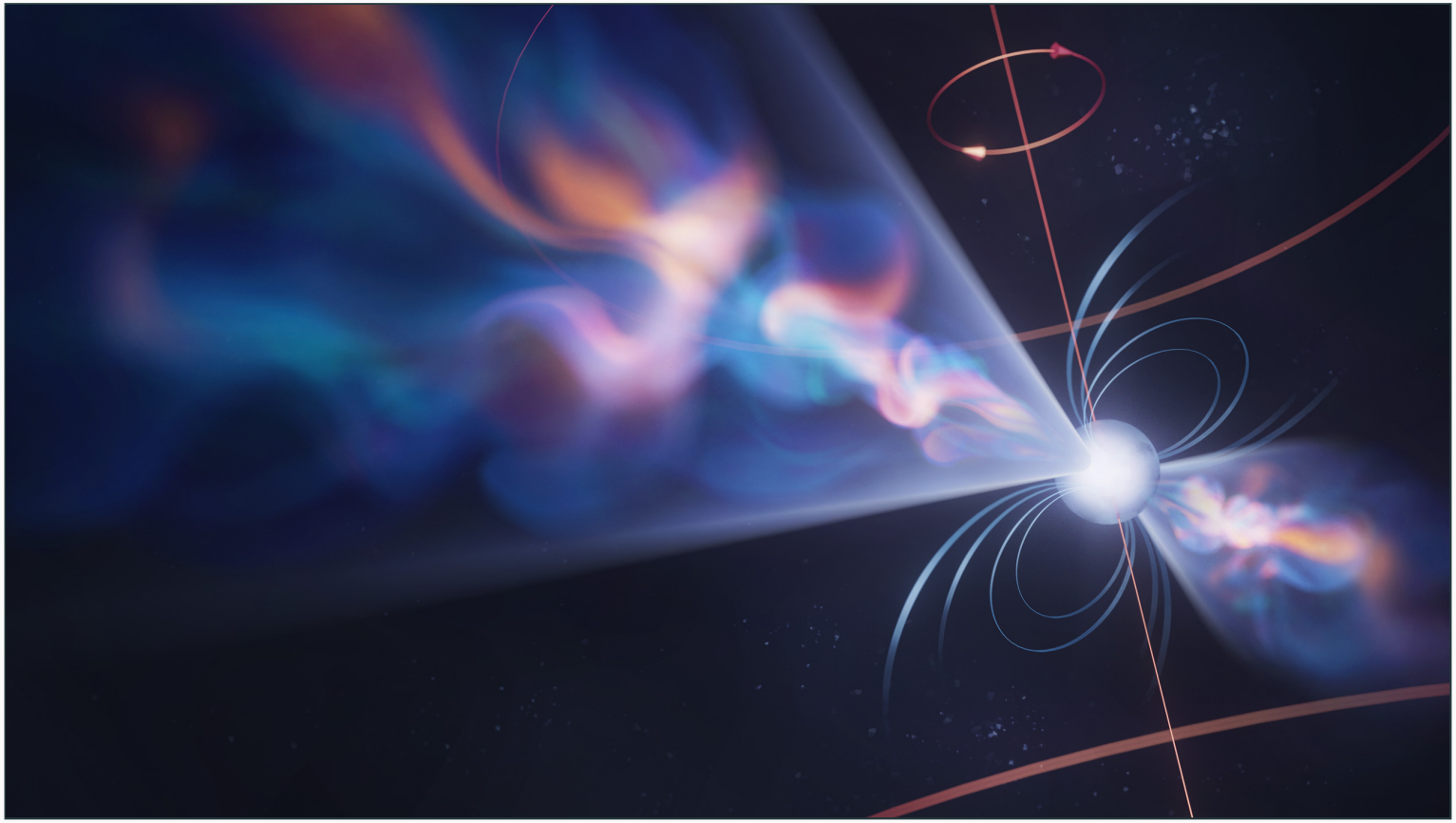

Highly magnetized rotating neutron stars, ultra-precise stellar clocks

- Beamed radio pulses emitted from magnetic poles $\rightarrow$ **cosmic lighthouses**
- Periods of $10^{-3\cdots1}$ s. Accretion in close-binary systems $\rightarrow$ **millisecond pulsars**

Discovery

[cam.ac.uk]

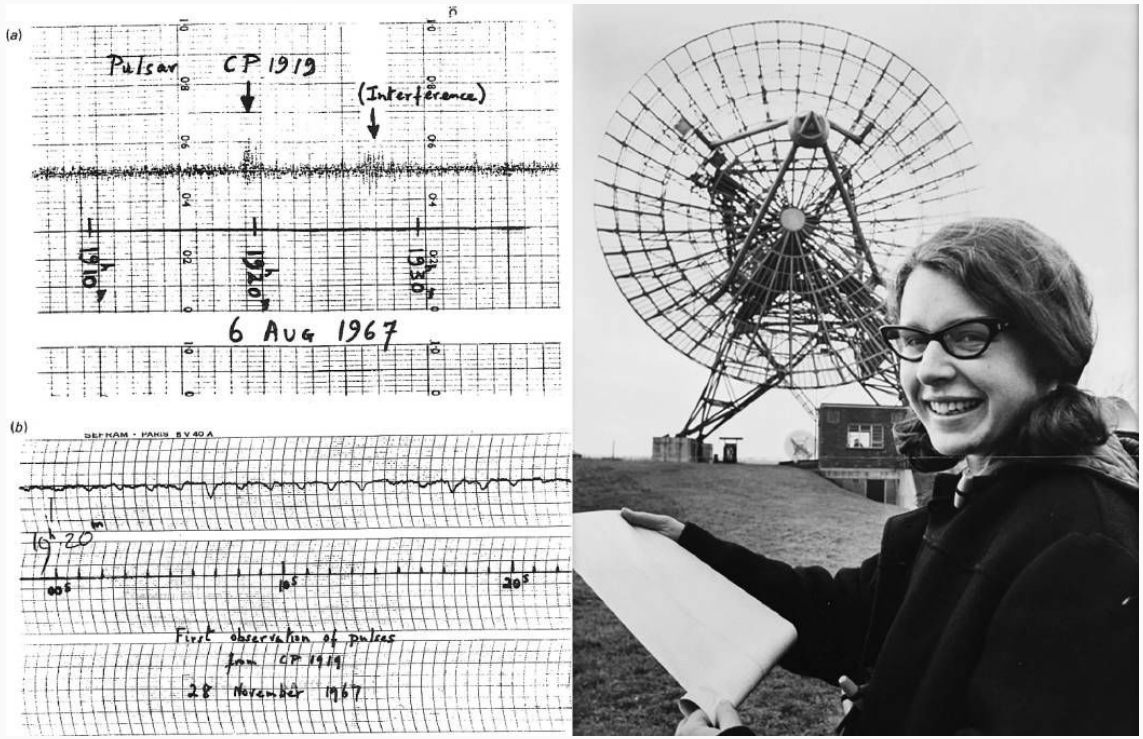

- First pulsar PSR B1919+21 (period 1.337 s), initially dubbed LGM-1
- Detected by Jocelyn Bell (PhD student) in 1967
- 1974 Nobel Prize in Physics awarded to Antony Hewish and Martin Ryle

Pulsar $P - \dot{P}$ diagram

[https://neutronstars.utk.edu/code/nstar-plot/ppdot.html]

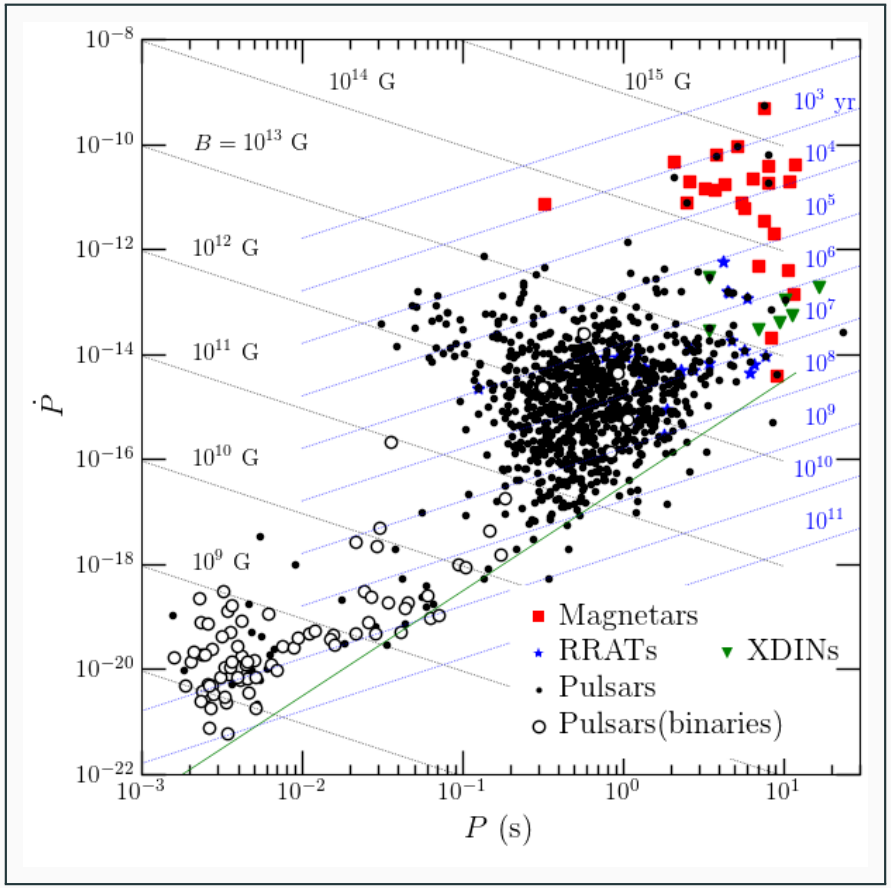

- Contours: constant characteristic age, constant surface magnetic field
- Three main populations: normal pulsars, millisecond pulsars, and magnetars
- MSPs: short P, small $\dot{P}$, small B, pass death line and then recycled

Hulse–Taylor binary system

PSR B1913+16: Binary system; pulsar + companion (most likely a neutron star)

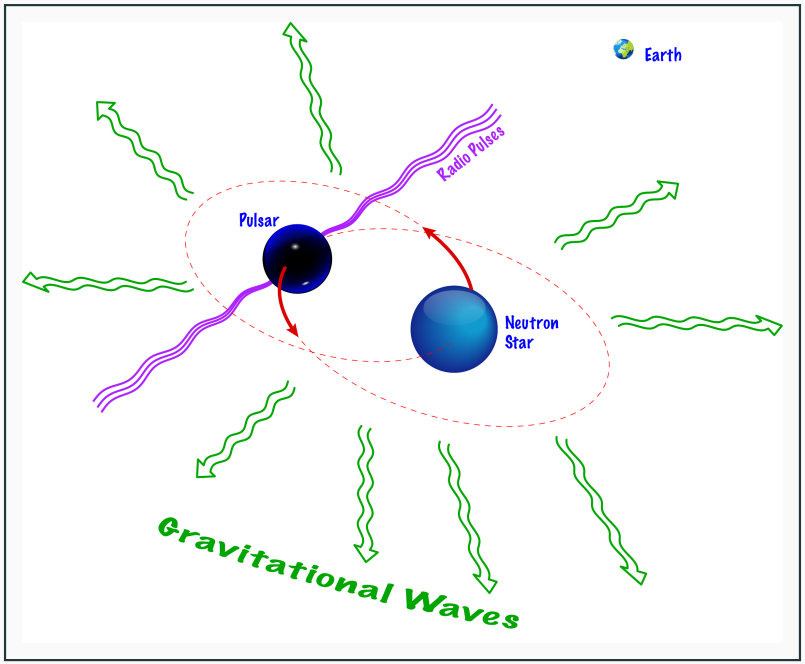

- Relativistic system, $v \sim 10^{-3}\, c$; excellent laboratory for probing general relativity
- Discovered in 1974. Orbital period decays because of GW emsission

First (indirect) detection of gravitational waves

Nobel prize in Physics awarded to Russell A. Hulse and Joseph H. Taylor in 1993

Period shift

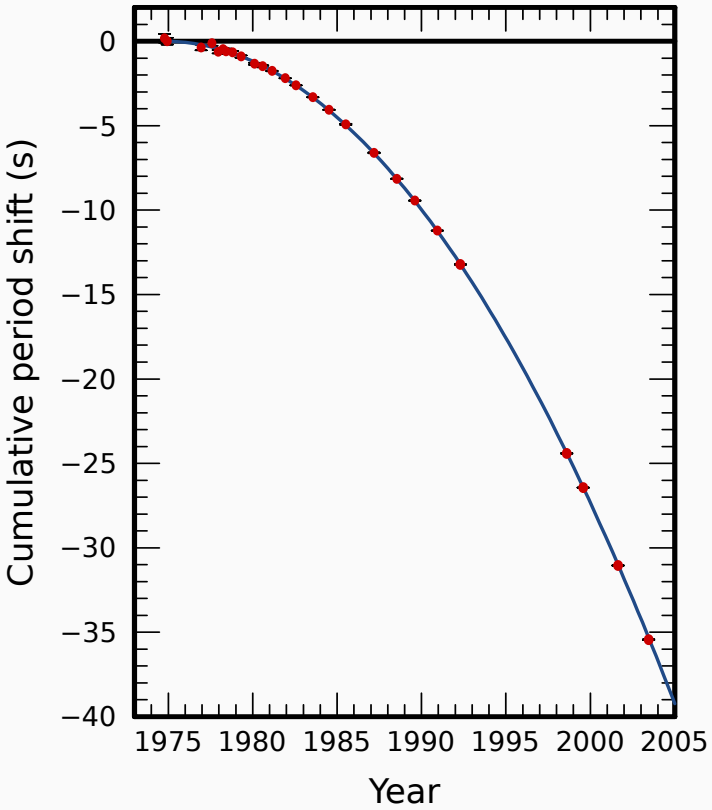

Orbital period

$$P_b = 0.322997448930(4)\,\mathrm{d}$$

Orbital decay rate

$$\dot{P}_b = -2.4184(9) \times 10^{-12}$$

Cumulative period shift

$$T_n - \frac{n}{\nu_b} = \frac{\dot{P}_b}{2\,P_b}\,T_n^2$$

Cumulative shift in the periastron epoch of PSR B1913+16 as a function of time

- Blue solid curve: theoretical prediction based on general relativity
- Red data points: measured values

Pulsar timing arrays (PTAs)

Array of pulsars across the Milky Way → GW detector of galactic dimensions!

- Look for tiny distortions in pulse travel times caused by nanohertz GWs
- Signal builds up over time; monitor PTA over years and decades

Times of arrival

[Alessandro Ridolfi, PhD thesis (2017)]

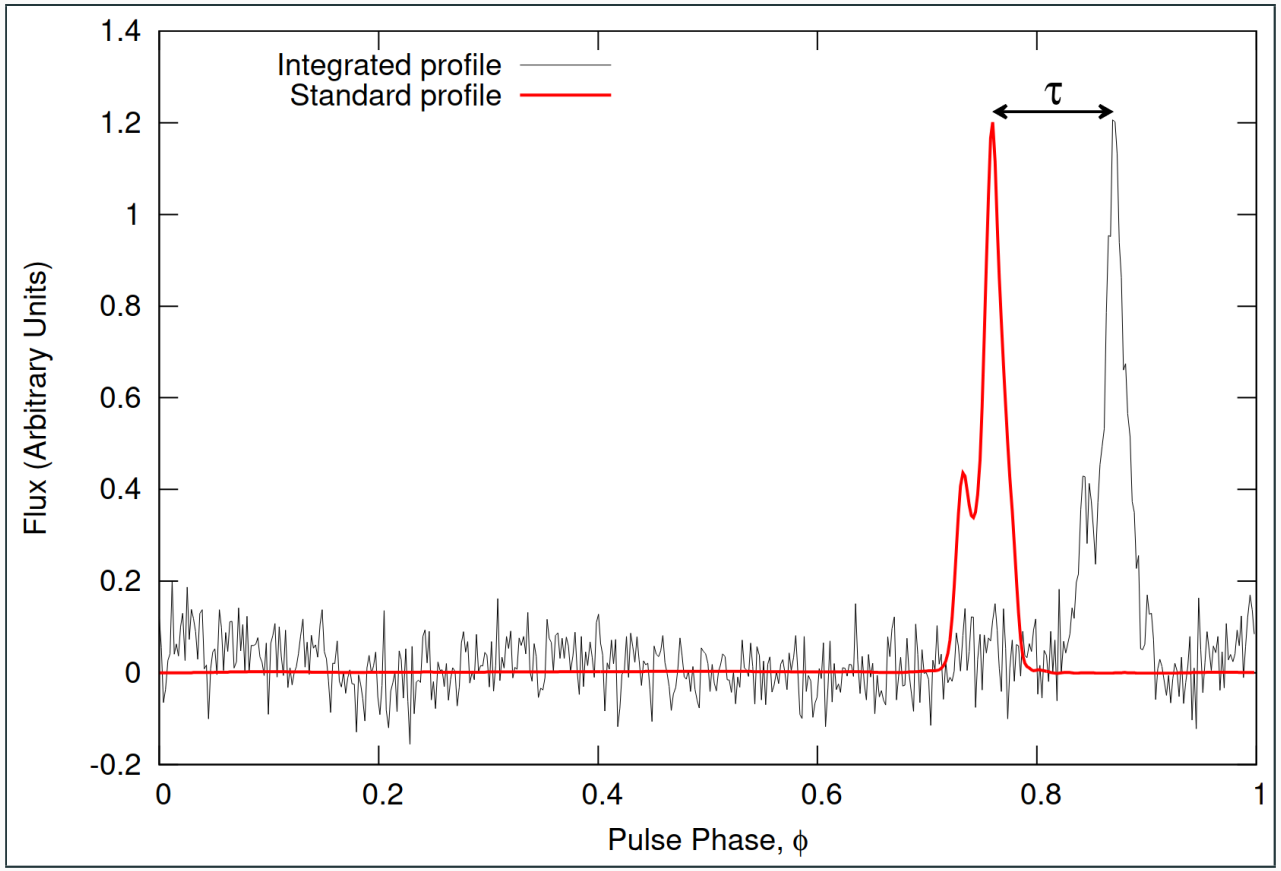

- Measure **times of arrival** and compare to predictions from a **timing model**
- **Timing residuals** for each individual pulsar → GW signature in cross-correlations

Timing model

1. Proper observer time $\tau_{\mathrm{obs},n} \leftrightarrow$ coordinate time at the solar system barycenter $t^{\mathrm{obs}}_{\mathrm{SSB},n}$

Timing model

1. Proper observer time $\tau_{\mathrm{obs},n} \leftrightarrow$ coordinate time at the solar system barycenter $t^{\mathrm{obs}}_{\mathrm{SSB},n}$

$$t_{\mathrm{SSB}} = \tau_{\mathrm{obs}} - \frac{D}{\nu^2} + \Delta_{E,\odot} + \Delta_{R,\odot} - \Delta_{S,\odot}$$

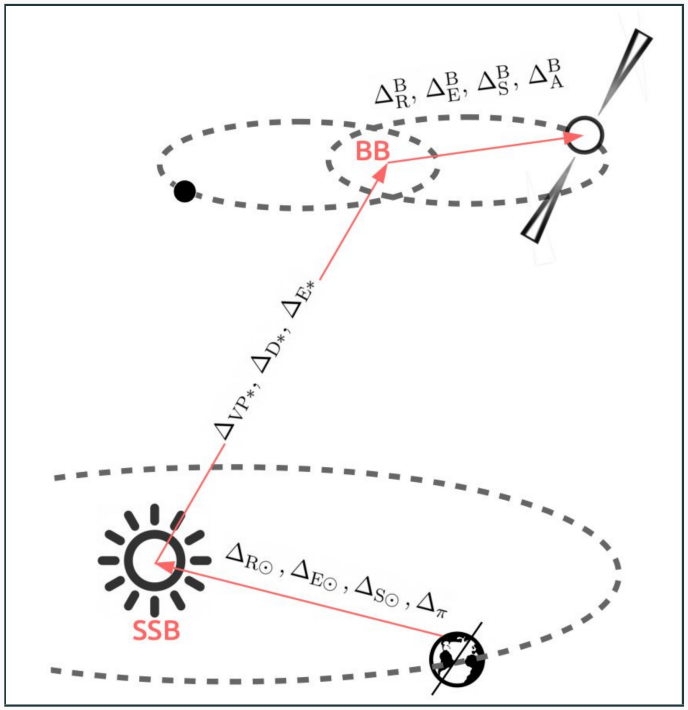

Timing model

1. Proper observer time $\tau_{\mathrm{obs},n} \leftrightarrow$ coordinate time at the solar system barycenter $t^{\mathrm{obs}}_{\mathrm{SSB},n}$

$$t_{\mathrm{SSB}} = \tau_{\mathrm{obs}} - \frac{D}{\nu^2} + \Delta_{E,\odot} + \Delta_{R,\odot} - \Delta_{S,\odot}$$

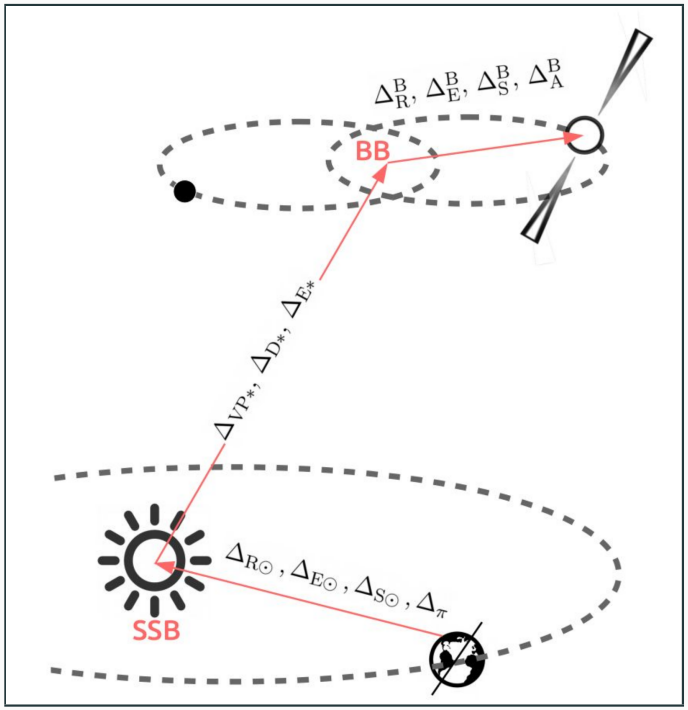

Roemer delay

Motion of the Earth w. r. t. to the SSB

$$\Delta_{R,\odot} = -\left(\boldsymbol{r}_b - \boldsymbol{r}_{\mathrm{obs}}\right) \cdot \hat{\boldsymbol{n}}$$

Timing model

1. Proper observer time $\tau_{\mathrm{obs},n} \leftrightarrow$ coordinate time at the solar system barycenter $t^{\mathrm{obs}}_{\mathrm{SSB},n}$

$$t_{\mathrm{SSB}} = \tau_{\mathrm{obs}} - \frac{D}{\nu^2} + \Delta_{E,\odot} + \Delta_{R,\odot} - \Delta_{S,\odot}$$

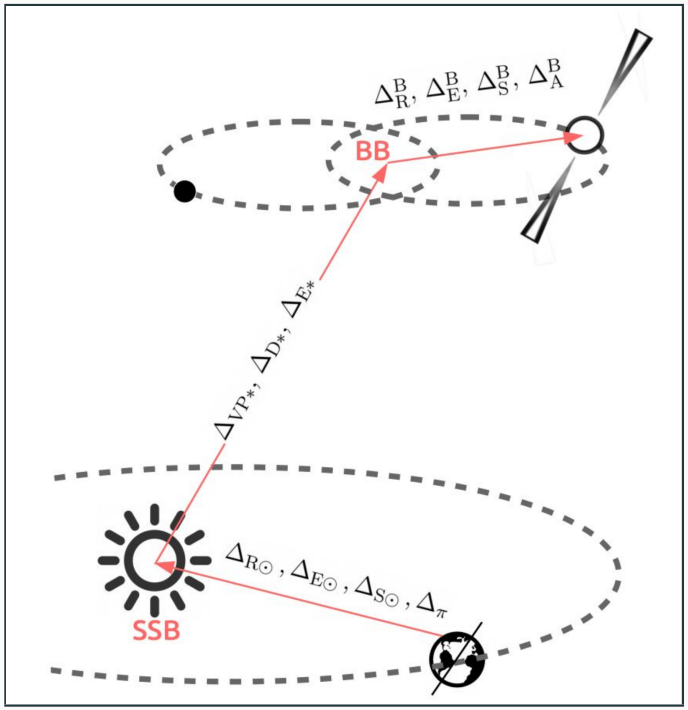

Roemer delay
Motion of the Earth w. r. t. to the SSB

$$\Delta_{R,\odot} = -\left(\boldsymbol{r}_b - \boldsymbol{r}_{\mathrm{obs}}\right) \cdot \hat{\boldsymbol{n}}$$

Shapiro delay
Time delay due to gravitational potential

$$\Delta_{S,\odot} = -2 \int_{\boldsymbol{r}_{\mathrm{obs}}}^{\boldsymbol{r}_p} |d\boldsymbol{x}|\, \phi\left(\boldsymbol{x}\right)$$

Timing model

1. Proper observer time $\tau_{\mathrm{obs},n} \leftrightarrow$ coordinate time at the solar system barycenter $t^{\mathrm{obs}}_{\mathrm{SSB},n}$

$$t_{\mathrm{SSB}} = \tau_{\mathrm{obs}} - \frac{D}{\nu^2} + \Delta_{E,\odot} + \Delta_{R,\odot} - \Delta_{S,\odot}$$

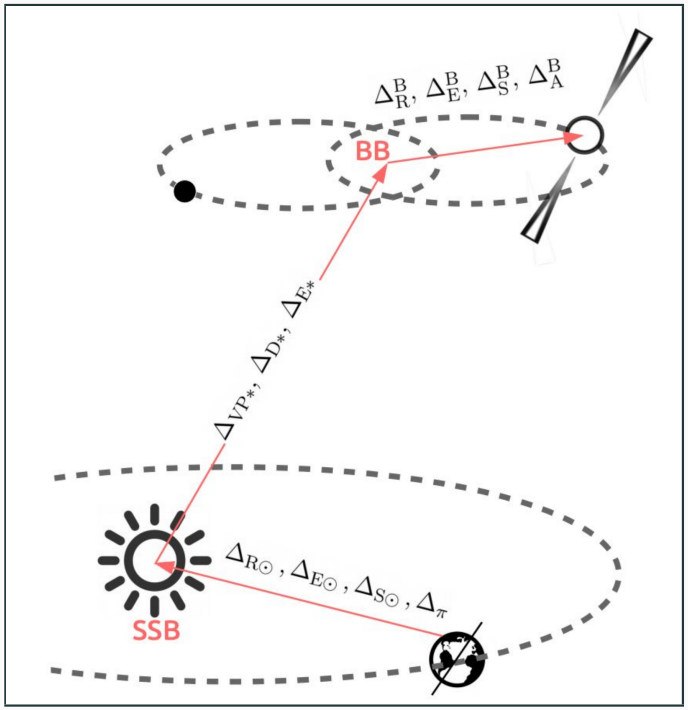

Roemer delay
Motion of the Earth w. r. t. to the SSB

$$\Delta_{R,\odot} = -\left(\boldsymbol{r}_b - \boldsymbol{r}_{\mathrm{obs}}\right) \cdot \hat{\boldsymbol{n}}$$

Shapiro delay
Time delay due to gravitational potential

$$\Delta_{S,\odot} = -2 \int_{\boldsymbol{r}_{\mathrm{obs}}}^{\boldsymbol{r}_p} |d\boldsymbol{x}|\, \phi\left(\boldsymbol{x}\right)$$

Einstein delay
Doppler shift and gravitational redshift

$$\Delta_{E,\odot} = \int^{t_{\mathrm{obs}}} dt' \left[1/2\, v^2_{\mathrm{obs}}(t') - \phi\left(\boldsymbol{r}_{\mathrm{obs}}(t')\right)\right]$$

Timing model

1. Proper observer time $\tau_{\mathrm{obs},n} \leftrightarrow$ coordinate time at the solar system barycenter $t^{\mathrm{obs}}_{\mathrm{SSB},n}$

$$t_{\mathrm{SSB}} = \tau_{\mathrm{obs}} - \frac{D}{\nu^2} + \Delta_{E,\odot} + \Delta_{R,\odot} - \Delta_{S,\odot}$$

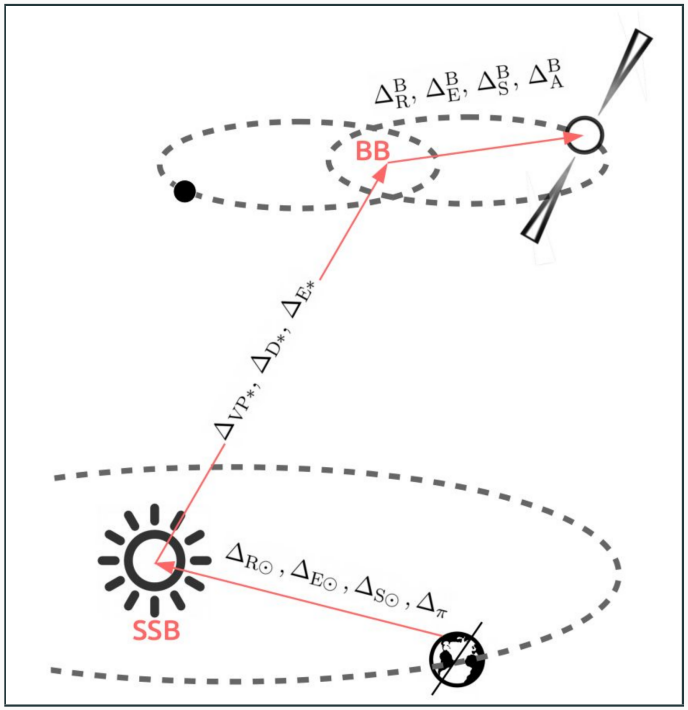

Roemer delay
Motion of the Earth w. r. t. to the SSB

$$\Delta_{R,\odot} = -\left(\boldsymbol{r}_b - \boldsymbol{r}_{\mathrm{obs}}\right) \cdot \hat{\boldsymbol{n}}$$

Shapiro delay
Time delay due to gravitational potential

$$\Delta_{S,\odot} = -2 \int_{\boldsymbol{r}_{\mathrm{obs}}}^{\boldsymbol{r}_p} |d\boldsymbol{x}|\, \phi\left(\boldsymbol{x}\right)$$

Einstein delay
Doppler shift and gravitational redshift

$$\Delta_{E,\odot} = \int^{t_{\mathrm{obs}}} dt' \left[1/2\, v^2_{\mathrm{obs}}(t') - \phi\left(\boldsymbol{r}_{\mathrm{obs}}(t')\right)\right]$$

2. Proper pulsar time $\tau_{\mathrm{em},n} \leftrightarrow$ coordinate time at binary barycenter $t_{\mathrm{em},n}$
3. Predict expected arrival time $t^{\mathrm{exp}}_{\mathrm{SSB},n} = t_{\mathrm{em},n} + \Delta t$ and compare to $t^{\mathrm{obs}}_{\mathrm{SSB},n} \leftrightarrow \tau_{\mathrm{obs},n}$

GW contribution to timing residuals

Relative shift in the pulse arrival time caused by GWs

$$z_a = \frac{\Delta T_a}{T_a} = \frac{1}{2}\, n_a^i n_a^j \int_{t_{\rm em}}^{t_{\rm em}+d_a} dt' \left[\frac{\partial}{\partial t'}\, h_{ij}^{\rm TT}\left(t', \boldsymbol{x}\right)\right]_{\boldsymbol{x}=(t_{\rm em}+d_a-t')\hat{\boldsymbol{n}}_a}$$

for pulsar a, with period T_a, at distance d_a, in the direction $\hat{\boldsymbol{n}}_a$, and GW strain $h_{ij}^{\rm TT}$

GW contribution to timing residuals

Relative shift in the pulse arrival time caused by GWs

$$z_a = \frac{\Delta T_a}{T_a} = \frac{1}{2}\, n_a^i n_a^j \int_{t_{\rm em}}^{t_{\rm em}+d_a} dt' \left[\frac{\partial}{\partial t'}\, h_{ij}^{\rm TT}\left(t', \boldsymbol{x}\right)\right]_{\boldsymbol{x}=(t_{\rm em}+d_a-t')\hat{\boldsymbol{n}}_a}$$

for pulsar a, with period T_a, at distance d_a, in the direction $\hat{\boldsymbol{n}}_a$, and GW strain $h_{ij}^{\rm TT}$

Example: Monochromatic GW

$$h_{ij}^{\rm TT}\left(t, \boldsymbol{x}\right) = \mathcal{A}_{ij}\left(\hat{\boldsymbol{n}}\right) \cos\left[\omega\left(t - \hat{\boldsymbol{n}}\cdot\boldsymbol{x}\right)\right]$$

$$z_a\left(t_{\rm obs}\right) = \frac{n_a^i n_a^j}{2\left(1+\hat{\boldsymbol{n}}\cdot\hat{\boldsymbol{n}}_a\right)}\left[h_{ij}^{\rm TT}\left(t_{\rm obs}, \boldsymbol{x}=0\right) - h_{ij}^{\rm TT}\left(t_{\rm em}, \boldsymbol{x}_a\right)\right]$$

GW contribution to timing residuals

Relative shift in the pulse arrival time caused by GWs

$$z_a = \frac{\Delta T_a}{T_a} = \frac{1}{2}\, n_a^i n_a^j \int_{t_{\rm em}}^{t_{\rm em}+d_a} dt' \left[\frac{\partial}{\partial t'}\, h_{ij}^{\rm TT}\left(t', \boldsymbol{x}\right)\right]_{\boldsymbol{x}=(t_{\rm em}+d_a-t')\hat{\boldsymbol{n}}_a}$$

for pulsar a, with period T_a, at distance d_a, in the direction $\hat{\boldsymbol{n}}_a$, and GW strain $h_{ij}^{\rm TT}$

Example: Monochromatic GW

$$h_{ij}^{\rm TT}\left(t, \boldsymbol{x}\right) = \mathcal{A}_{ij}\left(\hat{\boldsymbol{n}}\right) \cos\left[\omega\left(t - \hat{\boldsymbol{n}}\cdot\boldsymbol{x}\right)\right]$$

$$z_a\left(t_{\rm obs}\right) = \frac{n_a^i n_a^j}{2\left(1+\hat{\boldsymbol{n}}\cdot\hat{\boldsymbol{n}}_a\right)}\left[h_{ij}^{\rm TT}\left(t_{\rm obs}, \boldsymbol{x}=0\right) - h_{ij}^{\rm TT}\left(t_{\rm em}, \boldsymbol{x}_a\right)\right]$$

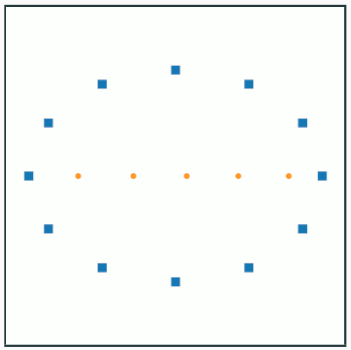

Timing residual: Integrate z_a to obtain cumulative effect

$$R_a\left(t\right) = \int_0^t dt'\, z_a\left(t'\right)$$

GW contribution to timing residuals

Relative shift in the pulse arrival time caused by GWs

$$z_a = \frac{\Delta T_a}{T_a} = \frac{1}{2}\, n_a^i n_a^j \int_{t_{\rm em}}^{t_{\rm em}+d_a} dt' \left[\frac{\partial}{\partial t'}\, h_{ij}^{\rm TT}\left(t', \boldsymbol{x}\right)\right]_{\boldsymbol{x}=(t_{\rm em}+d_a-t')\hat{\boldsymbol{n}}_a}$$

for pulsar a, with period T_a, at distance d_a, in the direction $\hat{\boldsymbol{n}}_a$, and GW strain $h_{ij}^{\rm TT}$

Example: Monochromatic GW

$$h_{ij}^{\rm TT}\left(t, \boldsymbol{x}\right) = \mathcal{A}_{ij}\left(\hat{\boldsymbol{n}}\right) \cos\left[\omega\left(t - \hat{\boldsymbol{n}}\cdot\boldsymbol{x}\right)\right]$$

$$z_a\left(t_{\rm obs}\right) = \frac{n_a^i n_a^j}{2\left(1+\hat{\boldsymbol{n}}\cdot\hat{\boldsymbol{n}}_a\right)}\left[h_{ij}^{\rm TT}\left(t_{\rm obs}, \boldsymbol{x}=0\right) - h_{ij}^{\rm TT}\left(t_{\rm em}, \boldsymbol{x}_a\right)\right]$$

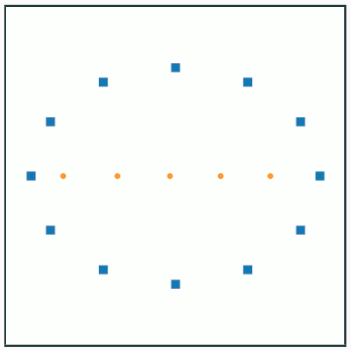

Timing residual: Integrate z_a to obtain cumulative effect

$$R_a\left(t\right) = \int_0^t dt'\, z_a\left(t'\right)$$

GW contribution to timing residuals

Relative shift in the pulse arrival time caused by GWs

$$z_a = \frac{\Delta T_a}{T_a} = \frac{1}{2}\, n_a^i n_a^j \int_{t_{\rm em}}^{t_{\rm em}+d_a} dt' \left[\frac{\partial}{\partial t'}\, h_{ij}^{\rm TT}\left(t', \boldsymbol{x}\right)\right]_{\boldsymbol{x}=(t_{\rm em}+d_a-t')\hat{\boldsymbol{n}}_a}$$

for pulsar a, with period T_a, at distance d_a, in the direction $\hat{\boldsymbol{n}}_a$, and GW strain $h_{ij}^{\rm TT}$

Example: Monochromatic GW

$$h_{ij}^{\rm TT}\left(t, \boldsymbol{x}\right) = \mathcal{A}_{ij}\left(\hat{\boldsymbol{n}}\right) \cos\left[\omega\left(t - \hat{\boldsymbol{n}}\cdot\boldsymbol{x}\right)\right]$$

$$z_a\left(t_{\rm obs}\right) = \frac{n_a^i n_a^j}{2\left(1+\hat{\boldsymbol{n}}\cdot\hat{\boldsymbol{n}}_a\right)}\left[h_{ij}^{\rm TT}\left(t_{\rm obs}, \boldsymbol{x}=0\right) - h_{ij}^{\rm TT}\left(t_{\rm em}, \boldsymbol{x}_a\right)\right]$$

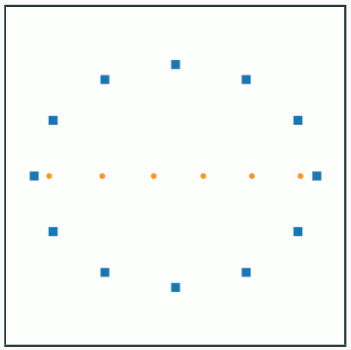

Timing residual: Integrate z_a to obtain cumulative effect

$$R_a\left(t\right) = \int_0^t dt'\, z_a\left(t'\right)$$

GW contribution to timing residuals

Relative shift in the pulse arrival time caused by GWs

$$z_a = \frac{\Delta T_a}{T_a} = \frac{1}{2}\, n_a^i n_a^j \int_{t_{\rm em}}^{t_{\rm em}+d_a} dt' \left[\frac{\partial}{\partial t'}\, h_{ij}^{\rm TT}\left(t', \boldsymbol{x}\right)\right]_{\boldsymbol{x}=(t_{\rm em}+d_a-t')\hat{\boldsymbol{n}}_a}$$

for pulsar a, with period T_a, at distance d_a, in the direction $\hat{\boldsymbol{n}}_a$, and GW strain $h_{ij}^{\rm TT}$

Example: Monochromatic GW

$$h_{ij}^{\rm TT}\left(t, \boldsymbol{x}\right) = \mathcal{A}_{ij}\left(\hat{\boldsymbol{n}}\right) \cos\left[\omega\left(t - \hat{\boldsymbol{n}}\cdot\boldsymbol{x}\right)\right]$$

$$z_a\left(t_{\rm obs}\right) = \frac{n_a^i n_a^j}{2\left(1+\hat{\boldsymbol{n}}\cdot\hat{\boldsymbol{n}}_a\right)}\left[h_{ij}^{\rm TT}\left(t_{\rm obs}, \boldsymbol{x}=0\right) - h_{ij}^{\rm TT}\left(t_{\rm em}, \boldsymbol{x}_a\right)\right]$$

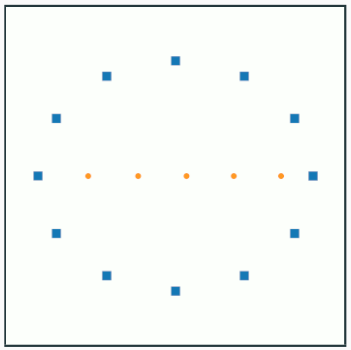

Timing residual: Integrate z_a to obtain cumulative effect

$$R_a\left(t\right) = \int_0^t dt'\, z_a\left(t'\right)$$

GW contribution to timing residuals

Relative shift in the pulse arrival time caused by GWs

$$z_a = \frac{\Delta T_a}{T_a} = \frac{1}{2}\, n_a^i n_a^j \int_{t_{\rm em}}^{t_{\rm em}+d_a} dt' \left[\frac{\partial}{\partial t'}\, h_{ij}^{\rm TT}\left(t', \boldsymbol{x}\right)\right]_{\boldsymbol{x}=(t_{\rm em}+d_a-t')\hat{\boldsymbol{n}}_a}$$

for pulsar a, with period T_a, at distance d_a, in the direction $\hat{\boldsymbol{n}}_a$, and GW strain $h_{ij}^{\rm TT}$

Example: Monochromatic GW

$$h_{ij}^{\rm TT}\left(t, \boldsymbol{x}\right) = \mathcal{A}_{ij}\left(\hat{\boldsymbol{n}}\right) \cos\left[\omega\left(t - \hat{\boldsymbol{n}}\cdot\boldsymbol{x}\right)\right]$$

$$z_a\left(t_{\rm obs}\right) = \frac{n_a^i n_a^j}{2\left(1+\hat{\boldsymbol{n}}\cdot\hat{\boldsymbol{n}}_a\right)}\left[h_{ij}^{\rm TT}\left(t_{\rm obs}, \boldsymbol{x}=0\right) - h_{ij}^{\rm TT}\left(t_{\rm em}, \boldsymbol{x}_a\right)\right]$$

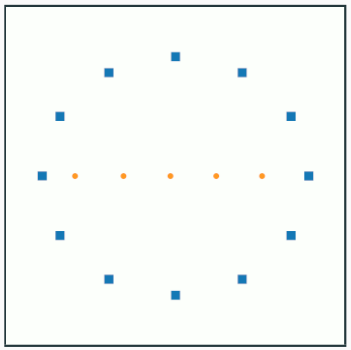

Timing residual: Integrate z_a to obtain cumulative effect

$$R_a\left(t\right) = \int_0^t dt'\, z_a\left(t'\right)$$

GW contribution to timing residuals

Relative shift in the pulse arrival time caused by GWs

$$z_a = \frac{\Delta T_a}{T_a} = \frac{1}{2}\, n_a^i n_a^j \int_{t_{\rm em}}^{t_{\rm em}+d_a} dt' \left[\frac{\partial}{\partial t'}\, h_{ij}^{\rm TT}\left(t', \boldsymbol{x}\right)\right]_{\boldsymbol{x}=(t_{\rm em}+d_a-t')\hat{\boldsymbol{n}}_a}$$

for pulsar a, with period T_a, at distance d_a, in the direction $\hat{\boldsymbol{n}}_a$, and GW strain $h_{ij}^{\rm TT}$

Example: Monochromatic GW

$$h_{ij}^{\rm TT}\left(t, \boldsymbol{x}\right) = \mathcal{A}_{ij}\left(\hat{\boldsymbol{n}}\right) \cos\left[\omega\left(t - \hat{\boldsymbol{n}}\cdot\boldsymbol{x}\right)\right]$$

$$z_a\left(t_{\rm obs}\right) = \frac{n_a^i n_a^j}{2\left(1+\hat{\boldsymbol{n}}\cdot\hat{\boldsymbol{n}}_a\right)}\left[h_{ij}^{\rm TT}\left(t_{\rm obs}, \boldsymbol{x}=0\right) - h_{ij}^{\rm TT}\left(t_{\rm em}, \boldsymbol{x}_a\right)\right]$$

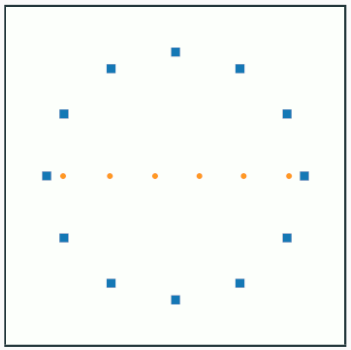

Timing residual: Integrate z_a to obtain cumulative effect

$$R_a\left(t\right) = \int_0^t dt'\, z_a\left(t'\right)$$

GW contribution to timing residuals

Relative shift in the pulse arrival time caused by GWs

$$z_a = \frac{\Delta T_a}{T_a} = \frac{1}{2}\, n_a^i n_a^j \int_{t_{\rm em}}^{t_{\rm em}+d_a} dt' \left[\frac{\partial}{\partial t'}\, h_{ij}^{\rm TT}\left(t', \boldsymbol{x}\right)\right]_{\boldsymbol{x}=(t_{\rm em}+d_a-t')\hat{\boldsymbol{n}}_a}$$

for pulsar a, with period T_a, at distance d_a, in the direction $\hat{\boldsymbol{n}}_a$, and GW strain $h_{ij}^{\rm TT}$

Example: Monochromatic GW

$$h_{ij}^{\rm TT}\left(t, \boldsymbol{x}\right) = \mathcal{A}_{ij}\left(\hat{\boldsymbol{n}}\right) \cos\left[\omega\left(t - \hat{\boldsymbol{n}}\cdot\boldsymbol{x}\right)\right]$$

$$z_a\left(t_{\rm obs}\right) = \frac{n_a^i n_a^j}{2\left(1+\hat{\boldsymbol{n}}\cdot\hat{\boldsymbol{n}}_a\right)}\left[h_{ij}^{\rm TT}\left(t_{\rm obs}, \boldsymbol{x}=0\right) - h_{ij}^{\rm TT}\left(t_{\rm em}, \boldsymbol{x}_a\right)\right]$$

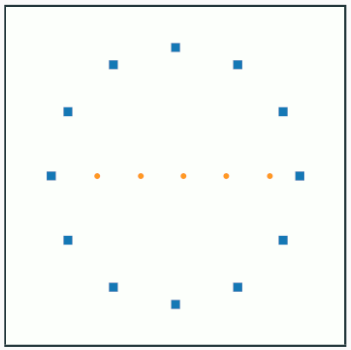

Timing residual: Integrate z_a to obtain cumulative effect

$$R_a\left(t\right) = \int_0^t dt'\, z_a\left(t'\right)$$

GW contribution to timing residuals

Relative shift in the pulse arrival time caused by GWs

$$z_a = \frac{\Delta T_a}{T_a} = \frac{1}{2}\, n_a^i n_a^j \int_{t_{\rm em}}^{t_{\rm em}+d_a} dt' \left[\frac{\partial}{\partial t'}\, h_{ij}^{\rm TT}\left(t', \boldsymbol{x}\right)\right]_{\boldsymbol{x}=(t_{\rm em}+d_a-t')\hat{\boldsymbol{n}}_a}$$

for pulsar a, with period T_a, at distance d_a, in the direction $\hat{\boldsymbol{n}}_a$, and GW strain $h_{ij}^{\rm TT}$

Example: Monochromatic GW

$$h_{ij}^{\rm TT}\left(t, \boldsymbol{x}\right) = \mathcal{A}_{ij}\left(\hat{\boldsymbol{n}}\right) \cos\left[\omega\left(t - \hat{\boldsymbol{n}}\cdot\boldsymbol{x}\right)\right]$$

$$z_a\left(t_{\rm obs}\right) = \frac{n_a^i n_a^j}{2\left(1+\hat{\boldsymbol{n}}\cdot\hat{\boldsymbol{n}}_a\right)}\left[h_{ij}^{\rm TT}\left(t_{\rm obs}, \boldsymbol{x}=0\right) - h_{ij}^{\rm TT}\left(t_{\rm em}, \boldsymbol{x}_a\right)\right]$$

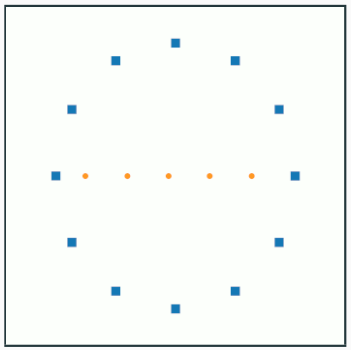

Timing residual: Integrate z_a to obtain cumulative effect

$$R_a\left(t\right) = \int_0^t dt'\, z_a\left(t'\right)$$

Cross correlations among timing residuals

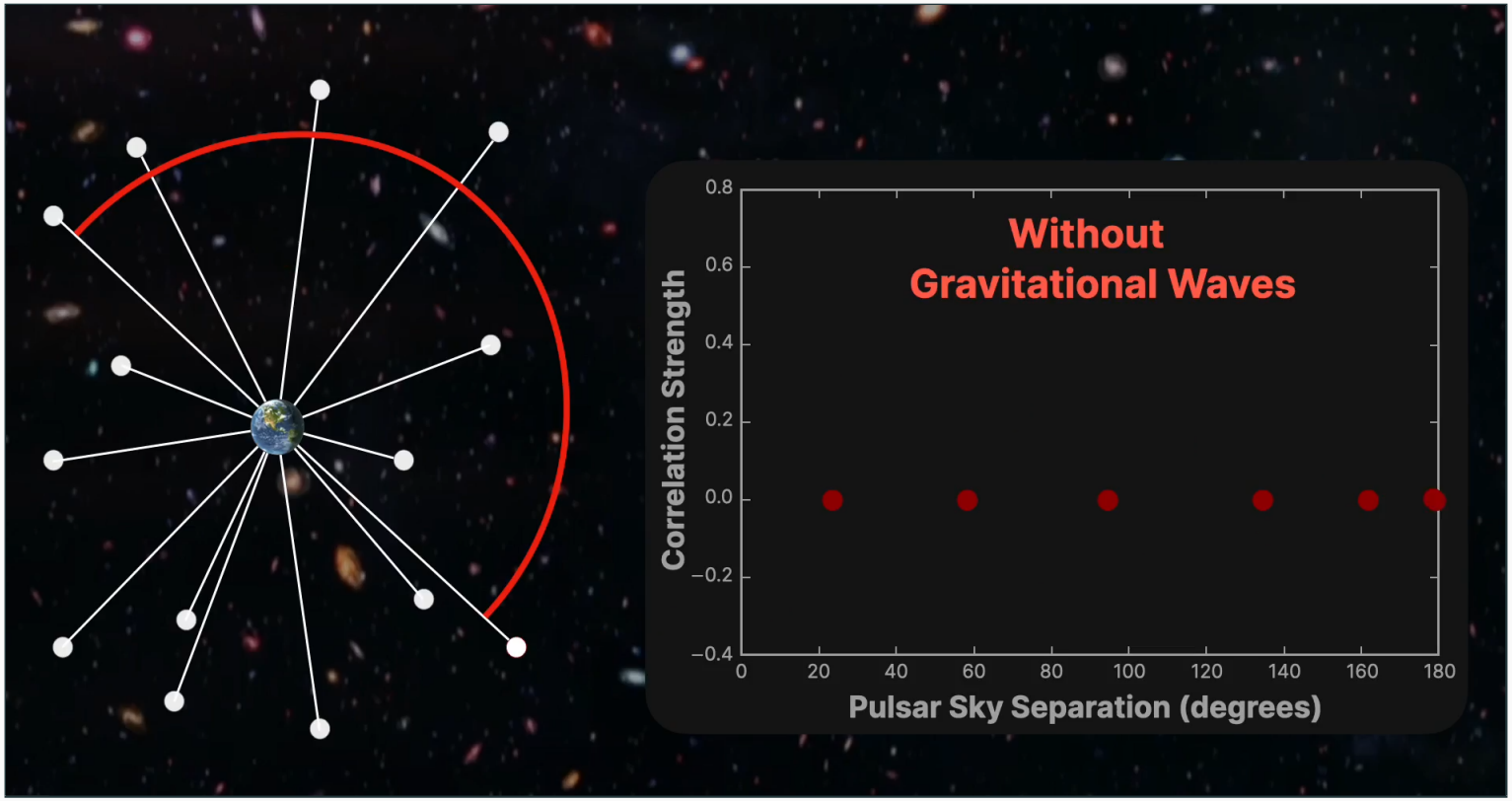

Cross correlations among timing residuals

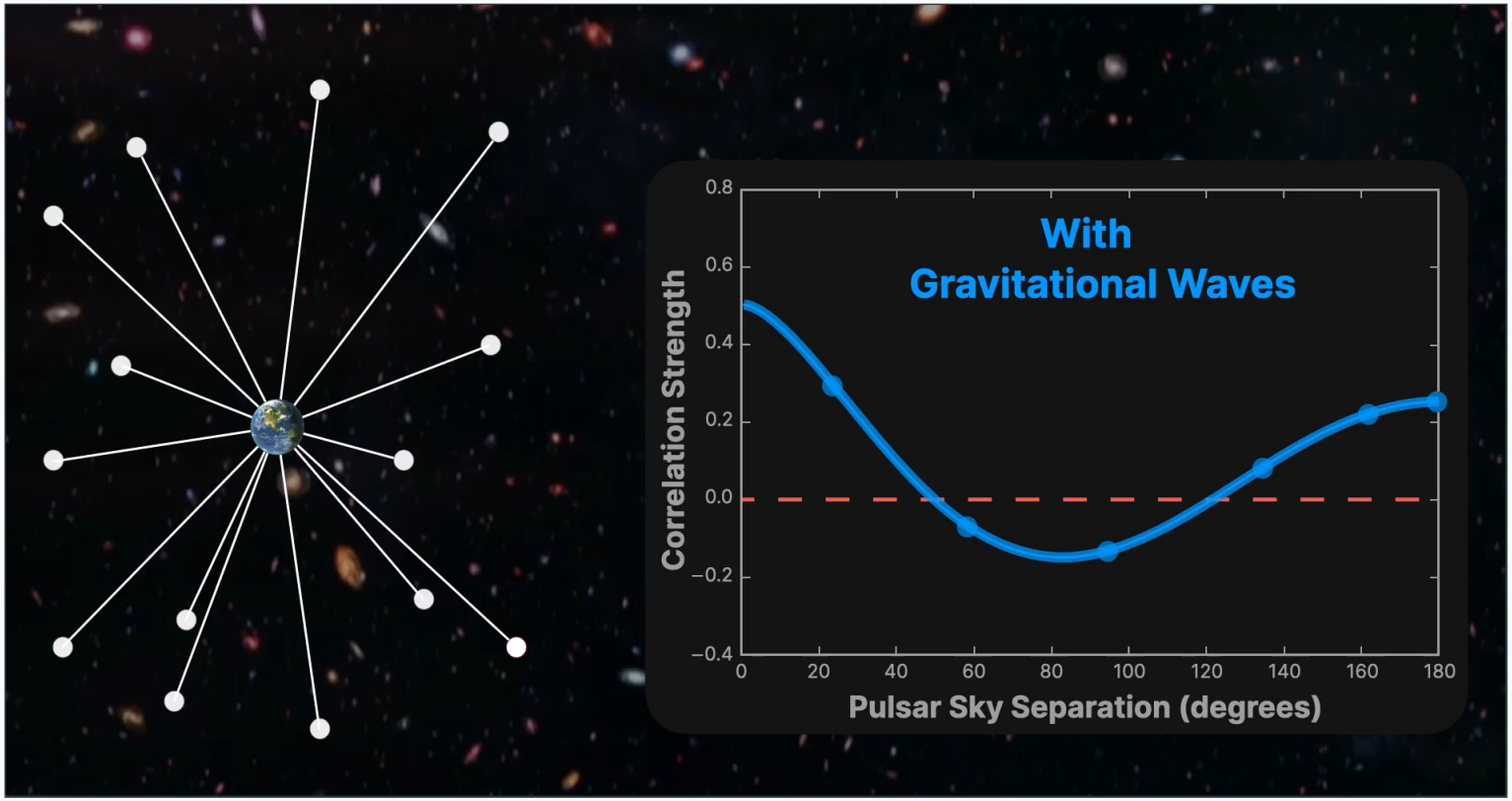

Hallmark signature of a stochastic gravitational-wave background signal:

Quadrupolar correlations described by Hellings–Downs (HD) curve $\Gamma(\xi_{ab})$

[Hellings, Downs: Astrophys. J. 265 (1983) L39]

Cross-power spectral density

Timing-residual cross-power spectral density for the pulsar pair (a, b)

$$\langle R_a(t)\, R_b(t)\rangle = \int_0^\infty df\, \Gamma(\xi_{ab})\, P_g\,, \qquad P_g(f) = \frac{h_c^2(f)}{12\pi^2 f^3}$$

Cross-power spectral density

Timing-residual cross-power spectral density for the pulsar pair (a, b)

$$\langle R_a(t)\, R_b(t)\rangle = \int_0^\infty df\, \Gamma(\xi_{ab})\, P_g\,, \qquad P_g(f) = \frac{h_c^2(f)}{12\pi^2 f^3}$$

Hellings–Downs cross-correlation coefficient

$$\Gamma(\xi_{ab}) = \frac{3}{2}\, x_{ab} \ln x_{ab} - \frac{x_{ab}}{4} + \frac{1}{2}\,, \qquad x_{ab} = \frac{1}{2}(1 - \cos\xi_{ab})$$

Cross-power spectral density

Timing-residual cross-power spectral density for the pulsar pair (a, b)

$$\langle R_a(t)\, R_b(t)\rangle = \int_0^\infty df\, \Gamma(\xi_{ab})\, P_g\,, \qquad P_g(f) = \frac{h_c^2(f)}{12\pi^2 f^3}$$

Hellings–Downs cross-correlation coefficient

$$\Gamma(\xi_{ab}) = \frac{3}{2}\, x_{ab} \ln x_{ab} - \frac{x_{ab}}{4} + \frac{1}{2}\,, \qquad x_{ab} = \frac{1}{2}(1 - \cos\xi_{ab})$$

Power-law ansatz for the characteristic strain amplitude

$$h_c(f) = A \left(\frac{f}{f_{\rm yr}}\right)^{\alpha} \qquad \Rightarrow \qquad P_g(f) = \frac{A^2}{12\pi^2\, f_{\rm yr}^3} \left(\frac{f}{f_{\rm yr}}\right)^{-\gamma}\,, \quad \gamma = 3 - 2\alpha$$

Excess timing delay: $\sqrt{\Delta f\, P_g} = \sqrt{P_g / T_{\rm obs}}$, after total observing time $T_{\rm obs}$

Existing pulsar timing arrays

Existing pulsar timing arrays

New results by CPTA, EPTA+InPTA, NANOGrav, and PPTA on June 29th, 2023!

Compelling evidence for HD correlations

2306.16213: NANOGrav

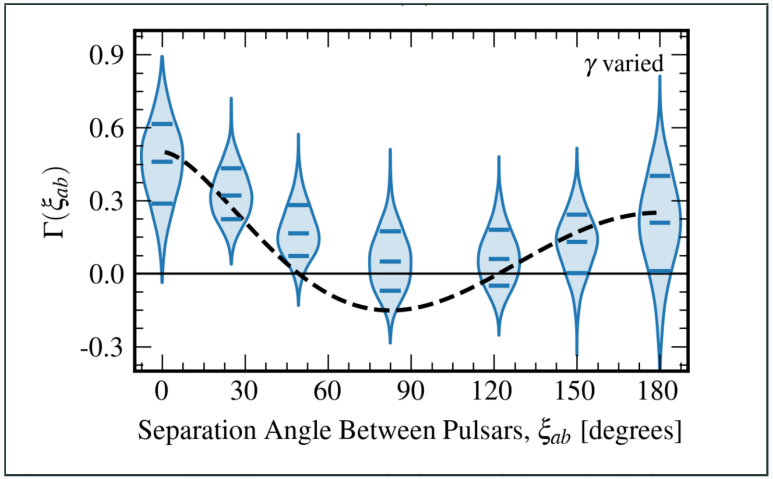

68 pulsars, 16 yr of data, HD at $\sim 3 \cdots 4\,\sigma$

2306.16214: EPTA+InPTA

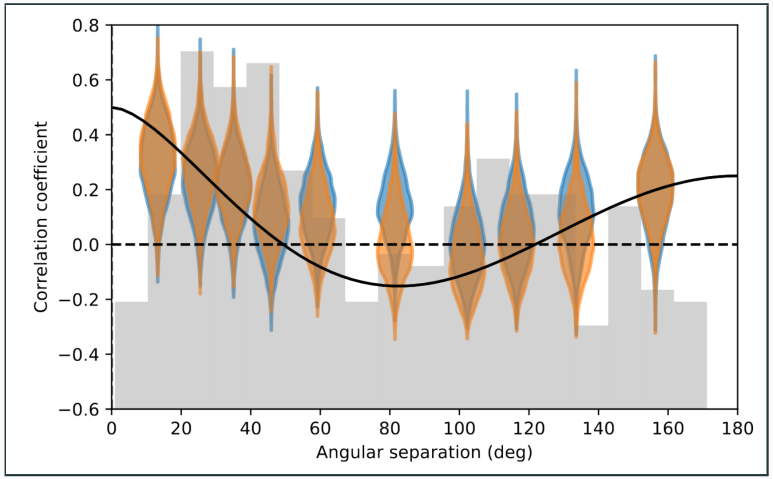

25 pulsars, 25 yr of data, HD at $\sim 3\,\sigma$

2306.16215: PPTA

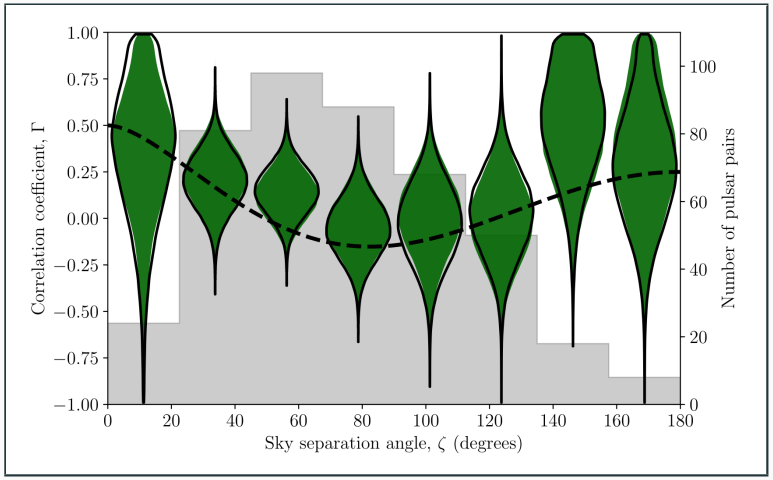

32 pulsars, 18 yr of data, HD at $\sim 2\,\sigma$

2306.16216: CPTA

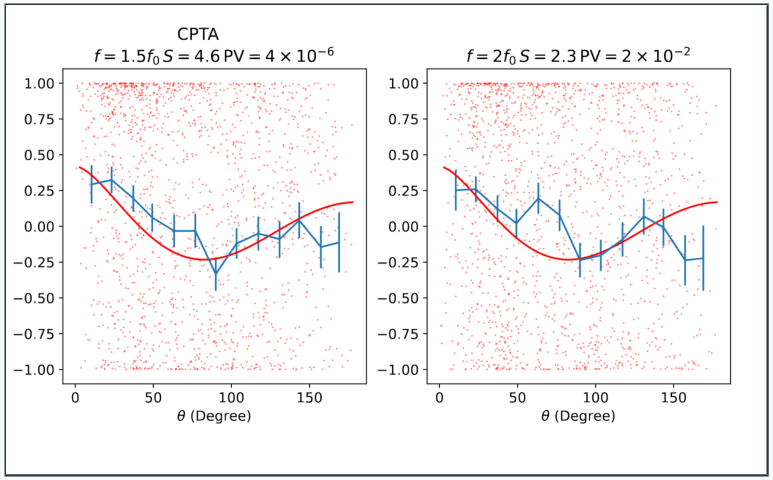

57 pulsars, 3.5 yr of data, HD at $\sim 4.6\,\sigma$

Spectral characterization

YouTube

2306.16213: NANOGrav

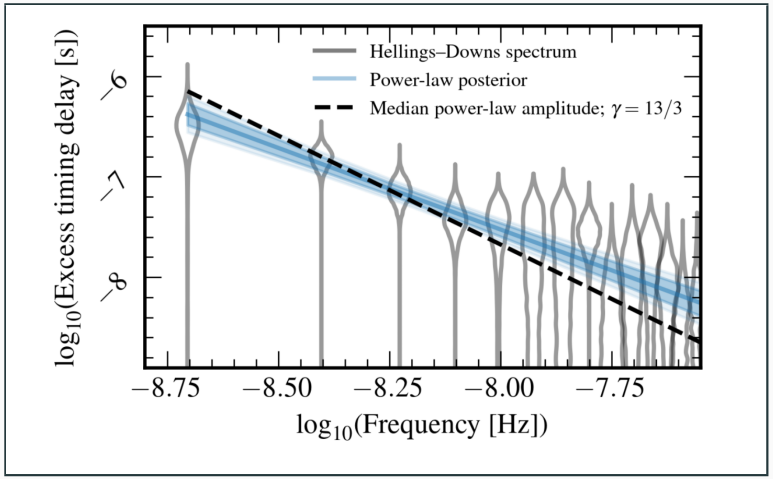

68 pulsars, 16 yr of data, HD at $\sim 3 \cdots 4\,\sigma$

2306.16214: EPTA+InPTA

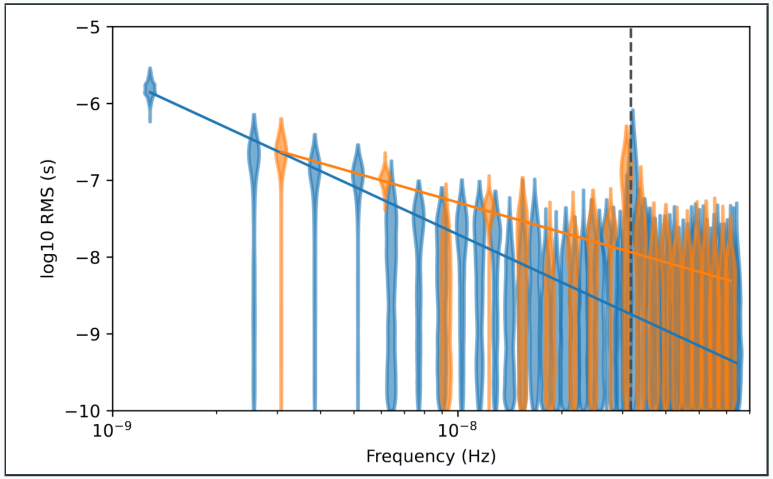

25 pulsars, 25 yr of data, HD at $\sim 3\,\sigma$

2306.16215: PPTA

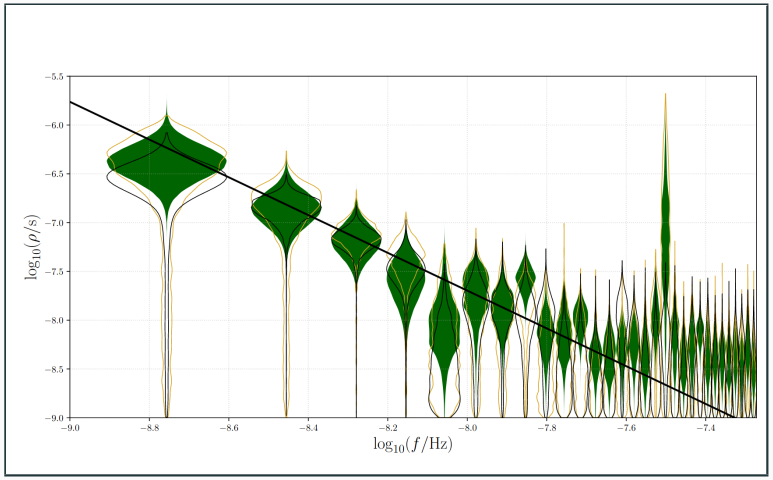

32 pulsars, 18 yr of data, HD at $\sim 2\,\sigma$

2306.16216: CPTA

57 pulsars, 3.5 yr of data, HD at $\sim 4.6\,\sigma$

Power-law fit

2306.16213: NANOGrav

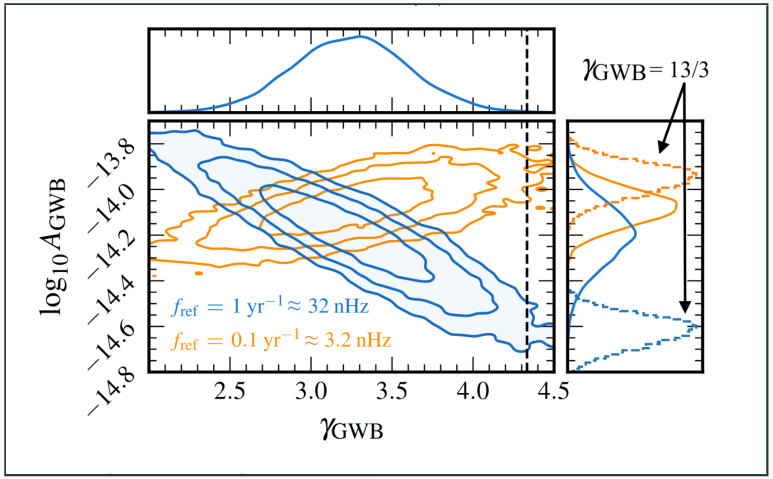

68 pulsars, 16 yr of data, HD at $\sim 3 \cdots 4\,\sigma$

2306.16214: EPTA+InPTA

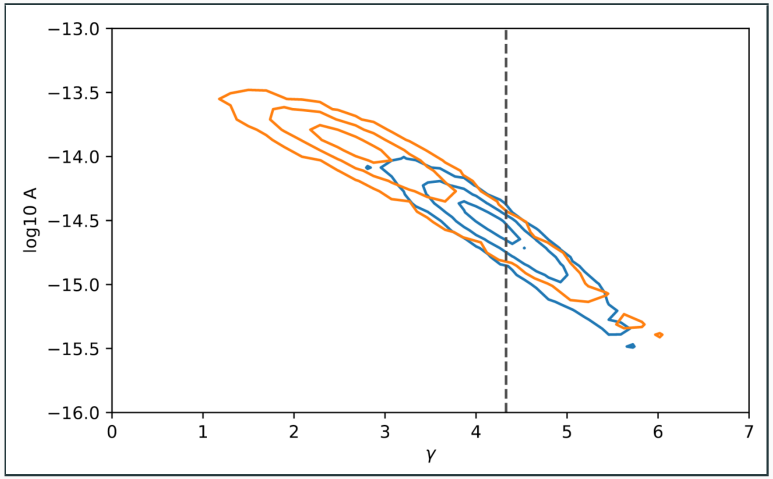

25 pulsars, 25 yr of data, HD at $\sim 3\,\sigma$

2306.16215: PPTA

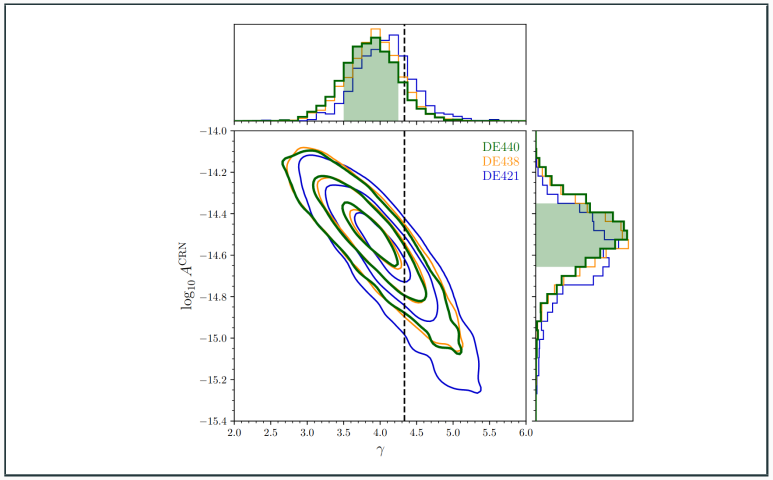

32 pulsars, 18 yr of data, HD at $\sim 2\,\sigma$

2306.16216: CPTA

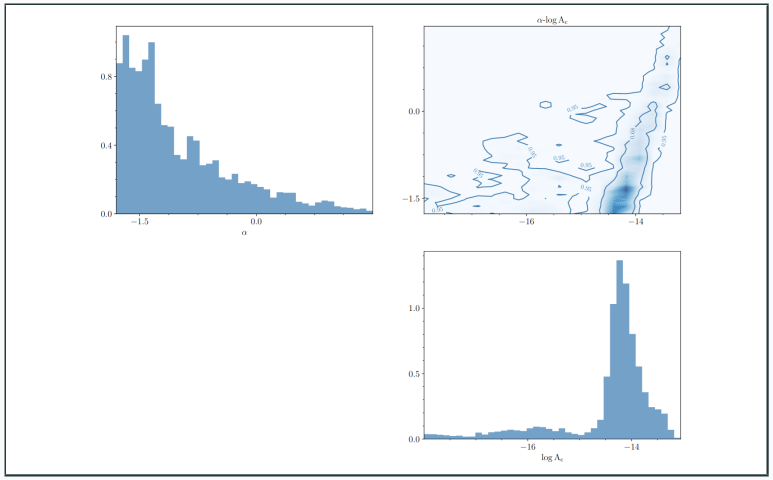

57 pulsars, 3.5 yr of data, HD at $\sim 4.6\,\sigma$

IPTA comparison

[IPTA 2309.00693]

Current world data on the HD-correlated common-spectrum process

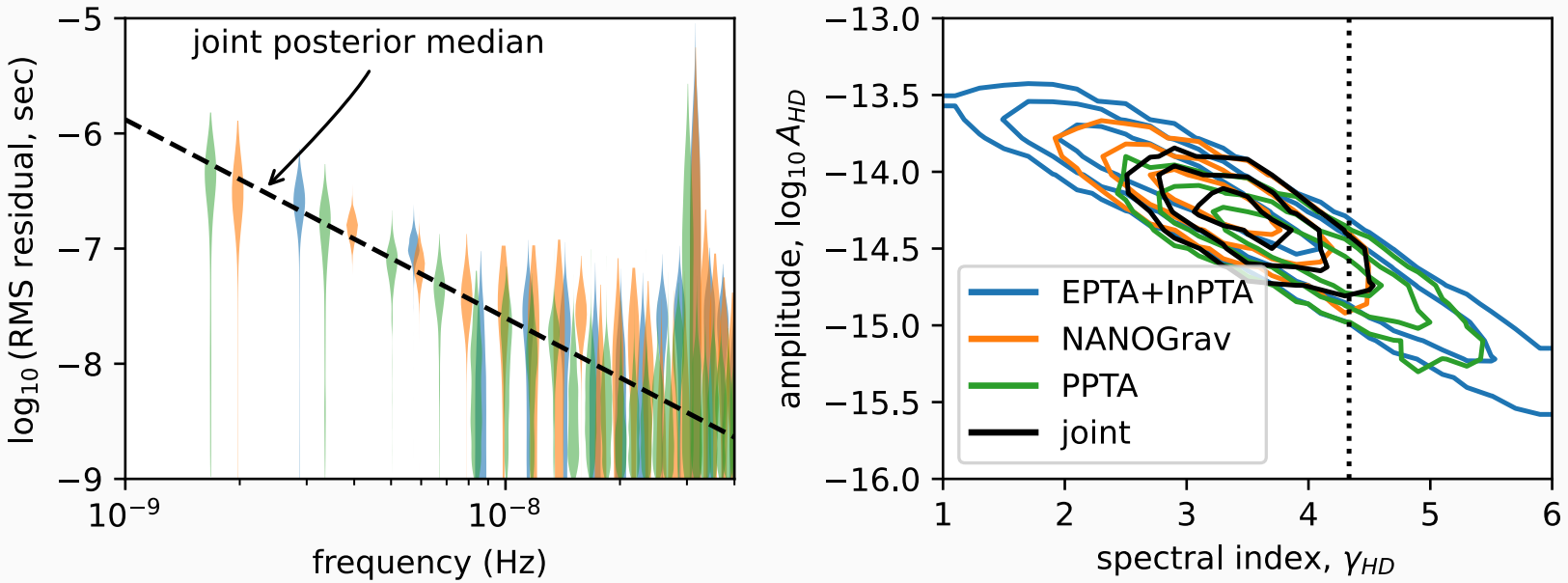

- Results from regional PTAs are consistent with each other (1σ posteriors overlap)
- Joint posterior = naive product (properly normalized) of individual posteriors
- Proper data combination and combined data analysis → IPTA DR3

Radio pulsars Venn diagram

[IPTA 2309.00693]

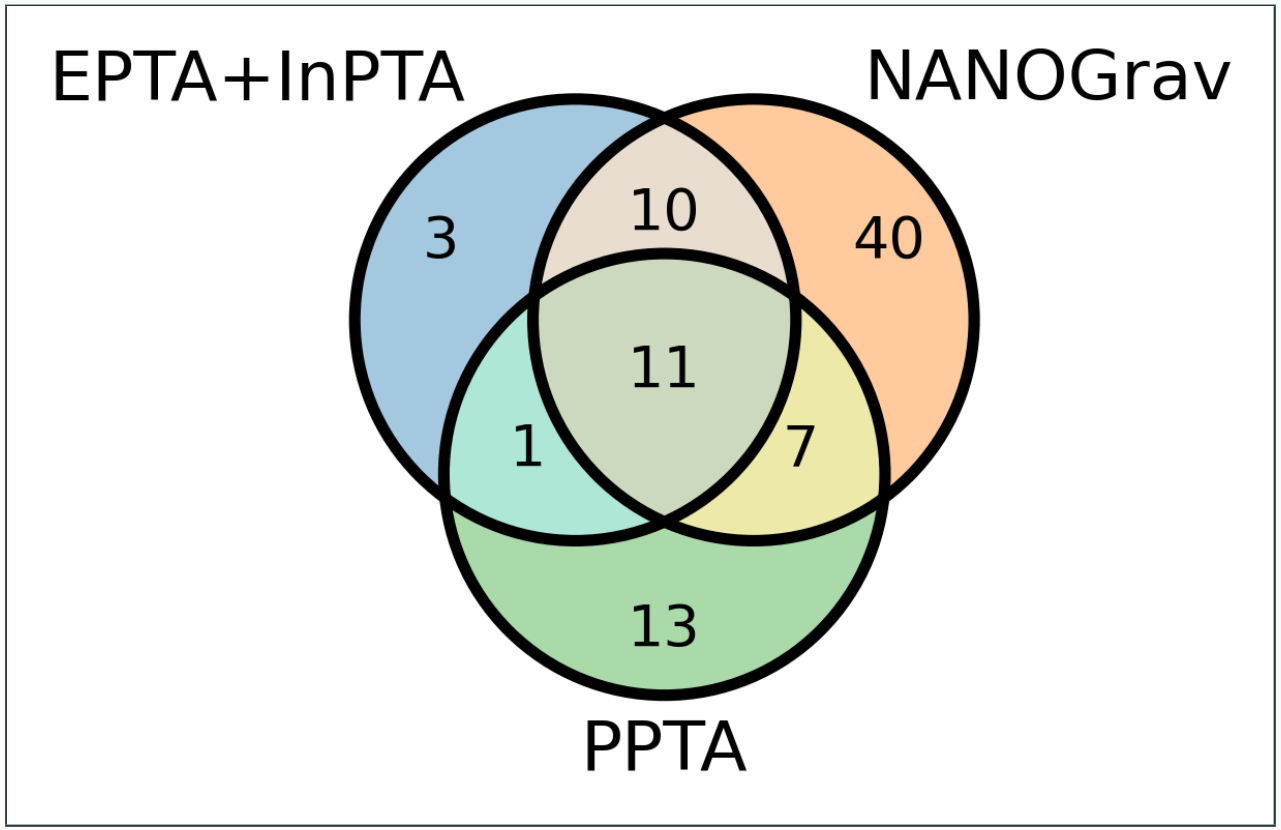

- 85 pulsars contained in latest PTA data sets
- IPTA DR3: 115 pulsars (CHIME, EPTA, InPTA, MeerKAT, NANOGrav, PPTA)

NANOGrav 15-year data set

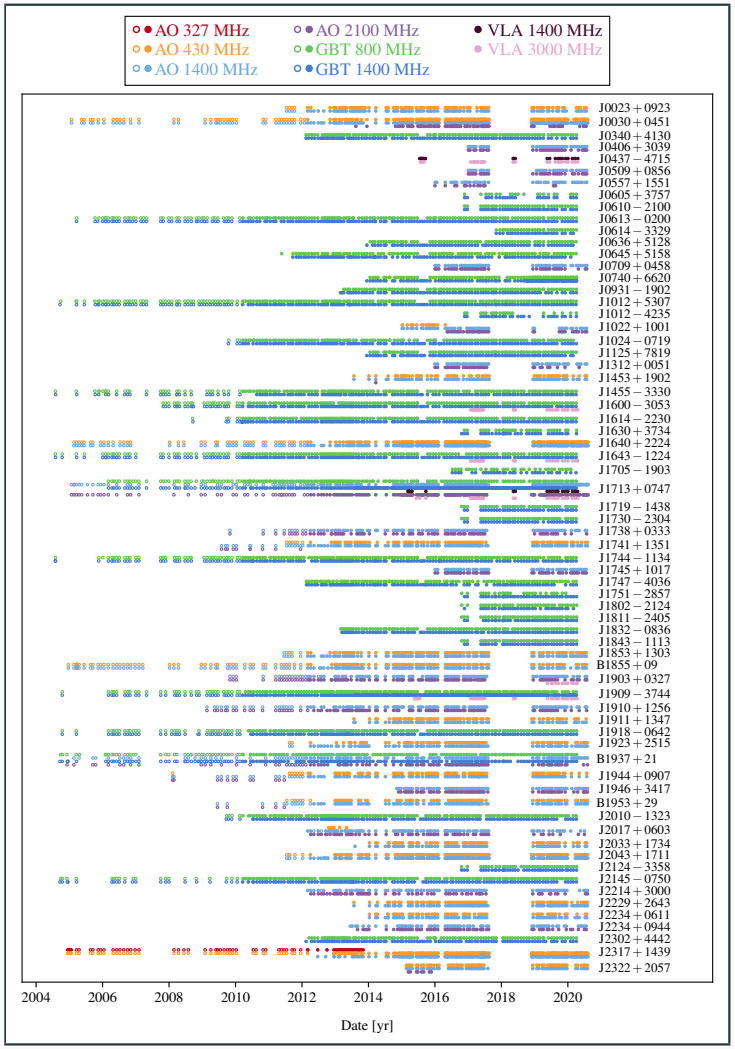

Telescopes

- AO: Arecibo Observatory
- GBT: Green Bank Telescope
- VLA: Very Large Array

Observations

- 68 millisecond pulsars (MSPs)
- 67 MSPs observed for $> 3\,\mathrm{yr}$
- 21 MSPs more than NG12.5
- 3 more years of observations
- Average cadence of one month

NANOGrav 15-year data set

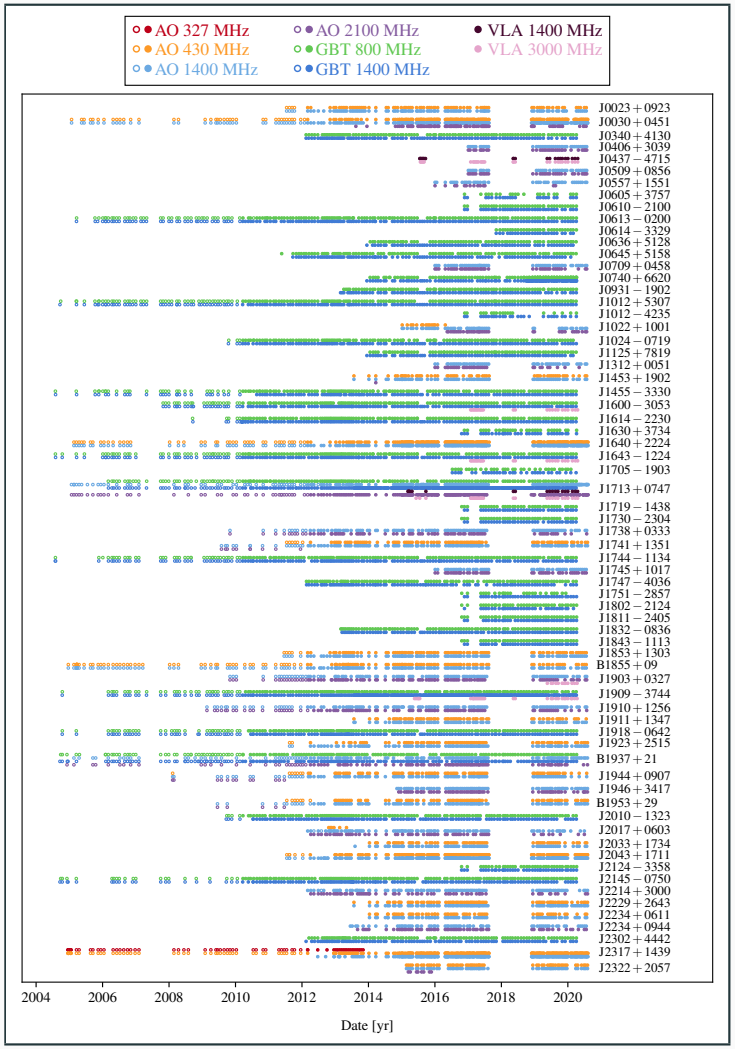

Telescopes

- AO: Arecibo Observatory
- GBT: Green Bank Telescope
- VLA: Very Large Array

Observations

- 68 millisecond pulsars (MSPs)
- 67 MSPs observed for $> 3\,\mathrm{yr}$
- 21 MSPs more than NG12.5
- 3 more years of observations
- Average cadence of one month

Apply Bayesian and frequentist statistical tools to fit the data to different models

Bayesian inference

- Typical problem in collider physics: signal on top of well-defined background
- Different situation for PTAs: only one measurement, noise a priori unknown

Model signal *and* noise by Gaussian processes and perform a global Bayesian fit

---

Bayesian inference

- Typical problem in collider physics: signal on top of well-defined background
- Different situation for PTAs: only one measurement, noise a priori unknown

Model signal *and* noise by Gaussian processes and perform a global Bayesian fit

---

Bayes' theorem for model $\mathcal{M}$ featuring parameters θ after collecting data D

$$P\left(\theta|D;\mathcal{M}\right) = \frac{\mathcal{L}\left(D|\theta;\mathcal{M}\right)\pi\left(\theta|\mathcal{M}\right)}{\mathcal{Z}\left(D|\mathcal{M}\right)}\,, \qquad \mathcal{Z}\left(D|\mathcal{M}\right) = \int d\theta\,\mathcal{L}\left(D|\theta;\mathcal{M}\right)\pi\left(\theta|\mathcal{M}\right)$$

with pior distribution π, likelihood $\mathcal{L}$, evidence $\mathcal{Z}$, and posterior distribution P

Bayesian inference

- Typical problem in collider physics: signal on top of well-defined background
- Different situation for PTAs: only one measurement, noise a priori unknown

Model signal *and* noise by Gaussian processes and perform a global Bayesian fit

---

Bayes' theorem for model $\mathcal{M}$ featuring parameters θ after collecting data D

$$P(\theta|D;\mathcal{M}) = \frac{\mathcal{L}(D|\theta;\mathcal{M})\,\pi(\theta|\mathcal{M})}{\mathcal{Z}(D|\mathcal{M})}, \qquad \mathcal{Z}(D|\mathcal{M}) = \int d\theta\,\mathcal{L}(D|\theta;\mathcal{M})\,\pi(\theta|\mathcal{M})$$

with pior distribution π, likelihood $\mathcal{L}$, evidence $\mathcal{Z}$, and posterior distribution P

Similarly, for a set of different models $\mathcal{M}_i$, where now $\mathcal{Z}(D|\mathcal{M}_i) \to \mathcal{L}(D|\mathcal{M}_i)$

$$P(\mathcal{M}_i|D) = \frac{\mathcal{L}(D|\mathcal{M}_i)\,\pi(\mathcal{M}_i)}{\mathcal{Z}(D)}, \qquad \mathcal{Z}(D) = \sum_i \mathcal{L}(D|\mathcal{M}_i)\,\pi(\mathcal{M}_i)$$

Bayes factor

Bayes factor: likelihood ratio for model $\mathcal{M}_1$ versus model $\mathcal{M}_0$

$$\mathcal{B} = \frac{\mathcal{L}\left(D|\mathcal{M}_1\right)}{\mathcal{L}\left(D|\mathcal{M}_0\right)} = \frac{\pi\left(\mathcal{M}_0\right)}{\pi\left(\mathcal{M}_1\right)} \frac{P\left(\mathcal{M}_1|D\right)}{P\left(\mathcal{M}_0|D\right)} .$$

Bayes factor

Bayes factor: likelihood ratio for model $\mathcal{M}_1$ versus model $\mathcal{M}_0$

$$\mathcal{B} = \frac{\mathcal{L}(D|\mathcal{M}_1)}{\mathcal{L}(D|\mathcal{M}_0)} = \frac{\pi(\mathcal{M}_0)}{\pi(\mathcal{M}_1)} \frac{P(\mathcal{M}_1|D)}{P(\mathcal{M}_0|D)} .$$

$\mathcal{B}$ quantifies levels of support for $\mathcal{M}_1$; Jeffreys scale:

$\mathcal{B} < 1$	disfavored
$\mathcal{B} \in \left[10^{0.0}, 10^{0.5}\right]$	weak
$\mathcal{B} \in \left[10^{0.5}, 10^{1.0}\right]$	substantial
$\mathcal{B} \in \left[10^{1.0}, 10^{1.5}\right]$	strong
$\mathcal{B} \in \left[10^{1.5}, 10^{2.0}\right]$	very strong
$\mathcal{B} > 100$	decisive

Bayesian model selection

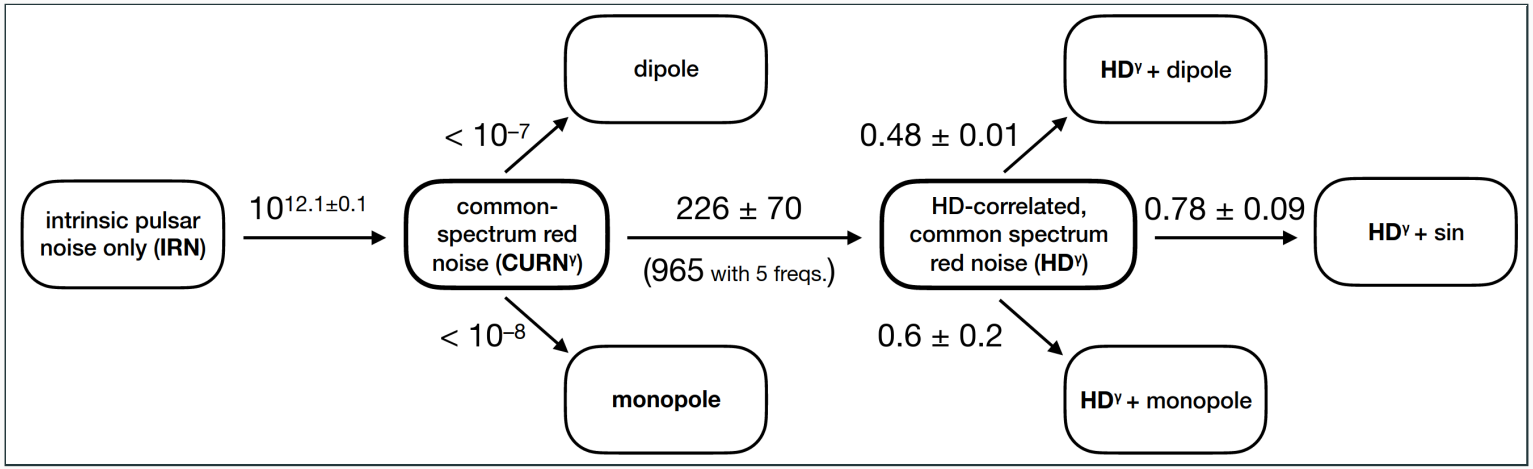

- **IRN:** Intrinsic pulsar noise only
- **CURN:** Common-spectrum spatially-uncorrelated red noise
- **HD:** Hellings–Downs correlations

Bayes factors

$$\frac{\mathcal{L}(D|\mathbf{CURN})}{\mathcal{L}(D|\mathbf{IRN})} = 10^{12.1\pm0.1}, \qquad \frac{\mathcal{L}(D|\mathbf{HD})}{\mathcal{L}(D|\mathbf{CURN})} \sim 200\cdots1000$$

Bayesian model selection

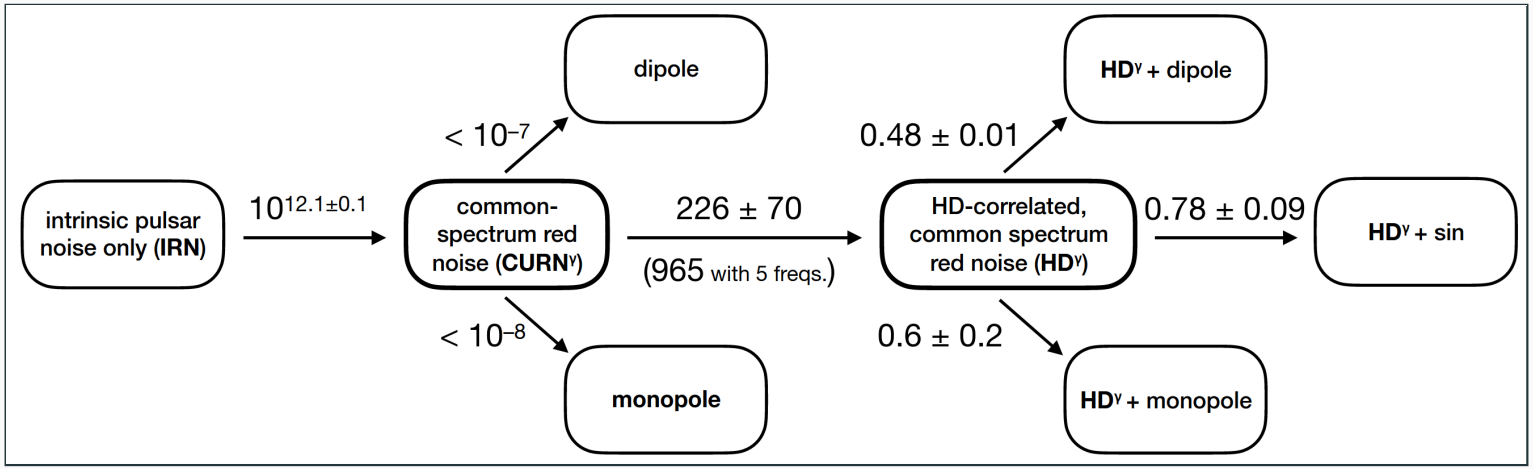

- **IRN:** Intrinsic pulsar noise only
- **CURN:** Common-spectrum spatially-uncorrelated red noise
- **HD:** Hellings–Downs correlations

Bayes factors

$$\frac{\mathcal{L}(D|\mathbf{CURN})}{\mathcal{L}(D|\mathbf{IRN})} = 10^{12.1\pm0.1}, \qquad \frac{\mathcal{L}(D|\mathbf{HD})}{\mathcal{L}(D|\mathbf{CURN})} \sim 200\cdots1000$$

Decisive evidence for a new common-spectrum process; compelling evidence for HD

(Range corresponds to spectral modelling choices, e.g., the number of frequency bins)

Hellings–Downs curve

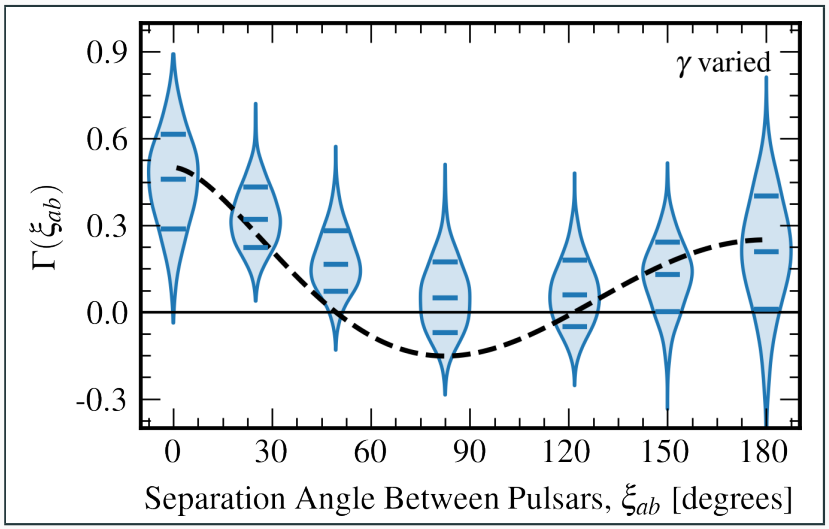

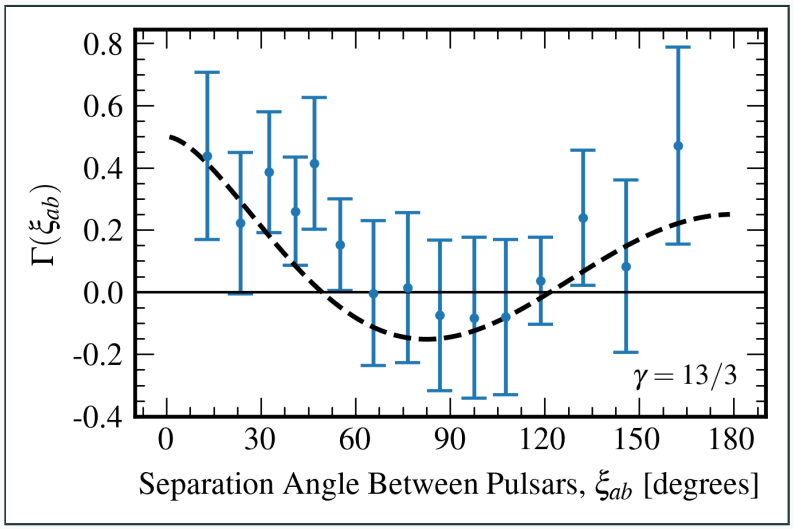

Bayesian analysis

Model correlations with cubic splines across seven nodes

Frequentist analysis

Measure correlations based on “optimal statistic” (matched filter)

Frequentist inference

Our frequentist friends want to know: "How many sigma?"

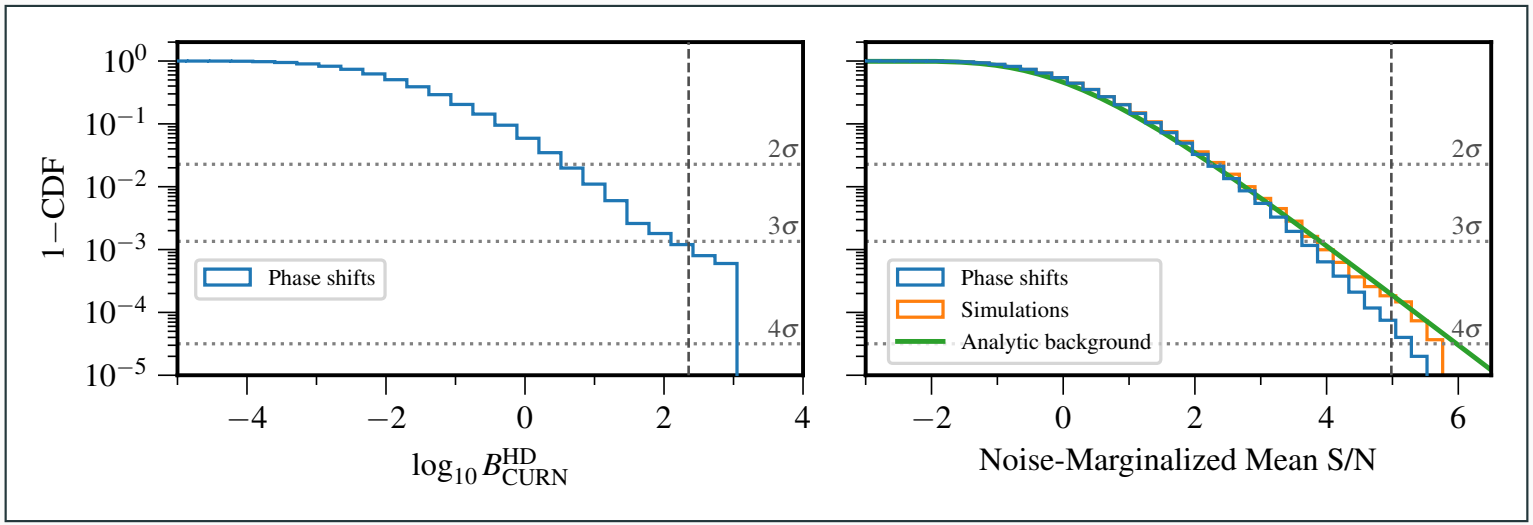

p-value test for two test statistics

- (1) HD-vs.-CURN Bayes factor, (2) signal-to-noise ratio for the optimal statistic
- Construct distributions under the null hypothesis $\mathcal{H}_0 = \{\text{no HD correlations}\}$
- Two techniques: (1) phase shifts, (2) sky scrambles
- Convert *p*-values to *z* scores: null hypothesis $\mathcal{H}_0$ rejected at the $3 \cdots 4\sigma$ level

Evidence for HD correlations *on top* of HUGE evidence for common-spectrum process

II) Astrophysical interpretation: Supermassive black-hole binaries

Astrophysical interpretation

YouTube

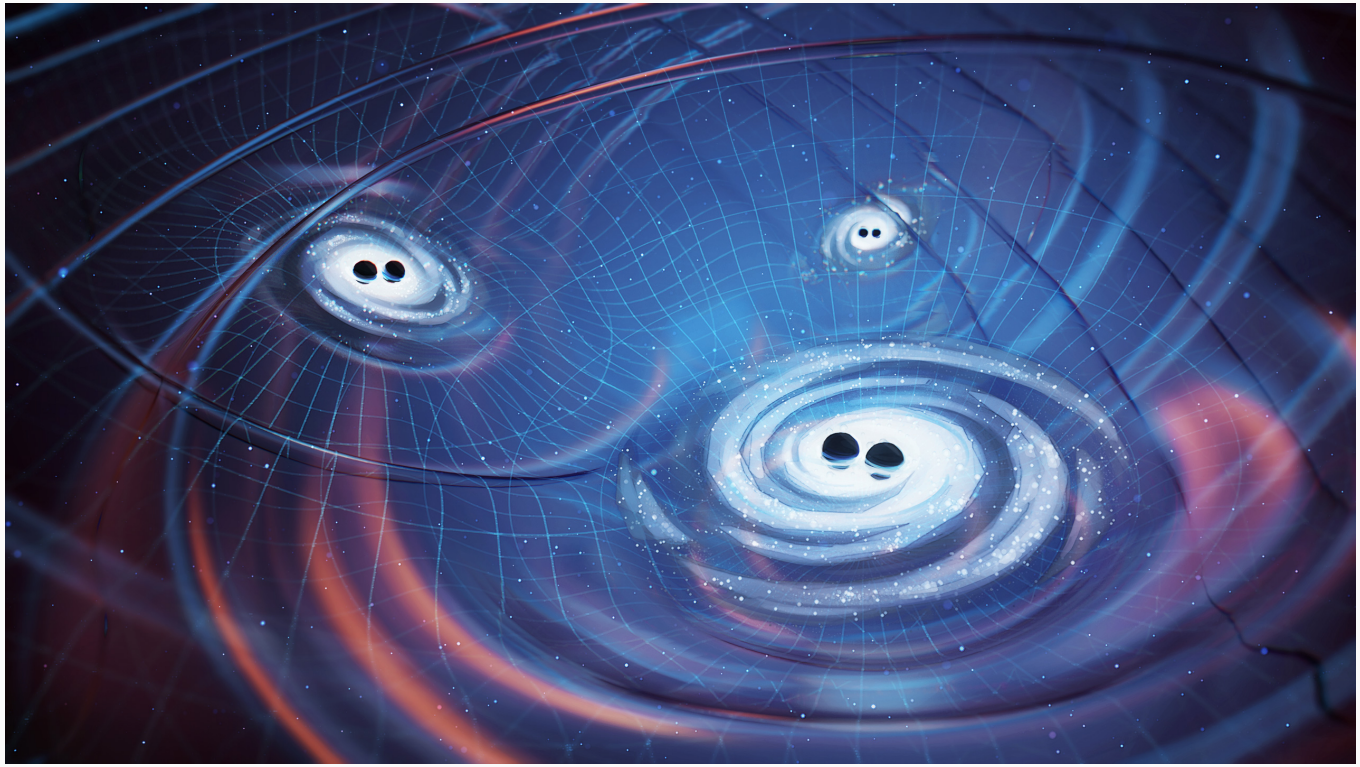

Inspiraling supermassive black-hole binaries (SMBHBs)

- Most galaxies host a SMBHB at their center; binaries form after galaxy mergers
- A few binaries are known; no SMBHB merger has been observed so far
- Hope is that PTA observations will shed more light on SMBHB evolution

Expected signal strength

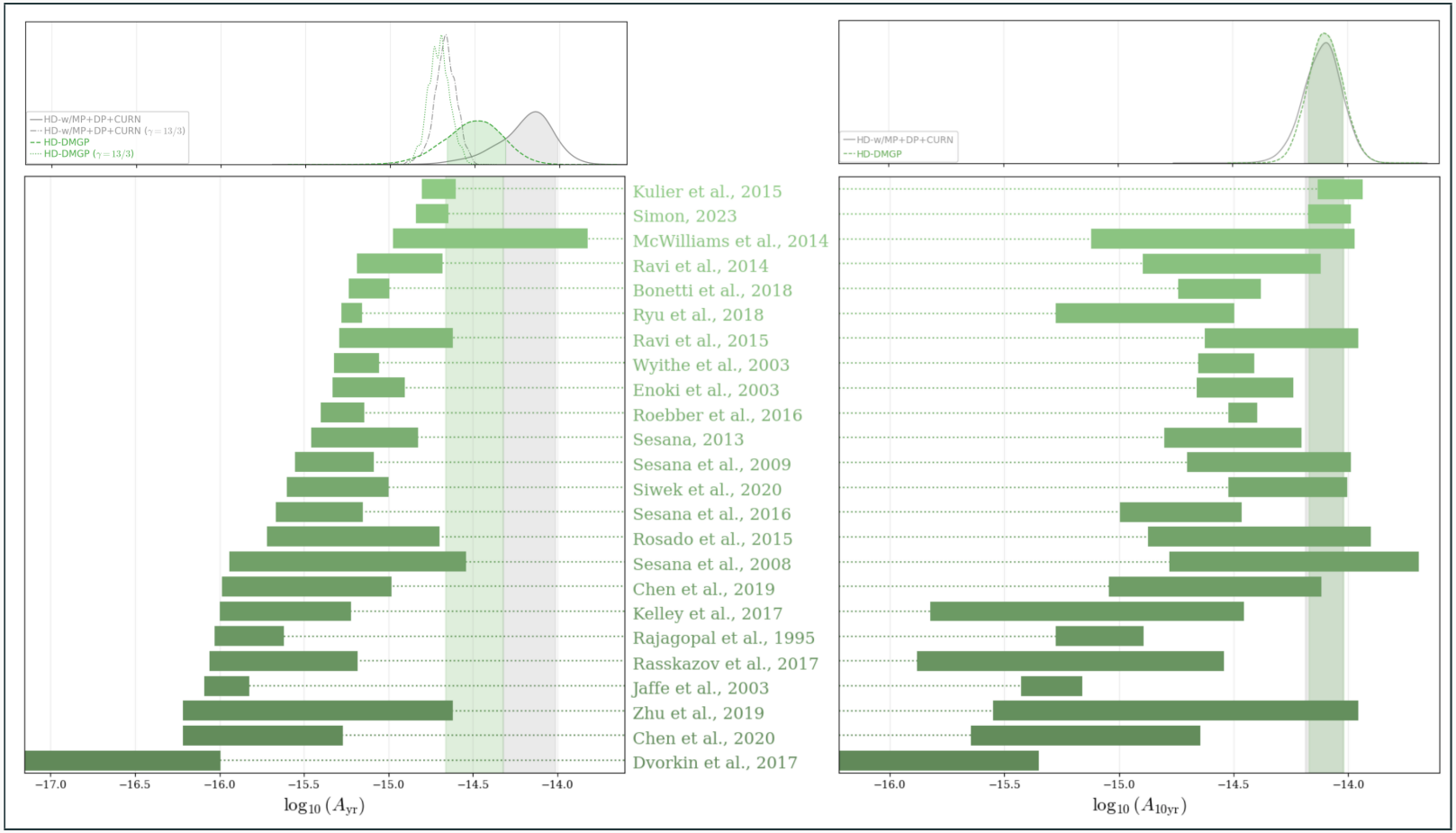

Loud signal! Signal amplitude A turns out to be surprisingly large

GW-driven binary evolution

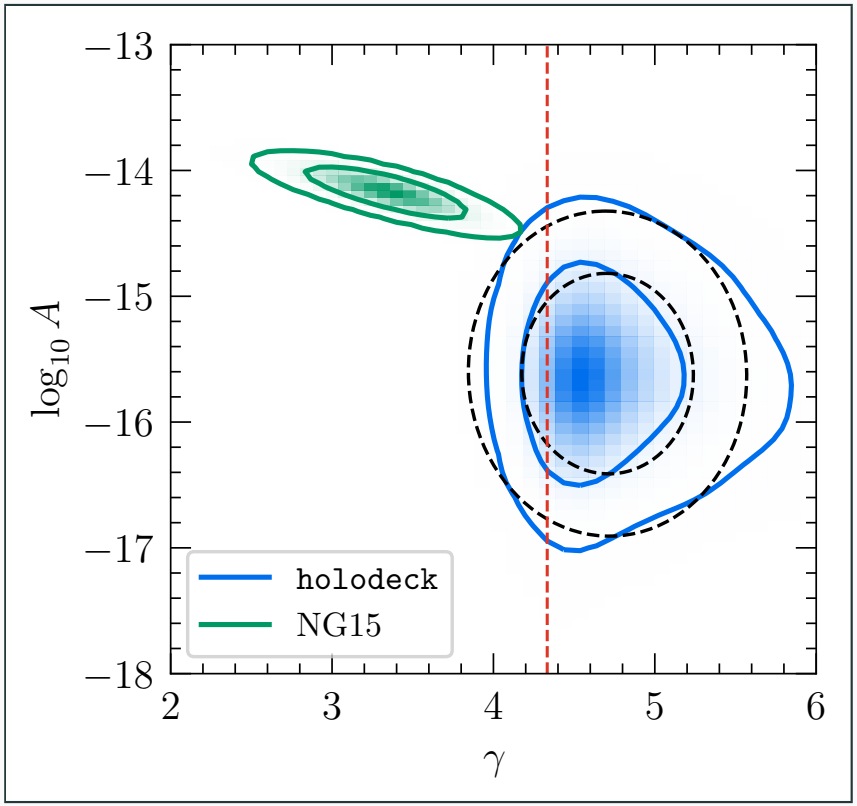

Compare observed spectrum (NG15) to theoretical expectation (`holodeck`)

- Assume SMBHBs on circular orbits and purely GW-driven orbital evolution
- 95 % regions barely touch $\rightarrow 2\sigma$ tension between observations and theory
- GW-only evolution unable to bring binaries to the PTA band within a Hubble time

Phenomenological models

Self-consistent phenomenological models accounting for environmental interactions

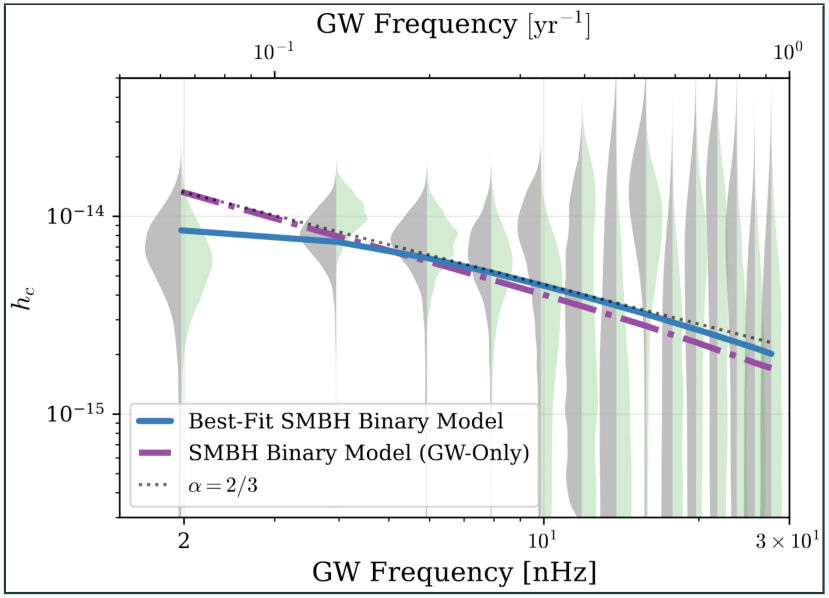

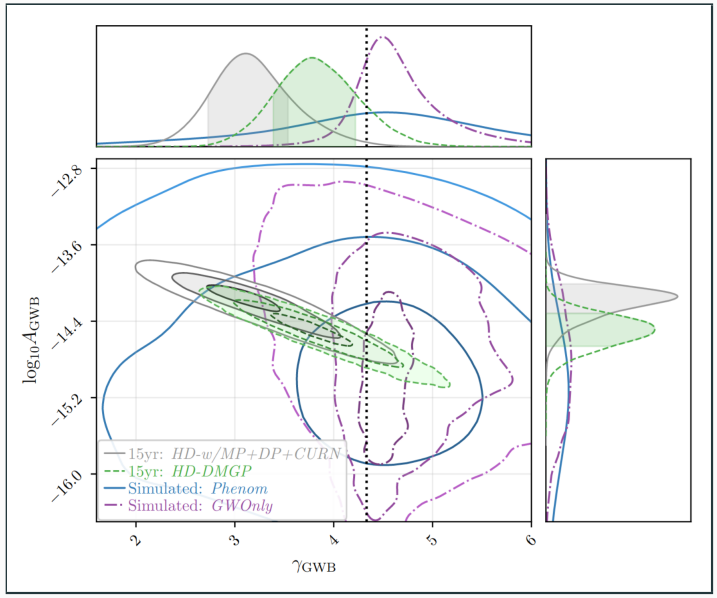

SMBHB interpretation: **Need to go to unexpected corners of parameter space!**

- Parameter shifts towards larger GWB amplitudes than previously expected
- Generally higher binary masses or densities, or highly efficient binary mergers

III) Cosmological interpretations: New physics in the early Universe

Gravitational waves from the Big Bang

[National Astronomical Observatory of Japan, gwpo.nao.ac.jp]

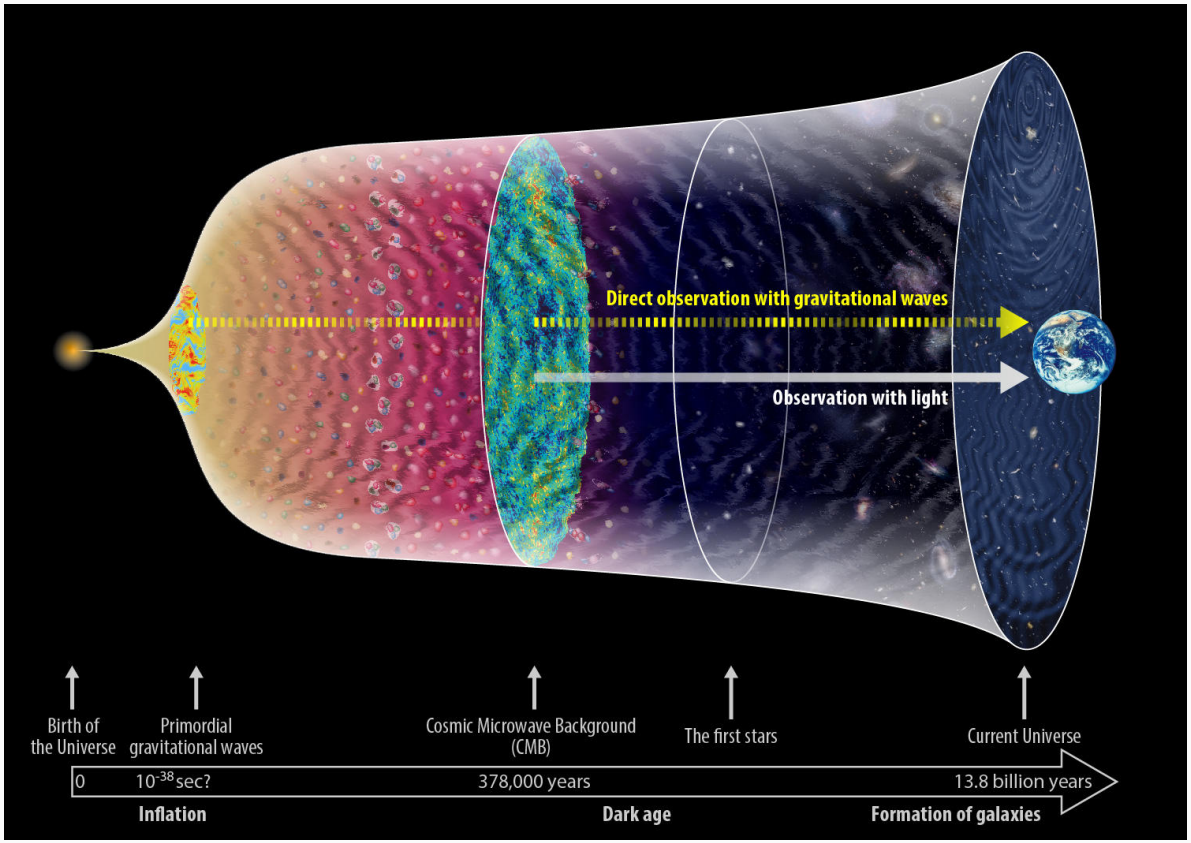

Logical possibility: PTA signal is not of SMBHB origin or receives several contributions

- *Probe* and *constrain* cosmology of the primordial Universe at **very early times**
- *Probe* and *constrain* particle physics at **extremely high energies** → New physics!?

Huge reaction in the literature

Top-cite 2023 papers: PTA papers on ranks #1 to #8

The NANOGrav 15 yr Data Set: Evidence for a Gravitational-wave Background #1

NANOGrav Collaboration • Gabriella Agazie (Marquette U.) et al. (Jun 28, 2023)

Published in: *Astrophys.J.Lett.* 951 (2023) 1, L8 • e-Print: 2306.16213 [astro-ph.HE]

pdf DOI cite claim reference search 236 citations

Searching for the Nano-Hertz Stochastic Gravitational Wave Background with the Chinese Pulsar Timing Array Data Release I #2

Heng Xu (NAOC, Beijing and Beijing, GUCAS), Siyuan Chen (Peking U., Beijing, KIAA and Peking U.), Yanjun Guo (Bonn, Max Planck Inst., Radioastron.), Jinchen Jiang (NAOC, Beijing and Beijing, GUCAS), Bojun Wang (NAOC, Beijing and Beijing, GUCAS) et al. (Jun 28, 2023)

Published in: *Res.Astron.Astrophys.* 23 (2023) 7, 075024 • e-Print: 2306.16216 [astro-ph.HE]

pdf DOI cite claim reference search 191 citations

The second data release from the European Pulsar Timing Array III. Search for gravitational wave signals #3

EPTA Collaboration • J. Antoniadis (Crete U. and IESL, Heraklion and Bonn, Max Planck Inst., Radioastron.) et al. (Jun 28, 2023)

Published in: *Astron.Astrophys.* 678 (2023) A50 • e-Print: 2306.16214 [astro-ph.HE]

pdf DOI cite claim reference search 190 citations

Search for an Isotropic Gravitational-wave Background with the Parkes Pulsar Timing Array #4

Daniel J. Reardon (Swinburne U., Ctr. Astrophys. Supercomput. and Australian Natl. U., Canberra (main)), Andrew Zic (Australia, CSIRO, Epping and Macquarie U.), Ryan M. Shannon (Swinburne U., Ctr. Astrophys. Supercomput. and Australian Natl. U., Canberra (main)), George B. Hobbs (Australia, CSIRO, Epping), Matthew Bailes (Swinburne U., Ctr. Astrophys. Supercomput. and Australian Natl. U., Canberra (main)) et al. (Jun 28, 2023)

Published in: *Astrophys.J.Lett.* 951 (2023) 1, L6 • e-Print: 2306.16215 [astro-ph.HE]

pdf DOI cite claim reference search 190 citations

The NANOGrav 15 yr Data Set: Search for Signals from New Physics #5

NANOGrav Collaboration • Adeela Afzal (Munster U. and Quaid-i-Azam U.) et al. (Jun 28, 2023)

Published in: *Astrophys.J.Lett.* 951 (2023) 1, L11 • e-Print: 2306.16219 [astro-ph.HE]

pdf DOI cite claim reference search 178 citations

The second data release from the European Pulsar Timing Array: V. Implications for massive black holes, dark matter and the early Universe #6

EPTA Collaboration • J. Antoniadis (Crete U. and IESL, Heraklion and Bonn, Max Planck Inst., Radioastron.) et al. (Jun 28, 2023)

e-Print: 2306.16227 [astro-ph.CO]

pdf cite claim reference search 102 citations

Huge reaction in the literature

Top-cite 2023 papers: PTA papers on ranks #1 to #8

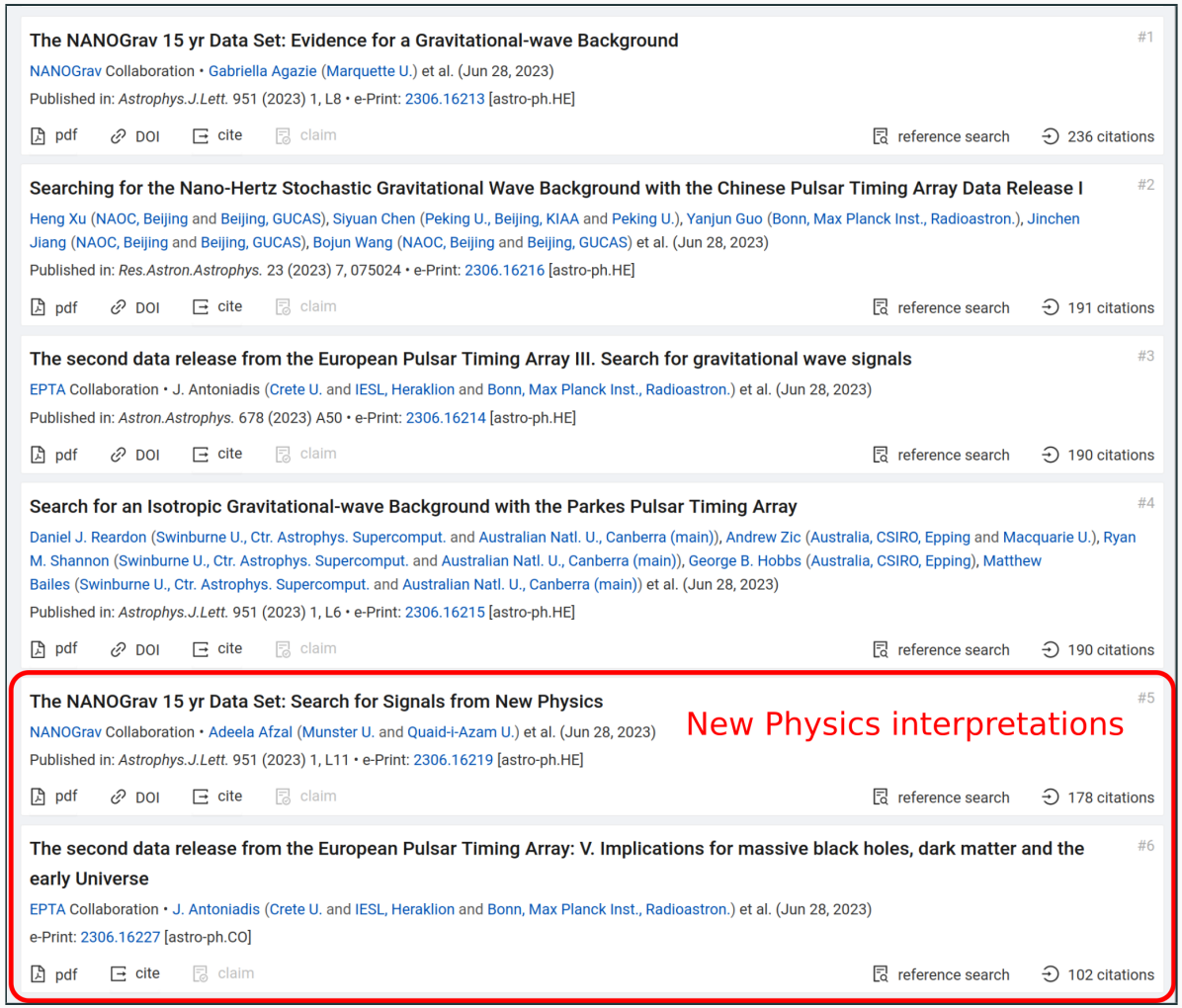

The NANOGrav 15 yr Data Set: Evidence for a Gravitational-wave Background #1

NANOGrav Collaboration • Gabriella Agazie (Marquette U.) et al. (Jun 28, 2023)

Published in: *Astrophys.J.Lett.* 951 (2023) 1, L8 • e-Print: 2306.16213 [astro-ph.HE]

pdf DOI cite claim reference search 236 citations

Searching for the Nano-Hertz Stochastic Gravitational Wave Background with the Chinese Pulsar Timing Array Data Release I #2

Heng Xu (NAOC, Beijing and Beijing, GUCAS), Siyuan Chen (Peking U., Beijing, KIAA and Peking U.), Yanjun Guo (Bonn, Max Planck Inst., Radioastron.), Jinchen Jiang (NAOC, Beijing and Beijing, GUCAS), Bojun Wang (NAOC, Beijing and Beijing, GUCAS) et al. (Jun 28, 2023)

Published in: *Res.Astron.Astrophys.* 23 (2023) 7, 075024 • e-Print: 2306.16216 [astro-ph.HE]

pdf DOI cite claim reference search 191 citations

The second data release from the European Pulsar Timing Array III. Search for gravitational wave signals #3

EPTA Collaboration • J. Antoniadis (Crete U. and IESL, Heraklion and Bonn, Max Planck Inst., Radioastron.) et al. (Jun 28, 2023)

Published in: *Astron.Astrophys.* 678 (2023) A50 • e-Print: 2306.16214 [astro-ph.HE]

pdf DOI cite claim reference search 190 citations

Search for an Isotropic Gravitational-wave Background with the Parkes Pulsar Timing Array #4

Daniel J. Reardon (Swinburne U., Ctr. Astrophys. Supercomput. and Australian Natl. U., Canberra (main)), Andrew Zic (Australia, CSIRO, Epping and Macquarie U.), Ryan M. Shannon (Swinburne U., Ctr. Astrophys. Supercomput. and Australian Natl. U., Canberra (main)), George B. Hobbs (Australia, CSIRO, Epping), Matthew Bailes (Swinburne U., Ctr. Astrophys. Supercomput. and Australian Natl. U., Canberra (main)) et al. (Jun 28, 2023)

Published in: *Astrophys.J.Lett.* 951 (2023) 1, L6 • e-Print: 2306.16215 [astro-ph.HE]

pdf DOI cite claim reference search 190 citations

The NANOGrav 15 yr Data Set: Search for Signals from New Physics #5

NANOGrav Collaboration • Adeela Afzal (Munster U. and Quaid-i-Azam U.) et al. (Jun 28, 2023)

Published in: *Astrophys.J.Lett.* 951 (2023) 1, L11 • e-Print: 2306.16219 [astro-ph.HE]

New Physics interpretations

pdf DOI cite claim reference search 178 citations

The second data release from the European Pulsar Timing Array: V. Implications for massive black holes, dark matter and the early Universe #6

EPTA Collaboration • J. Antoniadis (Crete U. and IESL, Heraklion and Bonn, Max Planck Inst., Radioastron.) et al. (Jun 28, 2023)

e-Print: 2306.16227 [astro-ph.CO]

pdf cite claim reference search 102 citations

Physics beyond the Standard Model (BSM)

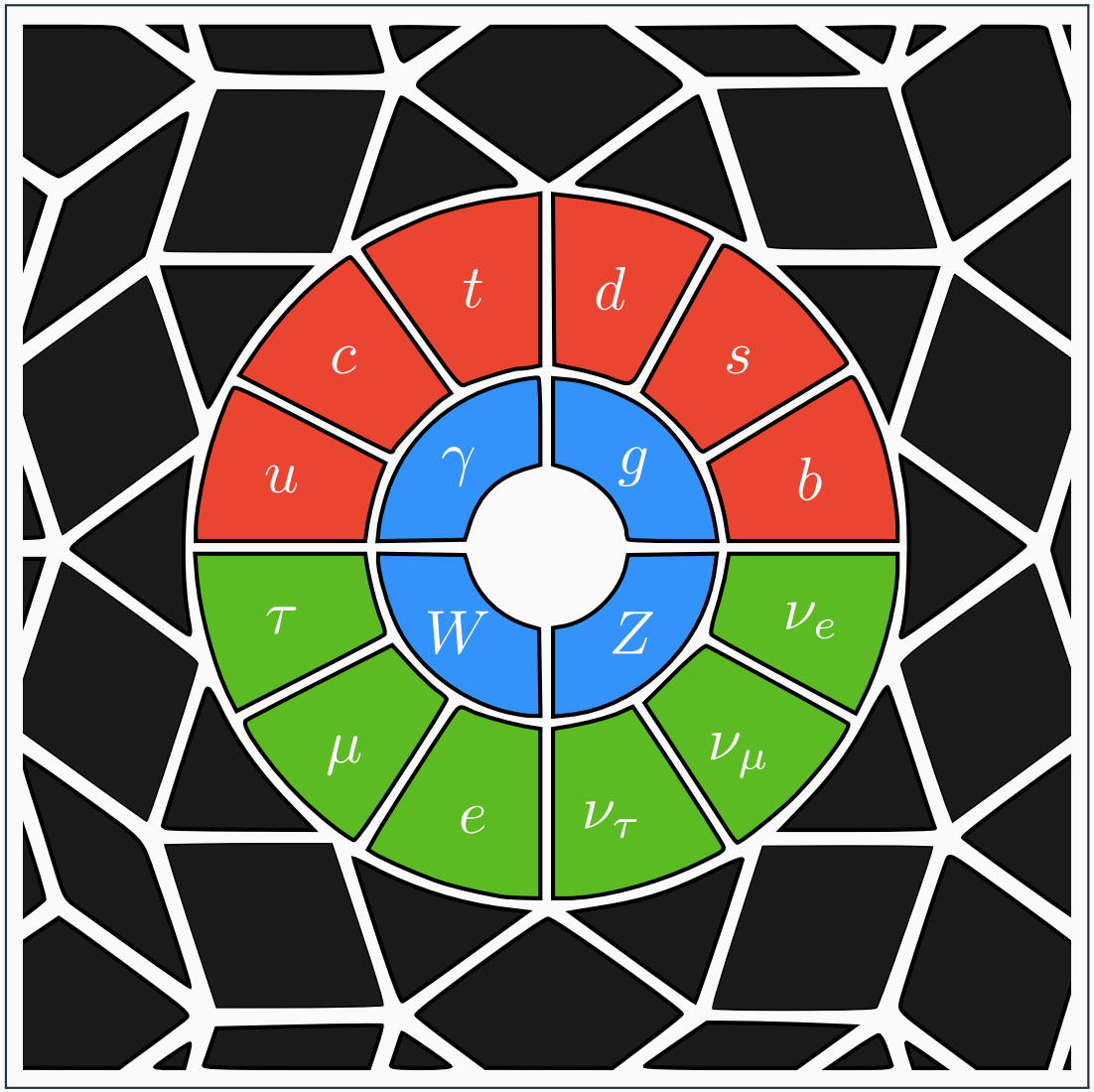

[Adapted from the movie *Particle Fever*]

20th-century particle physics:

Success story of the Standard Model (SM)

Physics beyond the Standard Model (BSM)

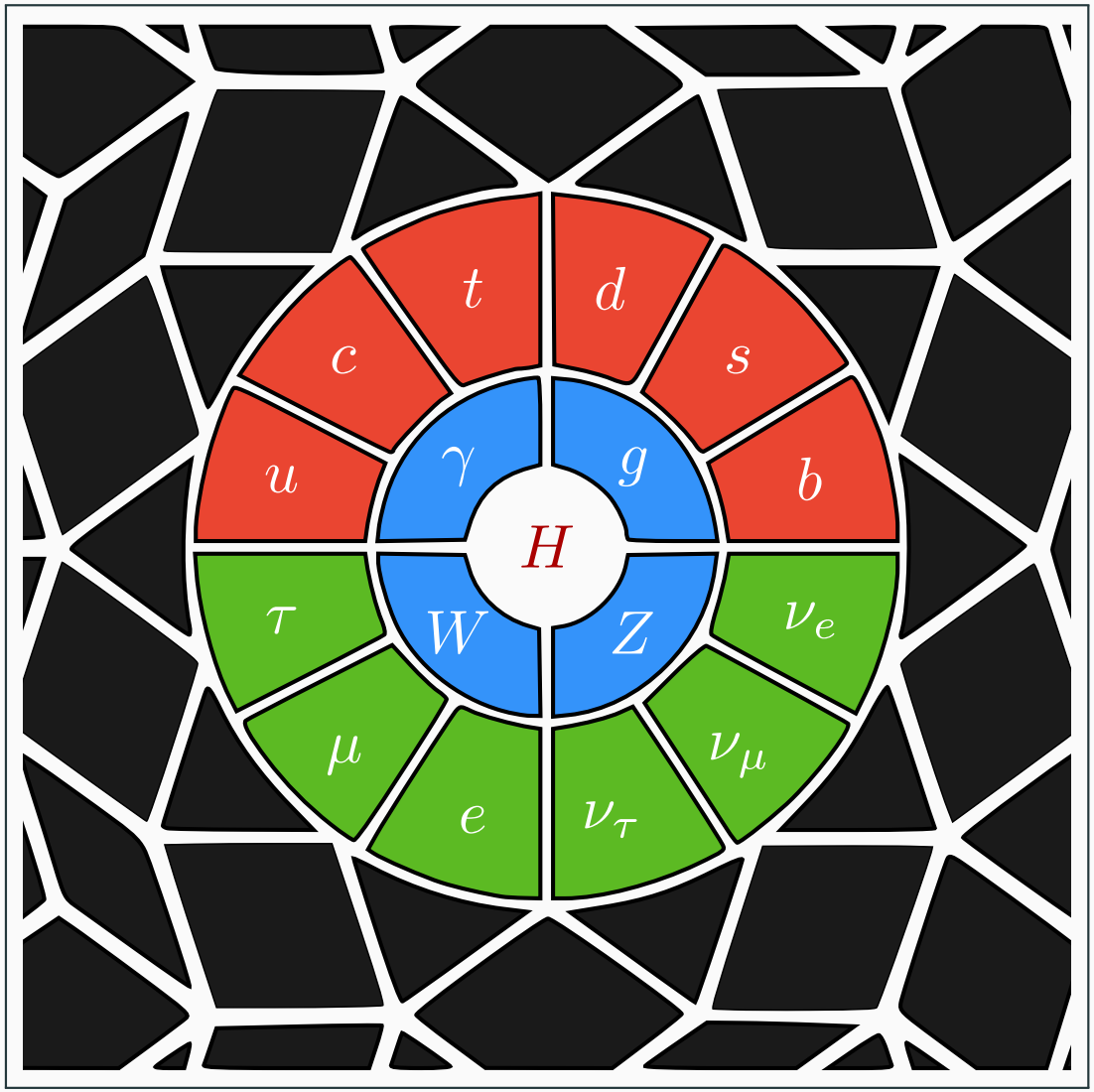

[Adapted from the movie *Particle Fever*]

20th-century particle physics:

Success story of the Standard Model (SM)

Physics beyond the Standard Model (BSM)

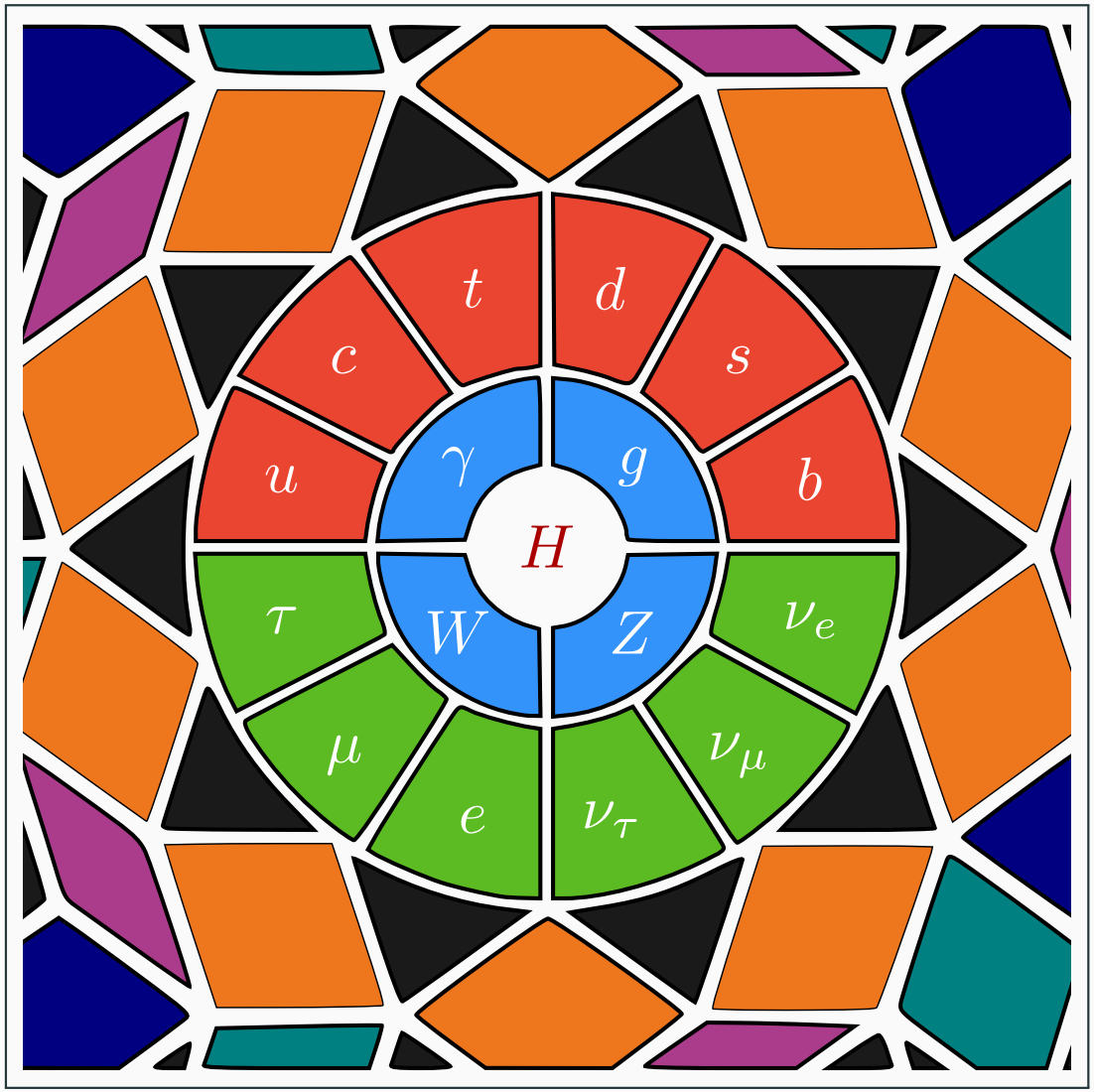

[Adapted from the movie *Particle Fever*]

20th-century particle physics:

Success story of the Standard Model (SM)

21st-century particle physics:

New era beyond the Standard Model (BSM)

Uncharted territory

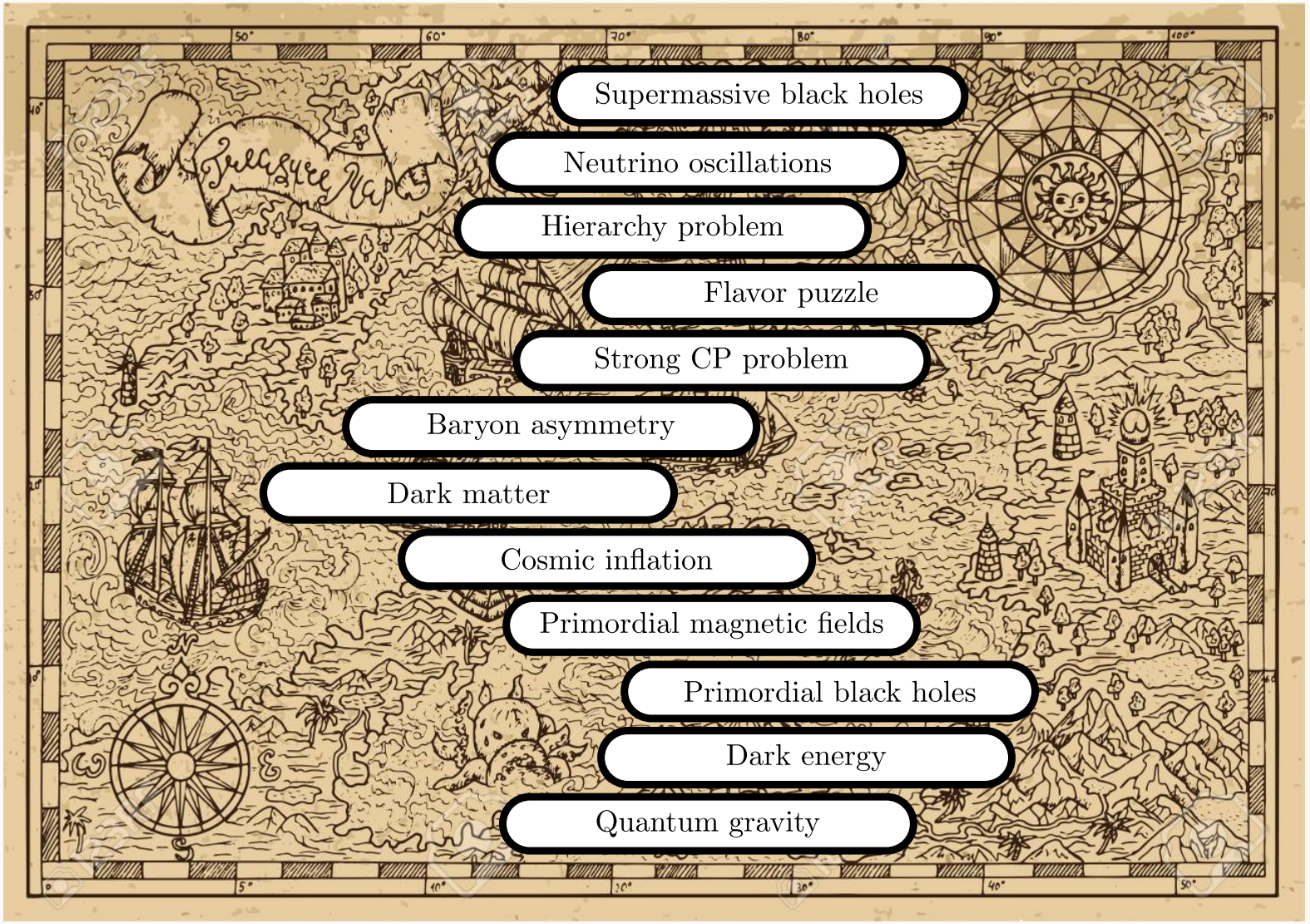

PTA frontier of particle physics

Energy frontier

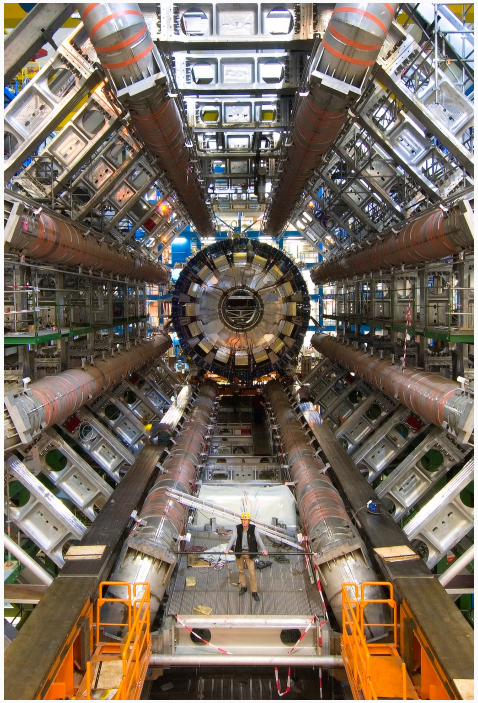

Intensity frontier

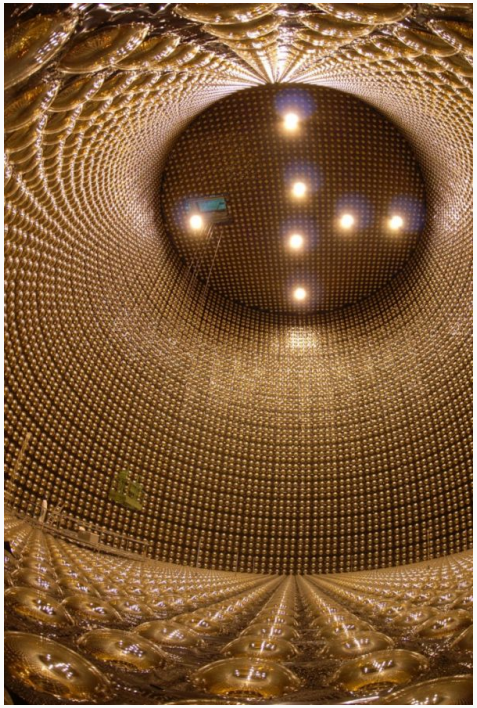

PTA frontier

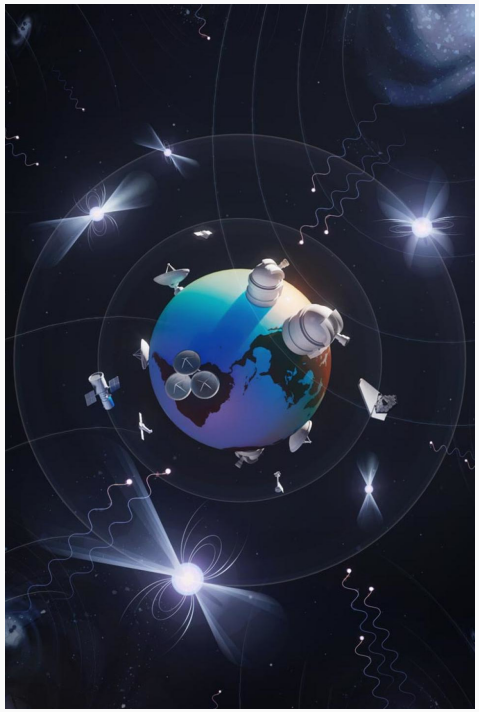

New physics at the PTA frontier

- Probe BSM models in regions of parameter space inaccessible by other methods
- Derive new constraints, irrespective of the origin of the PTA signal
- Complementary to laboratory searches at the energy and intensity frontiers

NANOGrav team

R. v. Eckardstein*

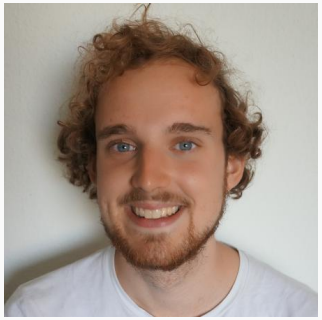

R. Lino d. Santos*

Andrea Mitridate

Jonathan Nay

Ken Olum

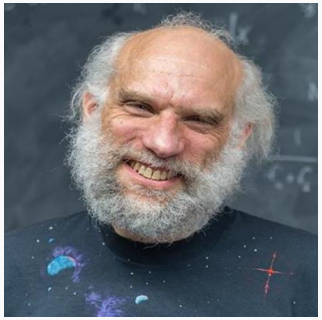

Kai Schmitz*

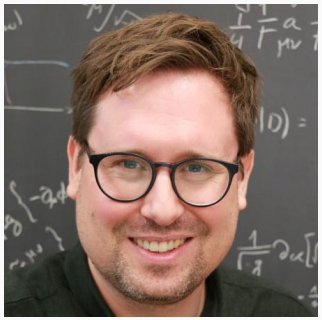

Tobias Schröder*

Tanner Trickle

David Wright

---

1. Searches for signals from new physics in NANOGrav data → 2306.16219
2. New software tools for fitting BSM models to PTA data → `PTArcade`

* Current or former members of my research group, *Particle Cosmology Münster*

2306.16219: Our contribution to the analysis of the NG15 data

arXiv > astro-ph > arXiv:2306.16219

Search... Help | Advanced

Astrophysics > High Energy Astrophysical Phenomena

[Submitted on 28 Jun 2023]

The NANOGrav 15-year Data Set: Search for Signals from New Physics

Adeela Afzal, Gabriella Agazie, Akash Anumarlapudi, Anne M. Archibald, Zaven Arzoumanian, Paul T. Baker, Bence Bécsy, Jose Juan Blanco-Pillado, Laura Blecha, Kimberly K. Boddy, Adam Brazier, Paul R. Brook, Sarah Burke-Spolaor, Rand Burnette, Robin Case, Maria Charisi, Shami Chatterjee, Katerina Chatziioannou, Belinda D. Cheeseboro, Siyuan Chen, Tyler Cohen, James M. Cordes, Neil J. Cornish, Fronefield Crawford, H. Thankful Cromartie, Kathryn Crowter, Curt J. Cutler, Megan E. DeCesar, Dallas DeGan, Paul B. Demorest, Heling Deng, Timothy Dolch, Brendan Drachler, Richard von Eckardstein, Elizabeth C. Ferrara, William Fiore, Emmanuel Fonseca, Gabriel E. Freedman, Nate Garver-Daniels, Peter A. Gentile, Kyle A. Gersbach, Joseph Glaser, Deborah C. Good, Lydia Guertin, Kayhan Gültekin, Jeffrey S. Hazboun, Sophie Hourihane, Kristina Islo, Ross J. Jennings, Aaron D. Johnson, Megan L. Jones, Andrew R. Kaiser, David L. Kaplan, Luke Zoltan Kelley, Matthew Kerr, Joey S. Key, Nima Laal, Michael T. Lam, William G. Lamb, T. Joseph W. Lazio, Vincent S. H. Lee, Natalia Lewandowska, Rafael R. Lino dos Santos, Tyson B. Littenberg, Tingting Liu, Duncan R. Lorimer, Jing Luo, Ryan S. Lynch, Chung-Pei Ma, Dustin R. Madison, Alexander McEwen, James W. McKee, Maura A. McLaughlin, Natasha McMann, Bradley W. Meyers, Patrick M. Meyers, Chiara M. F. Mingarelli, Andrea Mitridate, Jonathan Nay, Priyamvada Natarajan, Cherry Ng, David J. Nice, Stella Koch Ocker, Ken D. Olum, Timothy T. Pennucci, Benetge B. P. Perera, Polina Petrov, Nihan S. Pol, Henri A. Radovan, Scott M. Ransom, Paul S. Ray, Joseph D. Romano, Shashwat C. Sardesai, Ann Schmiedekamp, Carl Schmiedekamp, Kai Schmitz, Tobias Schröder, Levi Schult, Brent J. Shapiro-Albert, Xavier Siemens et al. (23 additional authors not shown)

The 15-year pulsar timing data set collected by the North American Nanohertz Observatory for Gravitational Waves (NANOGrav) shows positive evidence for the presence of a low-frequency gravitational-wave (GW) background. In this paper, we investigate potential cosmological interpretations of this signal, specifically cosmic inflation, scalar-induced GWs, first-order phase transitions, cosmic strings, and domain walls. We find that, with the exception of stable cosmic strings of field theory origin, all these models can reproduce the observed signal. When compared to the standard interpretation in terms of inspiraling supermassive black hole binaries (SMBHBs), many cosmological models seem to provide a better fit resulting in Bayes factors in the range from 10 to 100. However, these results strongly depend on modeling assumptions about the cosmic SMBHB population and, at this stage, should not be regarded as evidence for new physics. Furthermore, we identify excluded parameter regions where the predicted GW signal from cosmological sources significantly exceeds the NANOGrav signal. These parameter constraints are independent of the origin of the NANOGrav signal and illustrate how pulsar timing data provide a new way to constrain the parameter space of these models. Finally, we search for deterministic signals produced by models of ultralight dark matter (ULDM) and dark matter substructures in the Milky Way. We find no evidence for either of these signals and thus report updated constraints on these models. In the case of ULDM, these constraints outperform torsion balance and atomic clock constraints for ULDM coupled to electrons, muons, or gluons.

Comments: 74 pages, 31 figures, 4 tables; published in Astrophysical Journal Letters as part of Focus on NANOGrav's 15-year Data Set and the Gravitational Wave Background. For questions or comments, please email comments@nanograv.org

Subjects: **High Energy Astrophysical Phenomena (astro-ph.HE)**; Cosmology and Nongalactic Astrophysics (astro-ph.CO); General Relativity and Quantum Cosmology (gr-qc); High Energy Physics - Phenomenology (hep-ph)

Cite as: arXiv:2306.16219 **[astro-ph.HE]**
(or arXiv:2306.16219v1 **[astro-ph.HE]** for this version)
https://doi.org/10.48550/arXiv.2306.16219

Related DOI: https://doi.org/10.3847/2041-8213/acdc91

Submission history

From: Andrea Mitridate [view email]
[v1] Wed, 28 Jun 2023 13:51:07 UTC (27,492 KB)

Project leads: Andrea Mitridate, Kai Schmitz*

Richard von Eckardstein*	Cosmological phase transitions
Rafael Robson Lino dos Santos*	Inflation, scalar-induced gravitational waves
Jonathan Nay	Ultralight dark matter
Ken Olum	Cosmic strings, statistical tools
Tobias Schröder*	Cosmic strings
Tanner Trickle	Ultralight dark matter, dark-matter substructure
David Wright	Inflation, scalar-induced gravitational waves

PTArcade

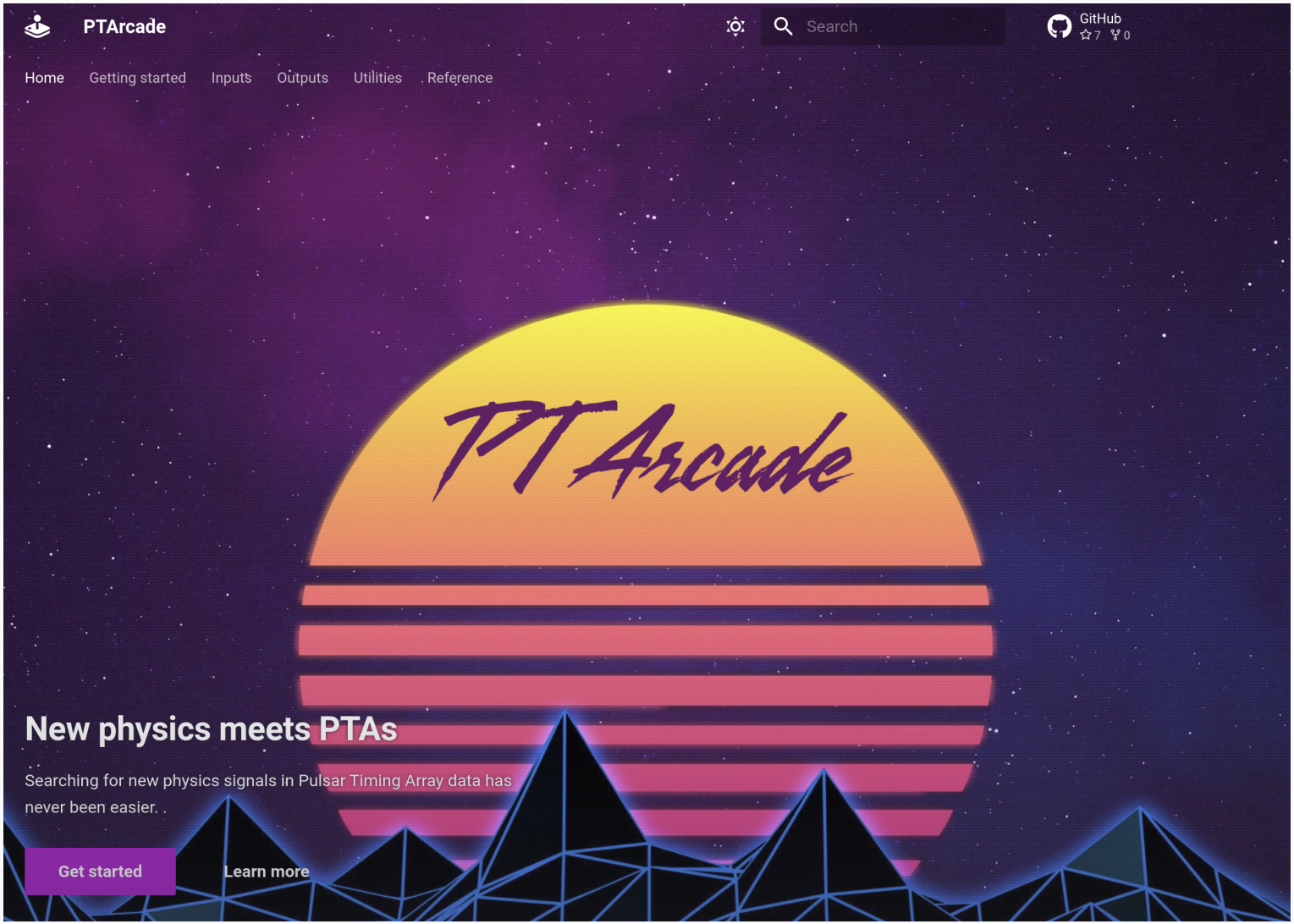

Our code developed for 2306.16219: Fit your favorite BSM model to the NG15 data!

Bayes factors

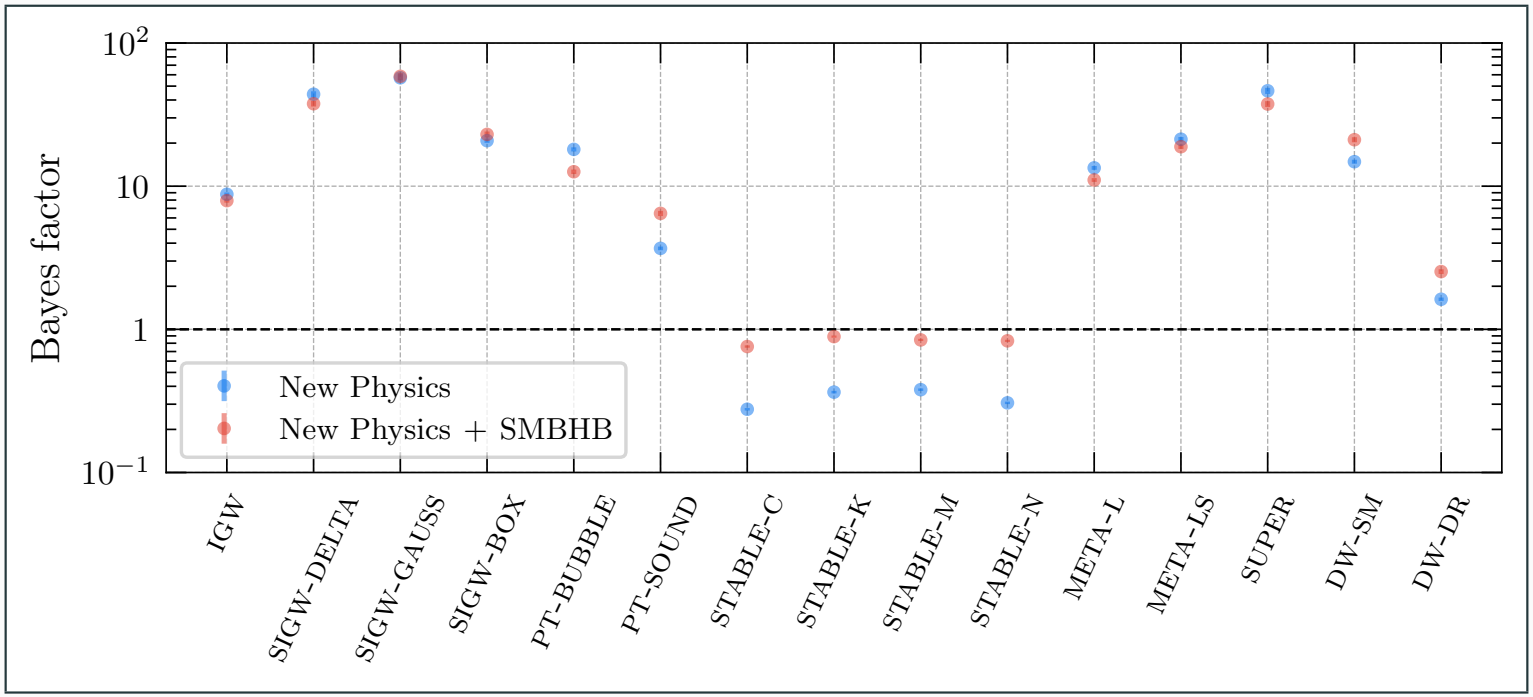

Bayesian model comparison

Reference model: $\mathcal{H}_0 = \{\text{SMBHBs only}\}$

- Many BSM models reach Bayes of order $10 \cdots 100$
- Interesting but not conclusive. Lots of uncertainties in SMBHB and BSM models
- Bayes factors are sensitive to prior choices. No unique null distribution for $\mathcal{H}_0$

Bayes factors

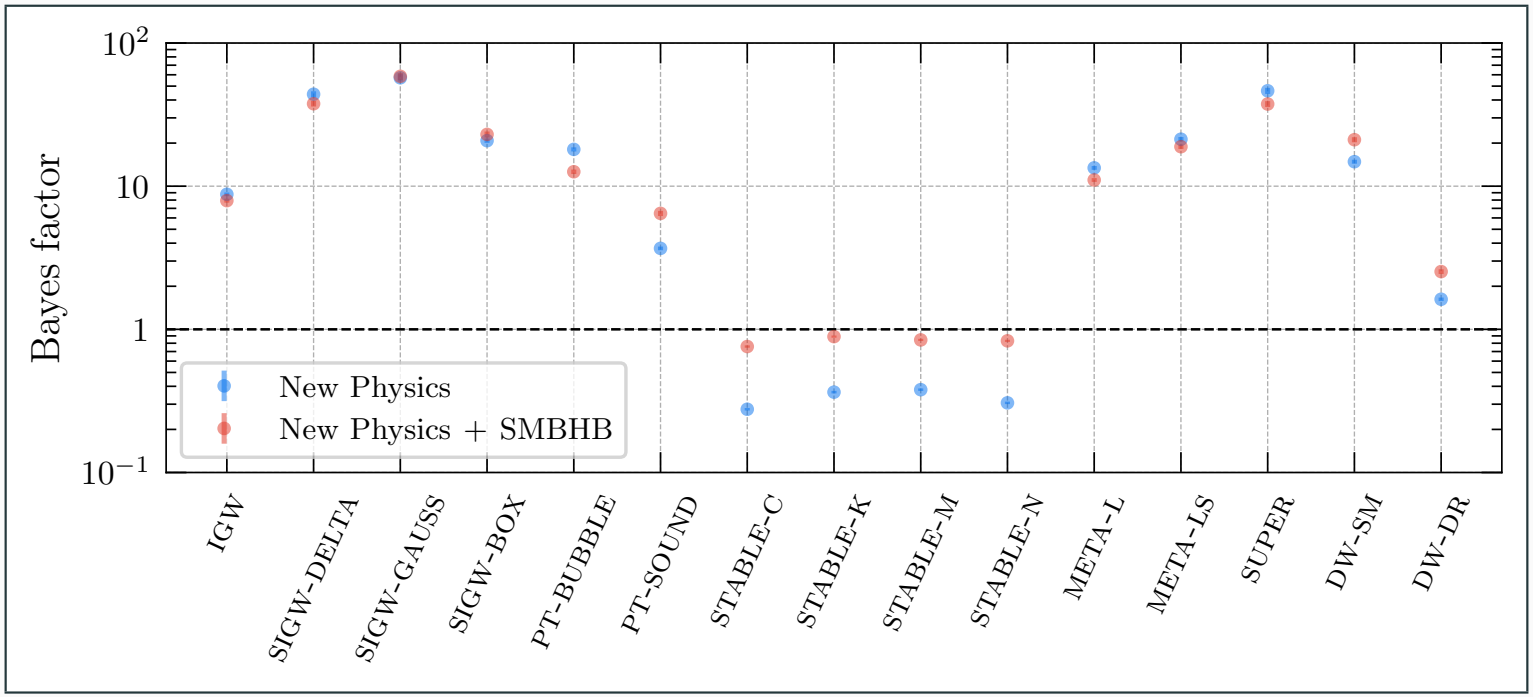

Bayesian model comparison Reference model: $\mathcal{H}_0 = \{\text{SMBHBs only}\}$

- Many BSM models reach Bayes of order $10 \cdots 100$
- Interesting but not conclusive. Lots of uncertainties in SMBHB and BSM models
- Bayes factors are sensitive to prior choices. No unique null distribution for $\mathcal{H}_0$

Bottom line: Stable strings don't look good; all other BSM models can fit the data

Median GW spectra

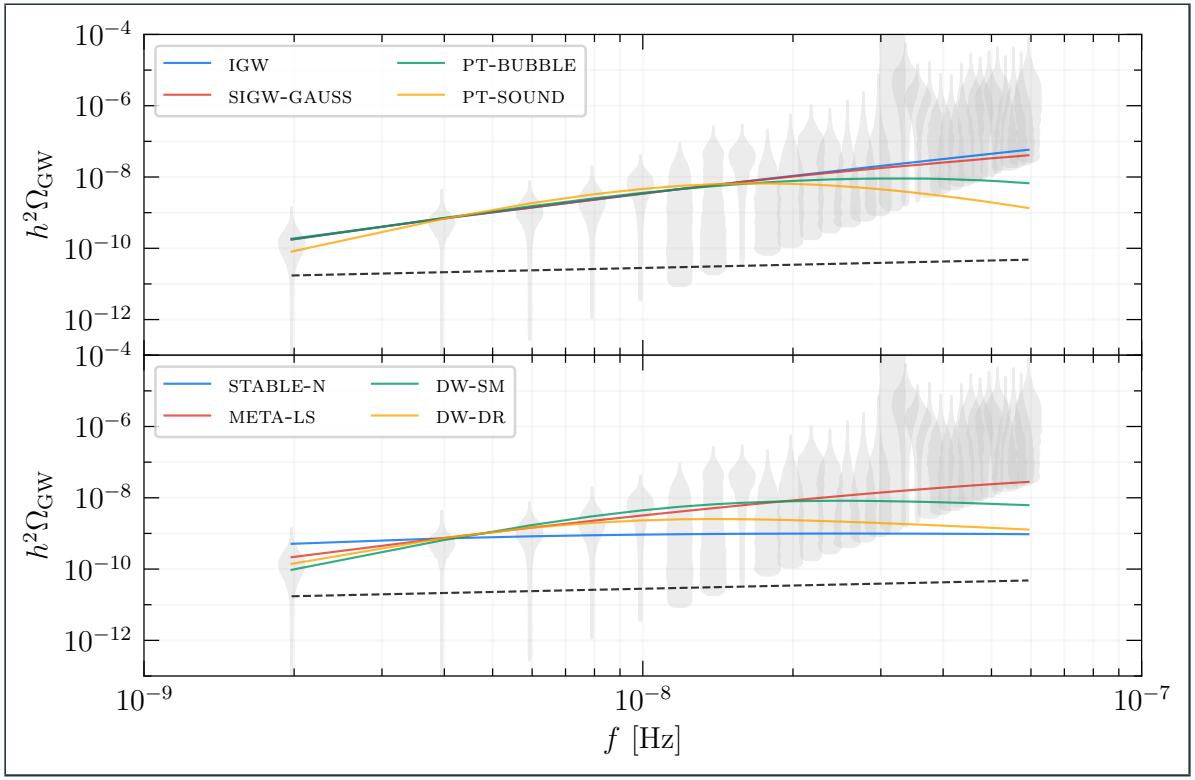

Solid lines: Median GW spectra for BSM models based on parameter posteriors

Dashed line: SMBHB prediction based on central values of our 2D parameter prior

Median GW spectra

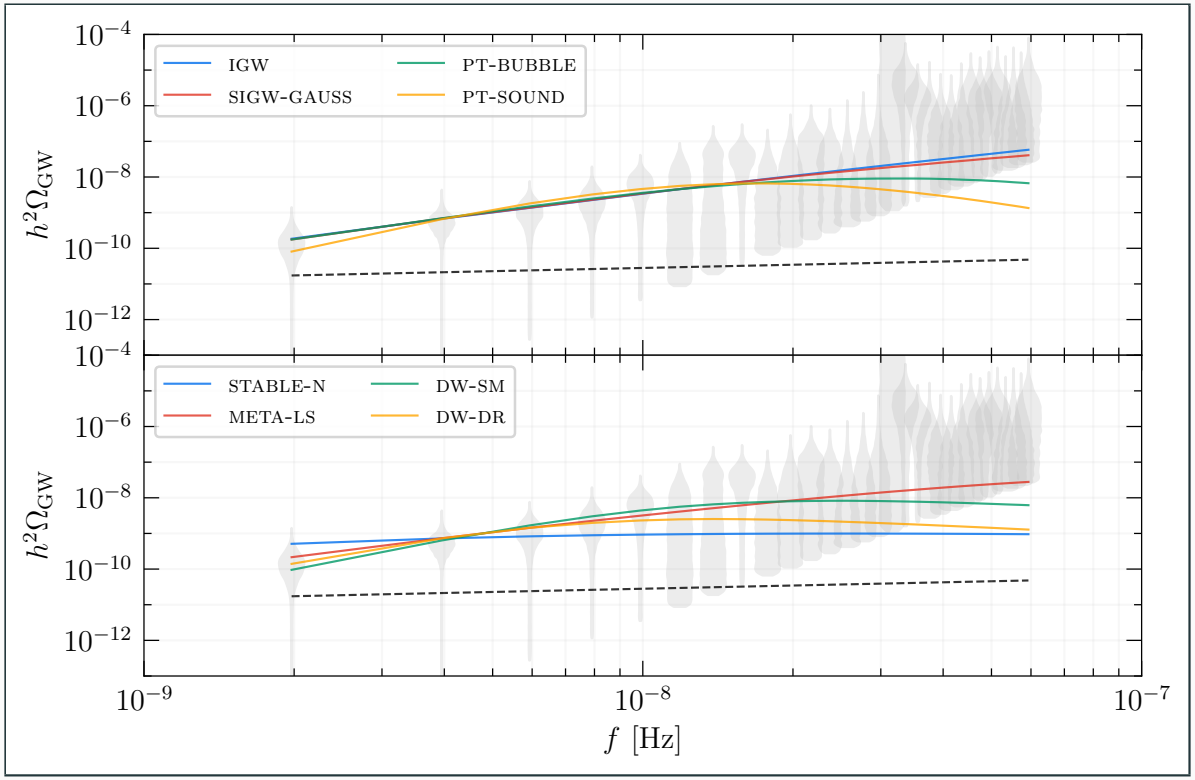

Solid lines: Median GW spectra for BSM models based on parameter posteriors
Dashed line: SMBHB prediction based on central values of our 2D parameter prior

---

Of course, GW spectra resulting in a good fit all look similar by construction.
→ Relevant question: Which parameter values predict GW spectrum of the right form?

❶ BSM scenario: Cosmic inflation

Big questions: What set the initial conditions of the Hot Big Bang: homogeneity, isotropy, spatial flatness? What seeded the temperature fluctuations in the CMB?

❶ BSM scenario: Cosmic inflation

Big questions: What set the initial conditions of the Hot Big Bang: homogeneity, isotropy, spatial flatness? What seeded the temperature fluctuations in the CMB?

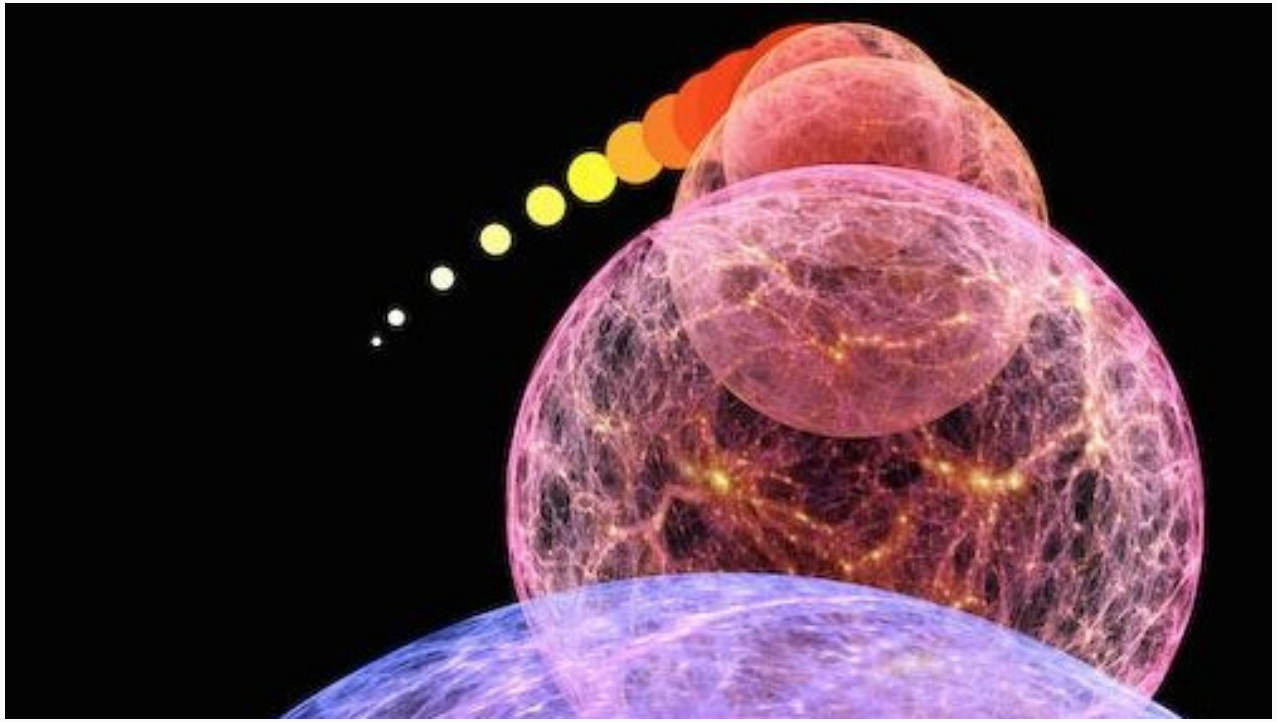

Cosmic inflation: Stage of exponentially fast expansion before the Hot Big Bang

- Requires form of dark energy, e.g., potential energy of a scalar "inflaton" field
- Inflaton and metric fluctuations $\rightarrow$ primordial scalar and tensor perturbations

Background dynamics

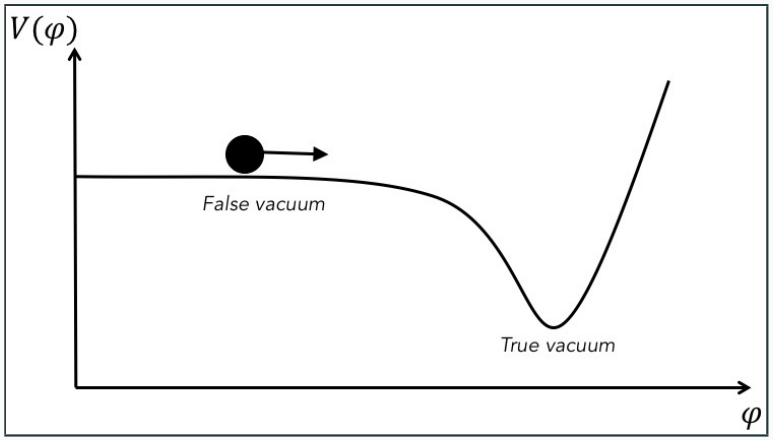

Klein–Gordon equation

$$\ddot{\phi}(t) + 3H\dot{\phi} + \frac{dV}{d\phi} = 0$$

Friedmann equation

$$H^2 = \left(\frac{\dot{a}}{a}\right)^2 \approx \frac{V}{3M_{\mathrm{Pl}}^2}$$

Slow-roll inflation

- Scalar inflaton field ϕ slowly rolls down scalar potential, $\ddot{\phi} \ll 3H\dot{\phi}, dV/d\phi$
- $V(\phi) \approx \mathrm{const} \approx$ slowly decaying cosmological constant $\rightarrow$ exponential expansion

Perturbation theory

Vacuum continuously sources perturbations in the inflaton field and in the metric

[Guth 1981] [Linde 1982] [Albrecht & Steinhardt 1982]

Primordial tensor perturbations

Action for transverse–traceless tensor perturbations from Einstein–Hilbert action

$$S = \frac{m_{\mathrm{Pl}}^2}{2} \int d^4x \sqrt{-g}\, R \qquad \supset \qquad S_h^{(2)} = -\frac{m_{\mathrm{Pl}}^2}{8} \int d\eta\, d^3\boldsymbol{x}\, a^2(\eta)\, \eta^{\mu\nu}\, \partial_\mu h_{ij}\, \partial_\nu h_{ij}$$

Primordial tensor perturbations

Action for transverse–traceless tensor perturbations from Einstein–Hilbert action

$$S = \frac{m_{\mathrm{Pl}}^2}{2} \int d^4x \sqrt{-g}\, R \qquad \supset \qquad S_h^{(2)} = -\frac{m_{\mathrm{Pl}}^2}{8} \int d\eta\, d^3\boldsymbol{x}\, a^2(\eta)\, \eta^{\mu\nu}\, \partial_\mu h_{ij}\, \partial_\nu h_{ij}$$

Go to Fourier space; introduce new field variables $v_p(\eta, \boldsymbol{k}) = m_{\mathrm{Pl}}/\sqrt{2}\, a(\eta)\, h_p(\eta, \boldsymbol{k})$:

$$S_h^{(2)} = \frac{1}{2} \sum_{p=+,\times} \int d\eta\, \frac{d^3\boldsymbol{k}}{(2\pi)^3} \left[|v_p'(\eta, \boldsymbol{k})|^2 - \left(k^2 - \frac{a''}{a} \right) |v_p(\eta, \boldsymbol{k})|^2 \right]$$

Primordial tensor perturbations

Action for transverse–traceless tensor perturbations from Einstein–Hilbert action

$$S = \frac{m_{\mathrm{Pl}}^2}{2} \int d^4x \sqrt{-g}\, R \qquad \supset \qquad S_h^{(2)} = -\frac{m_{\mathrm{Pl}}^2}{8} \int d\eta\, d^3\boldsymbol{x}\, a^2(\eta)\, \eta^{\mu\nu}\, \partial_\mu h_{ij}\, \partial_\nu h_{ij}$$

Go to Fourier space; introduce new field variables $v_p(\eta, \boldsymbol{k}) = m_{\mathrm{Pl}}/\sqrt{2}\, a(\eta)\, h_p(\eta, \boldsymbol{k})$:

$$S_h^{(2)} = \frac{1}{2} \sum_{p=+,\times} \int d\eta\, \frac{d^3\boldsymbol{k}}{(2\pi)^3} \left[|v_p'(\eta, \boldsymbol{k})|^2 - \left(k^2 - \frac{a''}{a} \right) |v_p(\eta, \boldsymbol{k})|^2 \right]$$

Solve equation of motion in inflationary background, $a(t) \approx a_0 e^{Ht}$, $a(\eta) \approx -1/(H\eta)$

$$v_k'' + \left(k^2 - \frac{a''}{a} \right) v_k = 0$$

Primordial tensor perturbations

Action for transverse–traceless tensor perturbations from Einstein–Hilbert action

$$S = \frac{m_{\rm Pl}^2}{2} \int d^4x \sqrt{-g}\, R \qquad \supset \qquad S_h^{(2)} = -\frac{m_{\rm Pl}^2}{8} \int d\eta\, d^3\boldsymbol{x}\, a^2(\eta)\, \eta^{\mu\nu}\, \partial_\mu h_{ij}\, \partial_\nu h_{ij}$$

Go to Fourier space; introduce new field variables $v_p(\eta, \boldsymbol{k}) = m_{\rm Pl}/\sqrt{2}\, a(\eta)\, h_p(\eta, \boldsymbol{k})$:

$$S_h^{(2)} = \frac{1}{2} \sum_{p=+,\times} \int d\eta\, \frac{d^3\boldsymbol{k}}{(2\pi)^3} \left[|v_p'(\eta, \boldsymbol{k})|^2 - \left(k^2 - \frac{a''}{a} \right) |v_p(\eta, \boldsymbol{k})|^2 \right]$$

Solve equation of motion in inflationary background, $a(t) \approx a_0 e^{Ht}$, $a(\eta) \approx -1/(H\eta)$

$$v_k'' + \left(k^2 - \frac{a''}{a} \right) v_k = 0$$

Primordial tensor spectrum

$$\langle 0|\, h_{ij}(\eta, \boldsymbol{k})\, h_{ij}^*(\eta, \ell)\, |0\rangle = \frac{2\pi^2}{k^3}\, \delta^{(3)}(\boldsymbol{k} - \ell)\, \mathcal{P}_h(k)\,, \qquad \boxed{\mathcal{P}_h(k) \approx 2 \left(\frac{H_k}{\pi\, m_{\rm Pl}} \right)^2}$$

CMB observables

[Review of Particle Physics (2020), pdg.lbl.gov]

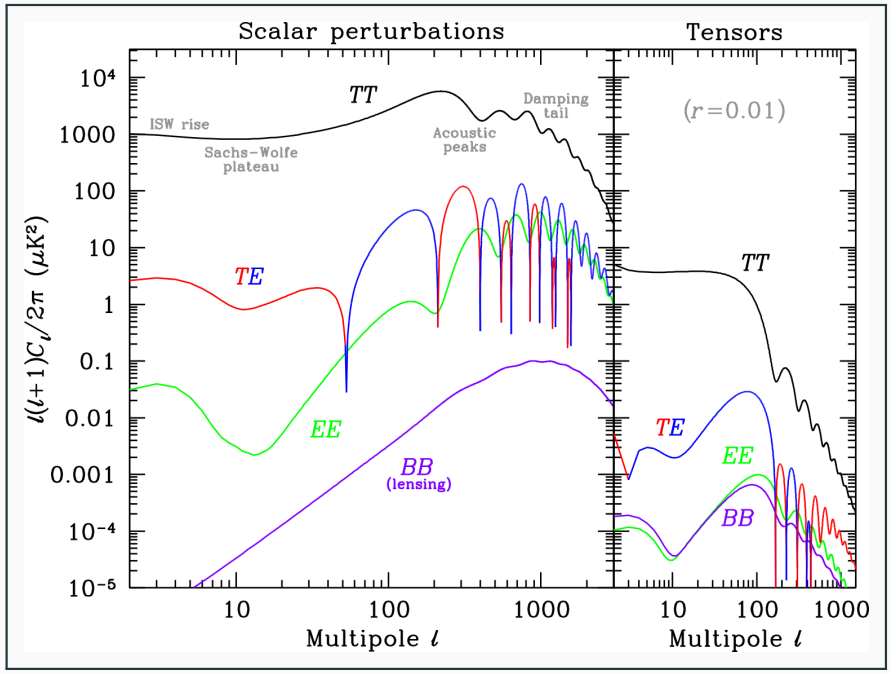

Primordial scalar + tensor perturbations source temperature + polarization anisotropies

$$\mathcal{P}_{\mathcal{R}}(k) = A_s \left(\frac{k}{k_*}\right)^{n_s-1} \approx \frac{1}{8\,\epsilon}\left(\frac{H_k}{\pi\, m_{\rm Pl}}\right)^2, \qquad \mathcal{P}_h(k) = r\, A_s \left(\frac{k}{k_*}\right)^{n_t} \approx 2\left(\frac{H_k}{\pi\, m_{\rm Pl}}\right)^2$$

with the slow-roll parameter $\epsilon = -\dot{H}/H^2$ measuring the deviation from dS expansion

CMB observables

[Review of Particle Physics (2020), pdg.lbl.gov]

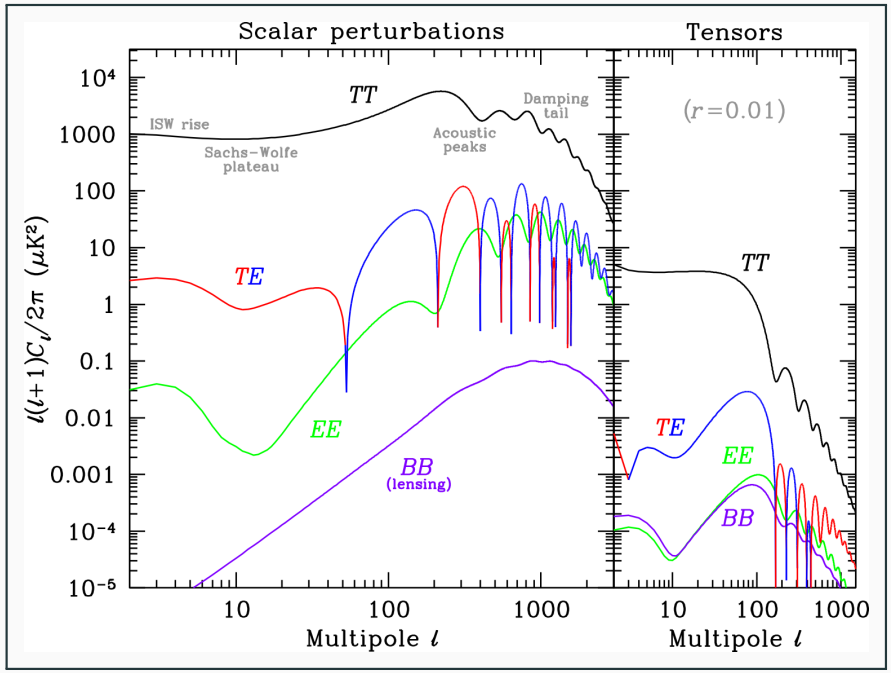

Primordial scalar + tensor perturbations source temperature + polarization anisotropies

$$\mathcal{P}_{\mathcal{R}}(k) = A_s \left(\frac{k}{k_*}\right)^{n_s-1} \approx \frac{1}{8\,\epsilon}\left(\frac{H_k}{\pi\, m_{\rm Pl}}\right)^2, \qquad \mathcal{P}_h(k) = r\, A_s \left(\frac{k}{k_*}\right)^{n_t} \approx 2\left(\frac{H_k}{\pi\, m_{\rm Pl}}\right)^2$$

with the slow-roll parameter $\epsilon = -\dot{H}/H^2$ measuring the deviation from dS expansion

Consistency relation in single-field slow-roll inflation: $\boxed{n_t = \dfrac{d\ln \mathcal{P}_h}{d\ln k} \approx -2\,\epsilon = -\dfrac{r}{8}}$

Observational constraints

Scalar spectral index versus $r_{0.002}$

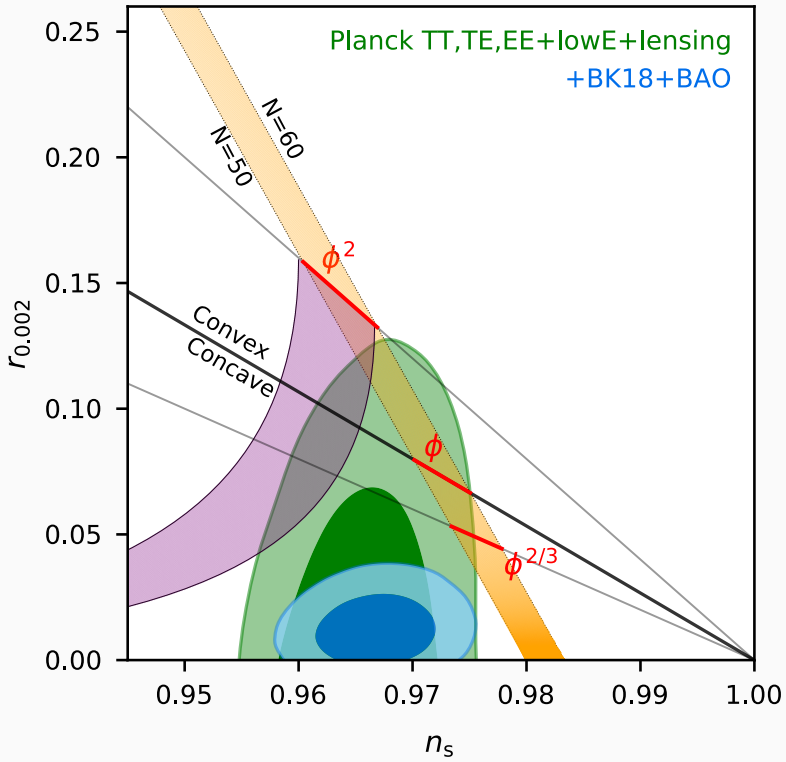

Tensor spectral index versus $r_{0.01}$

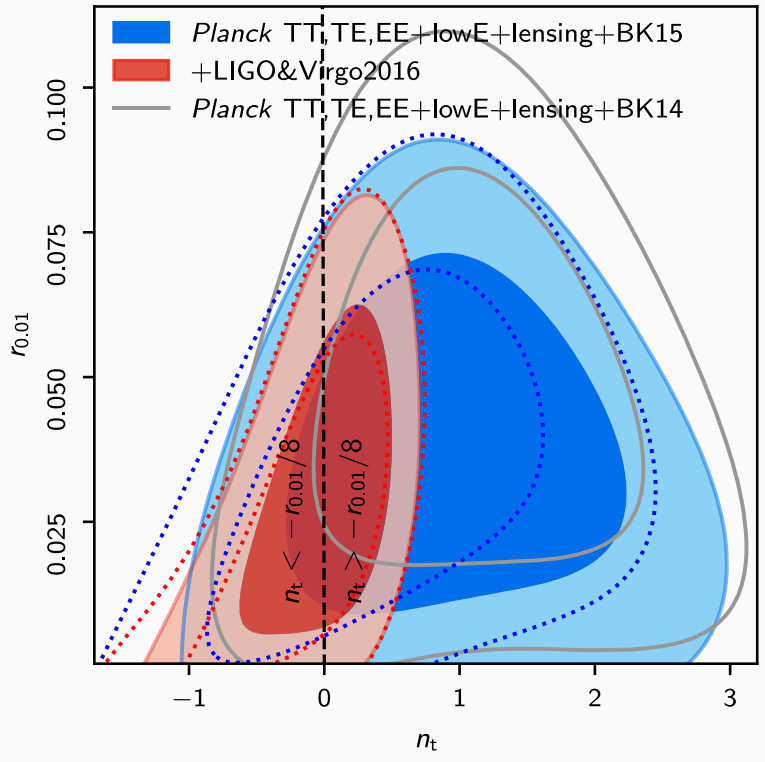

- Polynomial potentials disfavored; Higgs and Starobinsky inflation looking good
- Future CMB polarization experiments (e.g., LiteBIRD) will probe $r \gtrsim 10^{-4\cdots3}$
- In absence of a GW signal, tensor index only poorly constrained by CMB
- Tighter constraints if power law naively extrapolated to higher frequencies

Logbook of the expansion history

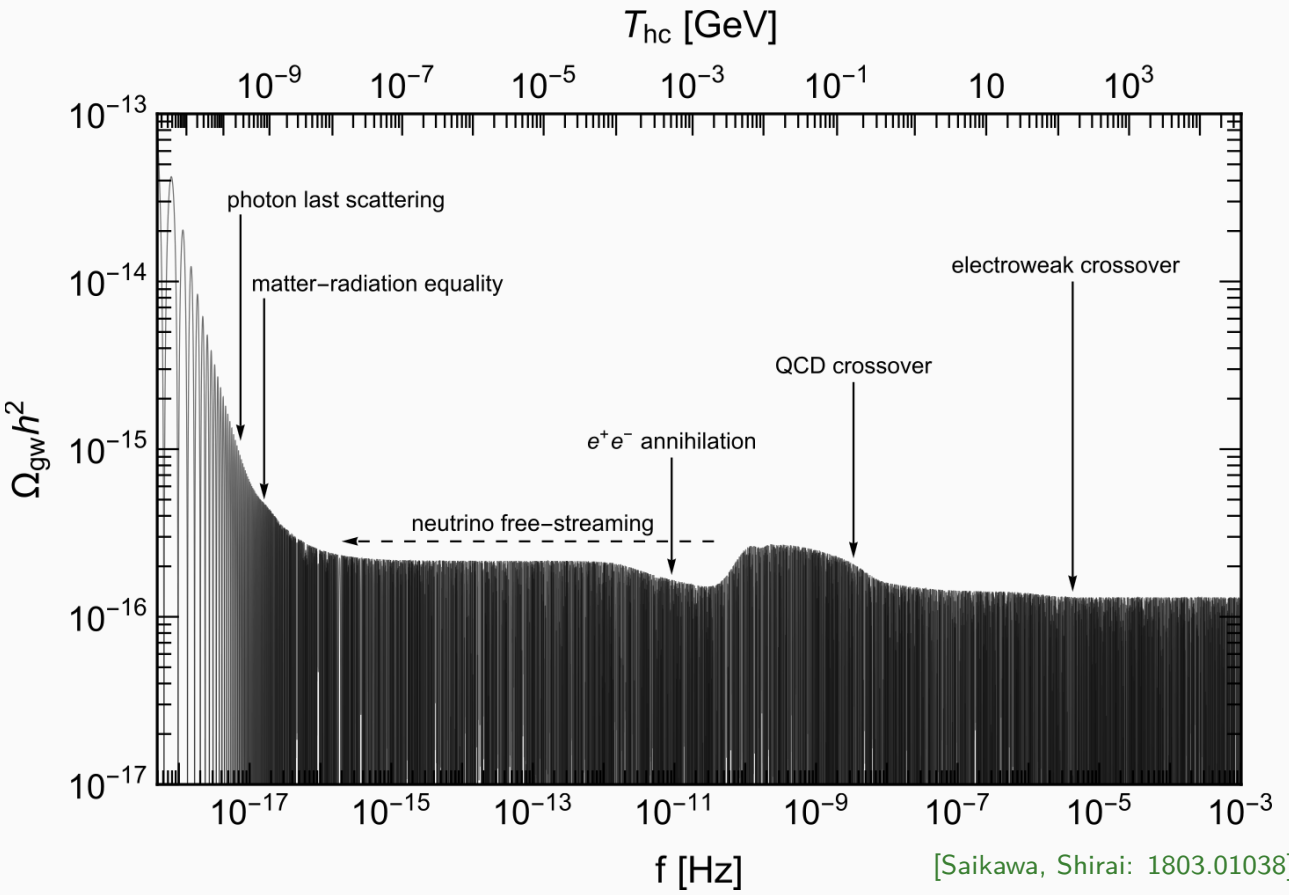

[Saikawa, Shirai: 1803.01038]

Scale-invariant GW spectrum from inflation, redshifted to the present epoch

- Cosmic logbook encoding the entire expansion history of the early Universe
- Major events in the early Universe leave their imprint in the SGWB signal
- Approximately flat plateau at $\Omega_{\rm gw} \sim \Omega_{\rm r}/24\, r A_s \sim 2 \times 10^{-16}\,(r/0.044)$

Primordial tensor spectrum

$$\mathcal{P}_h = r\, A_s \left(\frac{f}{f_{\rm cmb}}\right)^{n_t}$$

Parameters

$T_{\rm rh}$	Reheating temperature
r	Tensor-to-scalar ratio
n_t	Tensor spectral index

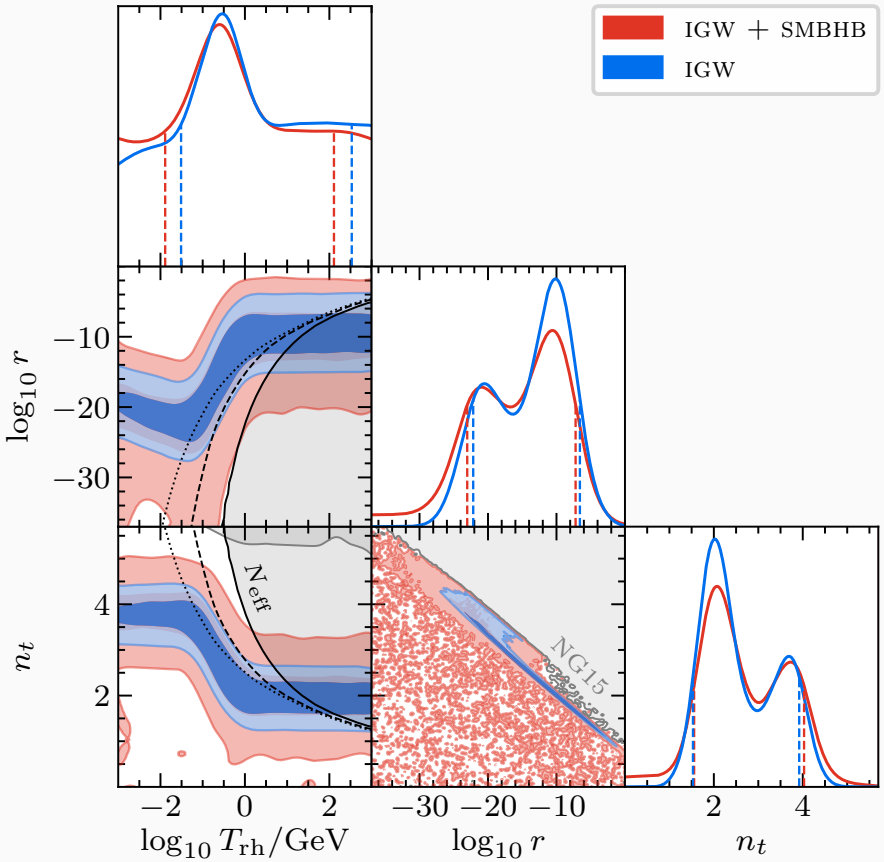

Lessons

- Strongly blue-tilted spectrum, $n_t \sim 2 \cdots 4 \rightarrow$ probe **nonminimal inflation models**
- Transition from **reheating** to the Hot Big Bang in the PTA band for $T_{\rm rh} \sim 1\,{\rm GeV}$
- If GWB extrapolated to higher frequencies $\rightarrow$ large contribution to **dark radiation**

❷ BSM scenario: Primordial black holes

Big questions: Are some of the black holes seen by LVK of primordial origin? To what extent do PBHs contribute to dark matter? How do galactic SMBHs form?

❷ BSM scenario: Primordial black holes

Big questions: Are some of the black holes seen by LVK of primordial origin? To what extent do PBHs contribute to dark matter? How do galactic SMBHs form?

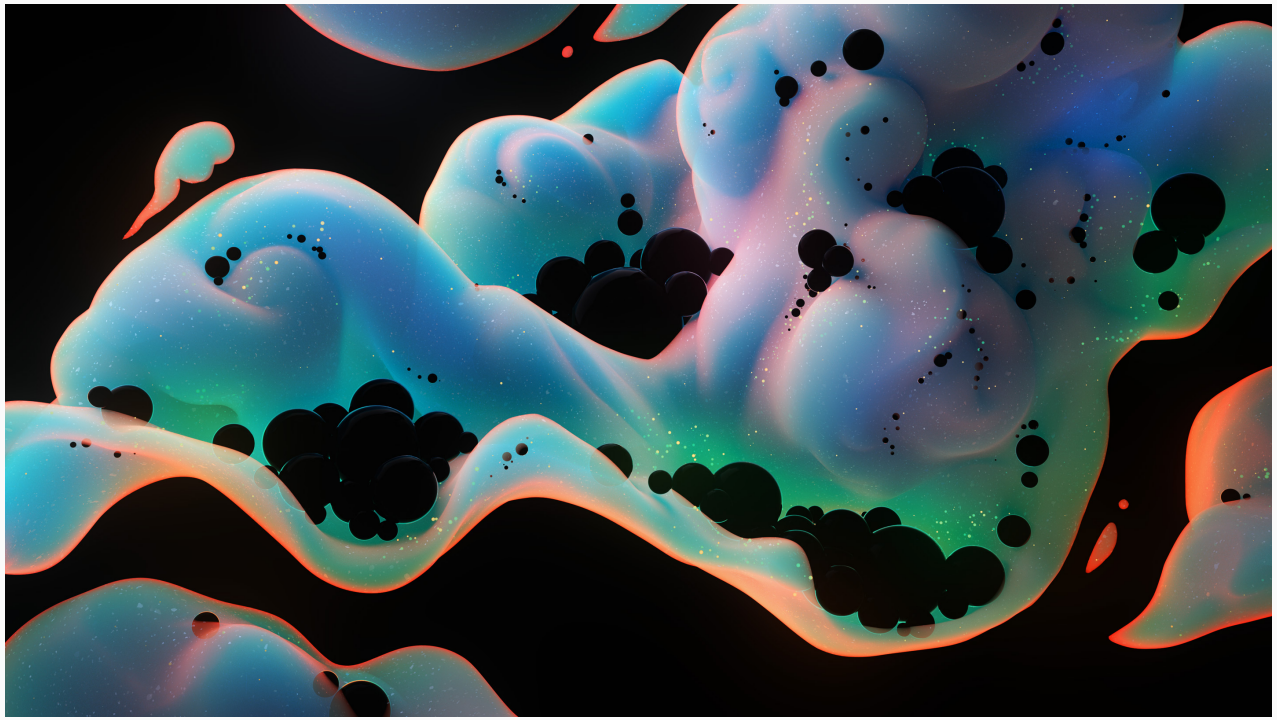

PBHs: Form in the gravitational collapse of large overdensities in the early Universe

- Typical scenario: Scalar perturbations enhanced during ultra-slow-roll inflation
- Enhanced scalar perturbations $\rightarrow$ GWs at second order in perturbation theory

Enhanced curvature perturbations

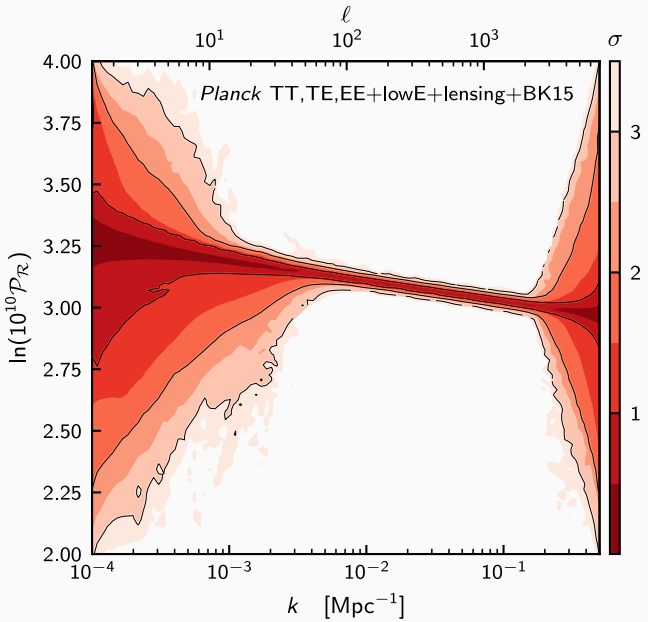

[PLANCK Collaboration: 1807.06211]

Primordial scalar power spectrum only well known at CMB scales

$$\mathcal{P}_{\mathcal{R}} = \frac{1}{24\pi^2}\frac{1}{\epsilon}\frac{V}{m_{\rm Pl}^4} \simeq (2.10 \pm 0.06) \times 10^{-9} \qquad \text{at} \qquad k_{\rm CMB} = 0.05\,\text{Mpc}^{-1}$$

Enhanced curvature perturbations

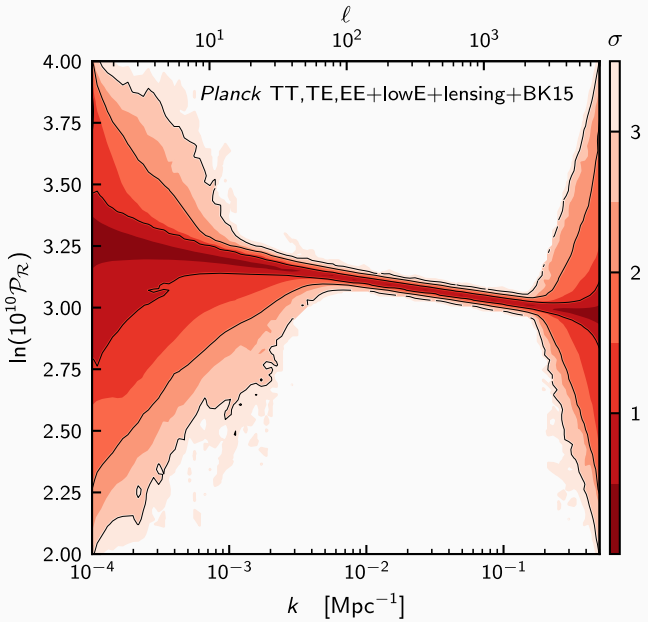

[PLANCK Collaboration: 1807.06211]

Primordial scalar power spectrum only well known at CMB scales

$$\mathcal{P}_{\mathcal{R}} = \frac{1}{24\pi^2}\frac{1}{\epsilon}\frac{V}{m_{\rm Pl}^4} \simeq (2.10 \pm 0.06) \times 10^{-9} \qquad \text{at} \qquad k_{\rm CMB} = 0.05\,\text{Mpc}^{-1}$$

- Standard slow-roll inflation + constant red tilt $\rightarrow$ even smaller $\mathcal{P}_{\mathcal{R}}$ on small scales

Enhanced curvature perturbations

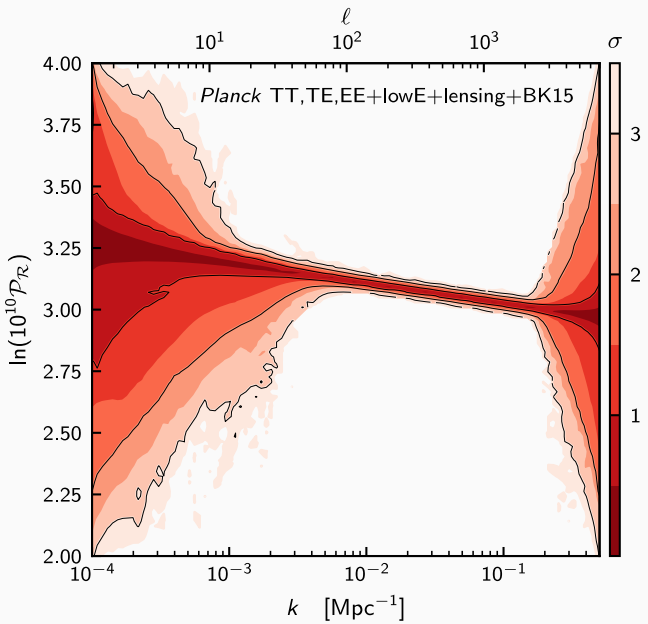

[PLANCK Collaboration: 1807.06211]

Primordial scalar power spectrum only well known at CMB scales

$$\mathcal{P}_\mathcal{R} = \frac{1}{24\pi^2}\frac{1}{\epsilon}\frac{V}{m_{\rm Pl}^4} \simeq (2.10 \pm 0.06) \times 10^{-9} \qquad \text{at} \qquad k_{\rm CMB} = 0.05\,\text{Mpc}^{-1}$$

- Standard slow-roll inflation + constant red tilt $\rightarrow$ even smaller $\mathcal{P}_\mathcal{R}$ on small scales
- Strong assumption! Many inflation models give rise to $\mathcal{P}_\mathcal{R} \gg \mathcal{P}_\mathcal{R}(k_{\rm CMB})$ at large k

Enhanced curvature perturbations

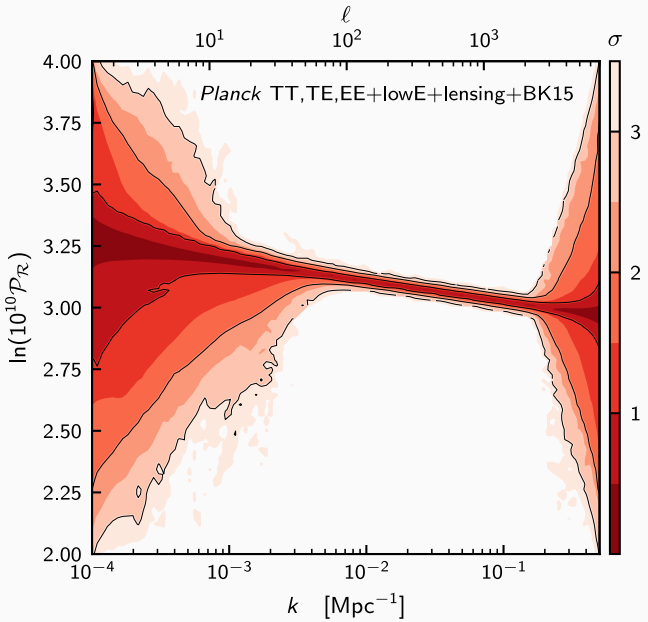

[PLANCK Collaboration: 1807.06211]

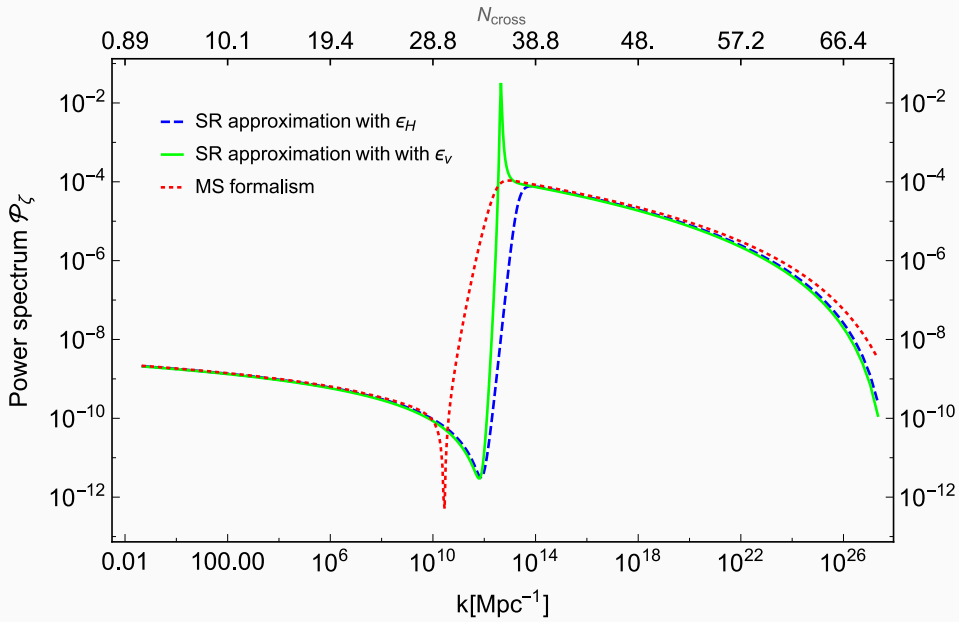

[Drees, Xu: 1905.13581]

Primordial scalar power spectrum only well known at CMB scales

$$\mathcal{P}_\mathcal{R} = \frac{1}{24\pi^2}\frac{1}{\epsilon}\frac{V}{m_{\rm Pl}^4} \simeq (2.10 \pm 0.06) \times 10^{-9} \qquad \text{at} \qquad k_{\rm CMB} = 0.05\,\text{Mpc}^{-1}$$

- Standard slow-roll inflation + constant red tilt $\rightarrow$ even smaller $\mathcal{P}_\mathcal{R}$ on small scales
- Strong assumption! Many inflation models give rise to $\mathcal{P}_\mathcal{R} \gg \mathcal{P}_\mathcal{R}(k_{\rm CMB})$ at large k
- E.g.: Critical Higgs inflation, saddle point in scalar potential at low field values

Scalar-induced GWs (SIGWs) at second order in perturbation theory

Cosmological perturbation theory

- Scalar and tensor modes couple to each other at second order, $h_{ij} \leftrightarrow \partial_i \Phi \partial_j \Phi$
- Enhanced density modes leave (re-enter) Hubble horizon during (after) inflation
- Collapse into PBHs and source SIGWs upon horizon re-entry during radiation era

---

Scalar-induced GWs (SIGWs) at second order in perturbation theory

Cosmological perturbation theory

- Scalar and tensor modes couple to each other at second order, $h_{ij} \leftrightarrow \partial_i \Phi \partial_j \Phi$
- Enhanced density modes leave (re-enter) Hubble horizon during (after) inflation
- Collapse into PBHs and source SIGWs upon horizon re-entry during radiation era

---

[Yuan, Huang: 2103.04739]

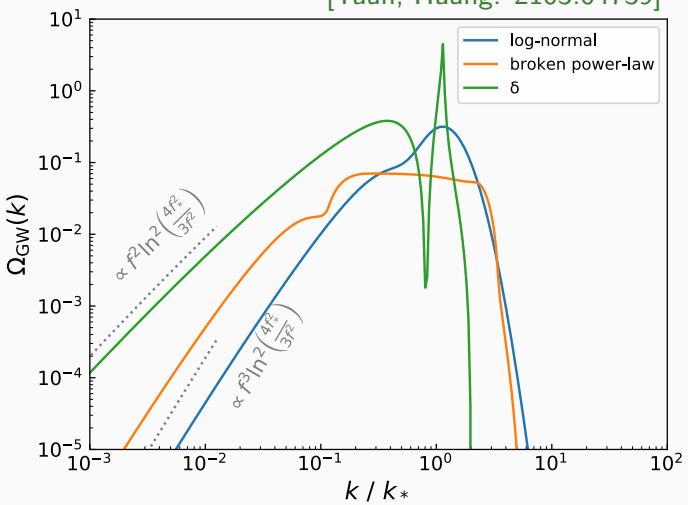

Solve tensor EOMs using Green's function:

$$\Omega_{\rm GW} = \int du \int dv\, f(u,v)\, \mathcal{P}_\zeta(uk) \mathcal{P}_\zeta(vk)$$

with some complicated transfer function f

- GW spectrum determined by shape of $\mathcal{P}_\zeta$
- Peak position set by feature in $\mathcal{P}_\zeta$ at k_*
- Characteristic log-dependent scaling at low k

Scalar-induced GWs (SIGWs) at second order in perturbation theory

Cosmological perturbation theory

- Scalar and tensor modes couple to each other at second order, $h_{ij} \leftrightarrow \partial_i \Phi \partial_j \Phi$
- Enhanced density modes leave (re-enter) Hubble horizon during (after) inflation
- Collapse into PBHs and source SIGWs upon horizon re-entry during radiation era

---

[Yuan, Huang: 2103.04739]

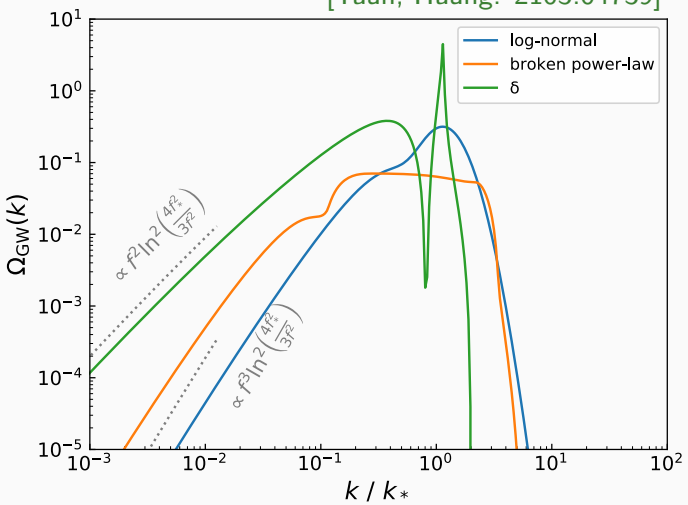

Solve tensor EOMs using Green's function:

$$\Omega_{\rm GW} = \int du \int dv\, f(u,v)\, \mathcal{P}_\zeta(uk) \mathcal{P}_\zeta(vk)$$

with some complicated transfer function f

- GW spectrum determined by shape of $\mathcal{P}_\zeta$
- Peak position set by feature in $\mathcal{P}_\zeta$ at k_*
- Characteristic log-dependent scaling at low k

Depending on $\mathcal{P}_\zeta$, second-order scalar-induced GWs can dominate the SGWB signal!

Associated PBH formation

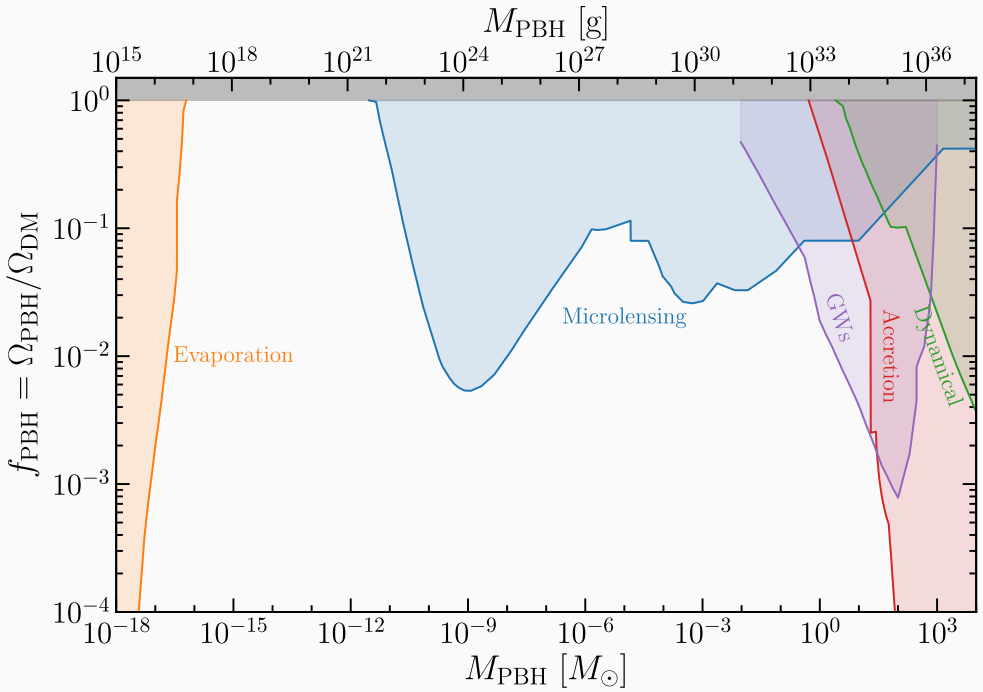

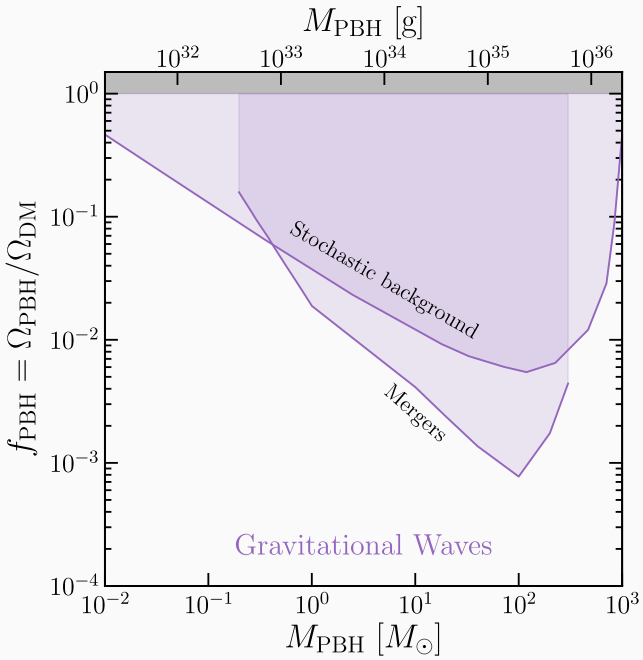

[Green, Kavanagh: 2007.10722]

Collapse of horizon mass when overdense regions re-enter the causal horizon

- Statistics of primordial density perturbations translate into PBH mass fraction
- Part of dark-matter (DM) relic density; up to 100 % for asteroid-scale masses
- DM mass fraction $f_{\rm PBH} \sim 10^{-3}$ and masses of $\mathcal{O}\,(10)\,M_\odot \rightarrow$ LIGO / Virgo!?
- Probe / constrain by searching for scalar-induced GWs at second order ...
- ... as well as for the GW signals / stochastic background from PBH mergers

Primordial scalar spectrum

$$\mathcal{P}_s = \frac{A}{\sqrt{2\pi}\,\Delta}\,\exp\left[-\frac{(\ln(f/f_*))^2}{2\,\Delta^2}\right]$$

Parameters

f_*	Peak frequency
A	Peak amplitude
Δ	Width

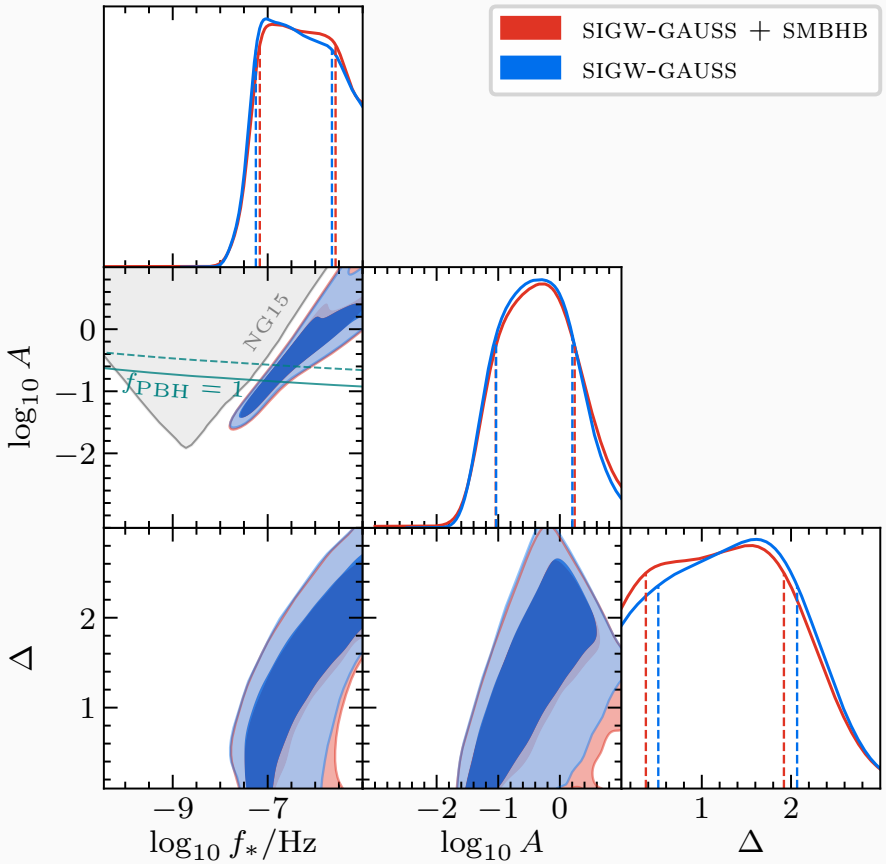

Lessons

- Require large-amplitude peak in $\mathcal{P}_s \rightarrow$ input for building models of **inflation**
- **PBH dark matter** might be possible; but some tension with PBH overproduction
- On-going debate on impact of **non-Gaussianities** on efficiency of PBH production

Alternative scenarios

Scalar-induced gravitational waves, δ-function-shaped $\mathcal{P}_\mathcal{R}$ (SIGW-DELTA)

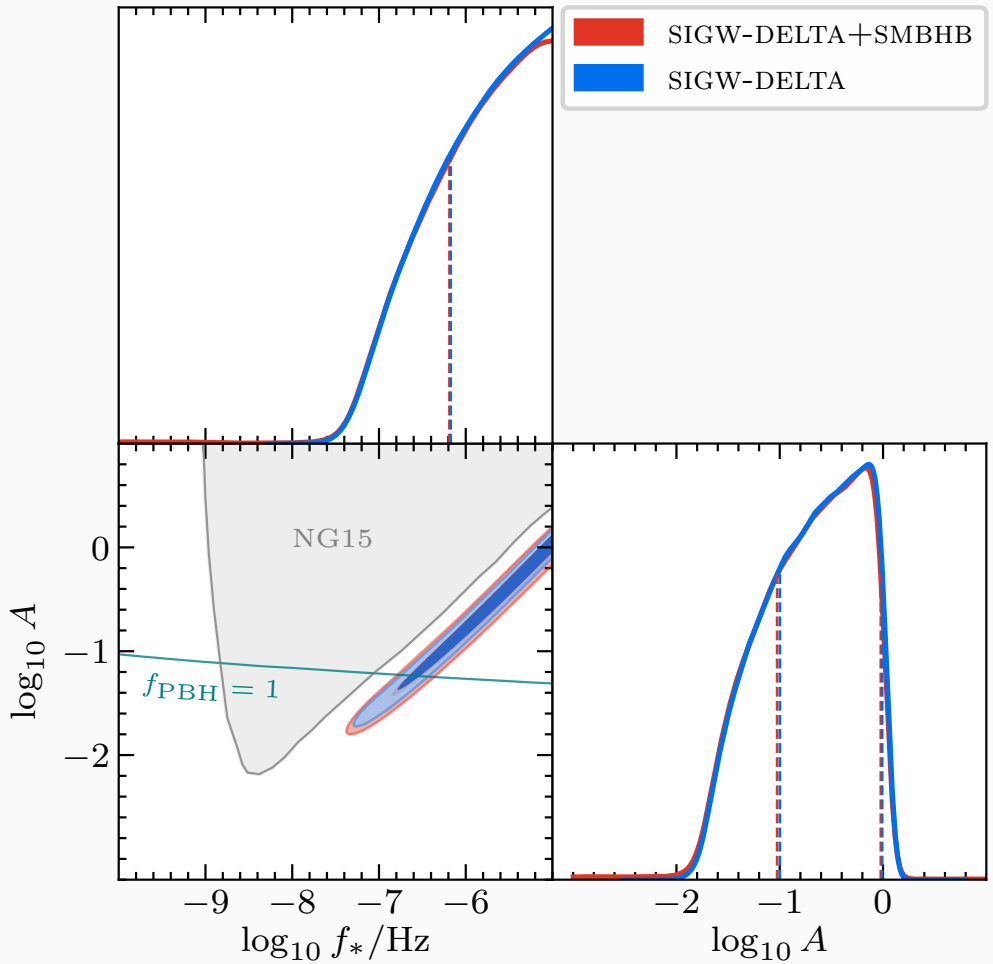

Alternative scenarios

Scalar-induced gravitational waves, box-shaped $\mathcal{P}_\mathcal{R}$ (SIGW-BOX)

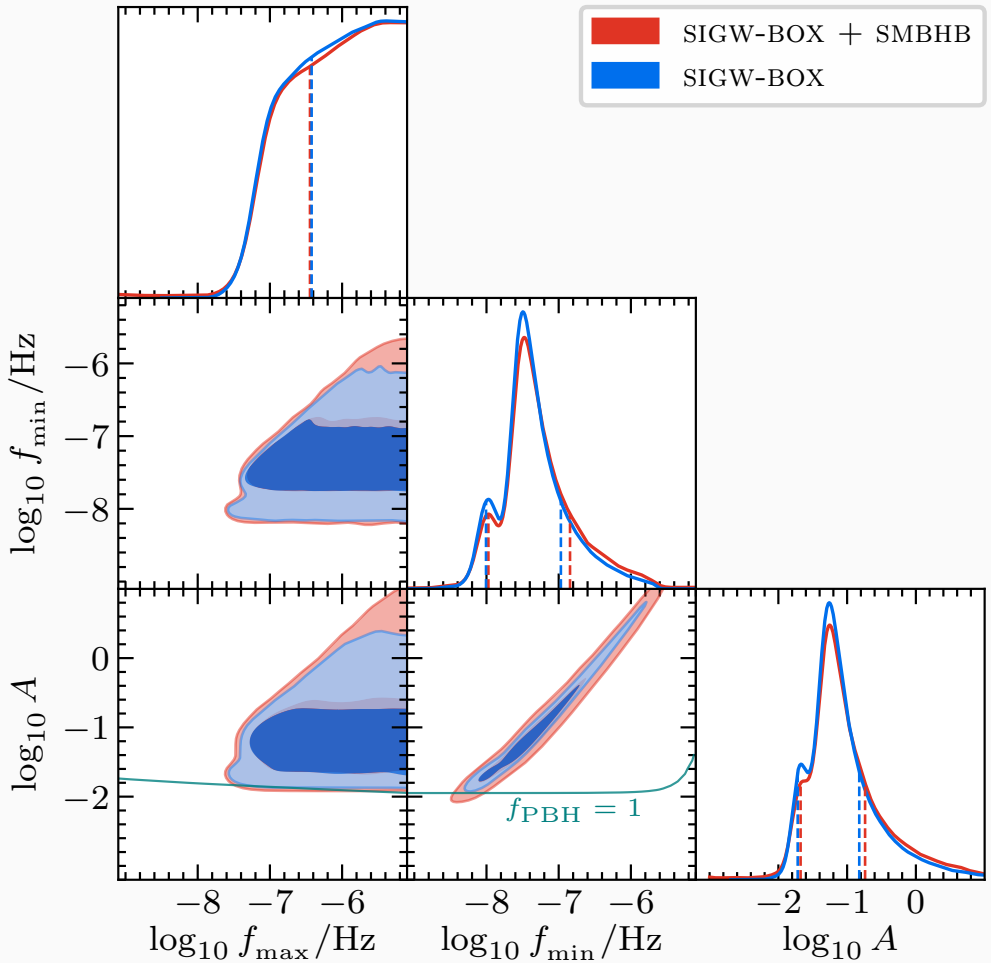

❸ BSM scenario: Phase transition

Big questions: How are the Higgs mechanism and the quark–hadron transition realized in the early Universe? Are there other fundamental forces beyond the Standard Model?

❸ BSM scenario: Phase transition

Big questions: How are the Higgs mechanism and the quark–hadron transition realized in the early Universe? Are there other fundamental forces beyond the Standard Model?

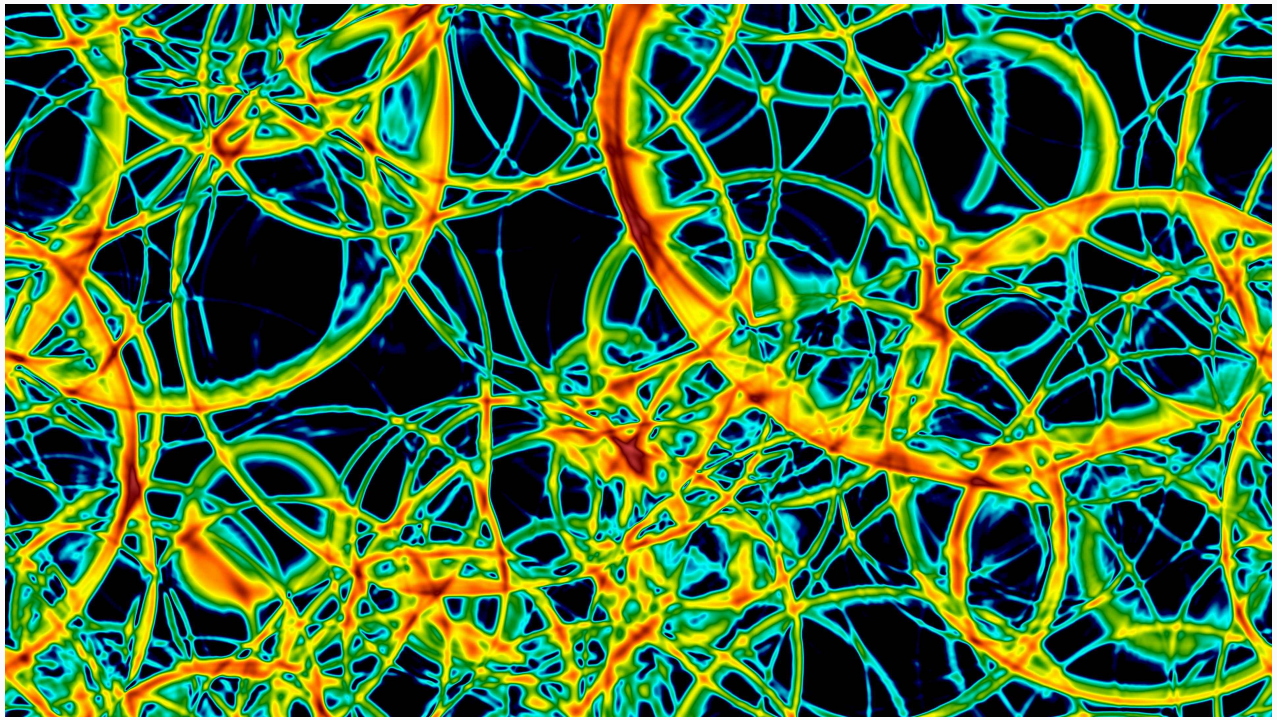

Cosmological phase transitions: Changes in the quantum field theory vacuum structure

- SM predicts smooth crossovers; strong first-order phase transitions require BSM
- GWs from bubble collisions, sound waves, and magnetohydrodynamic turbulence

First-order phase transitions

First-order phase transition

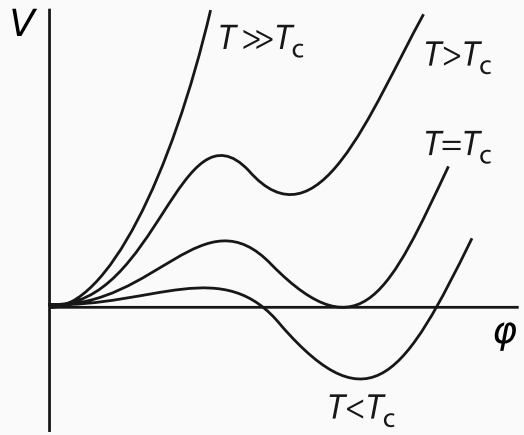

Second-order phase transition

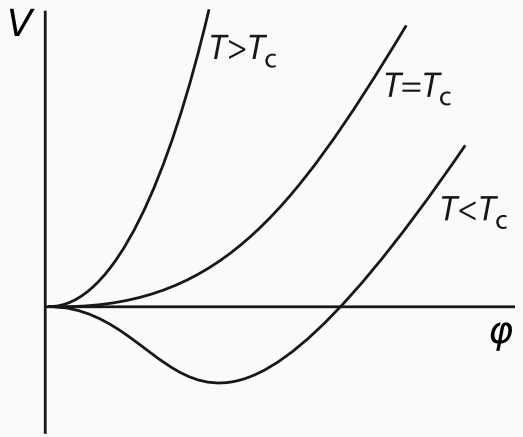

[Kinnunen, Baarsma, Martikainen, Törmä: 1706.07076]

GWs from strong first-order phase transitions (SFOPTs)

- Barrier in the effective potential of the order parameter (scalar field)
- Thermal jump or quantum tunneling $\rightarrow$ bubble nucleation in position space
- Bubbles expand, accelerate, transfer energy to the surrounding plasma, and collide

First-order phase transitions

First-order phase transition

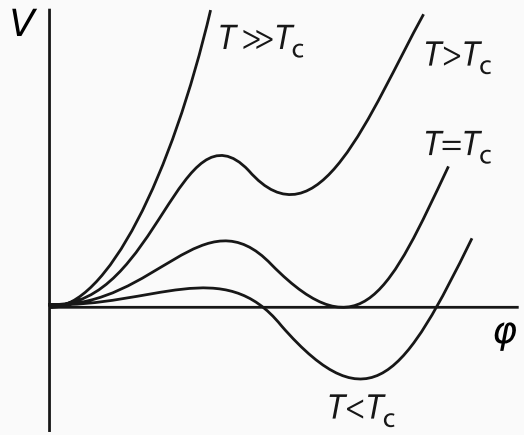

Second-order phase transition

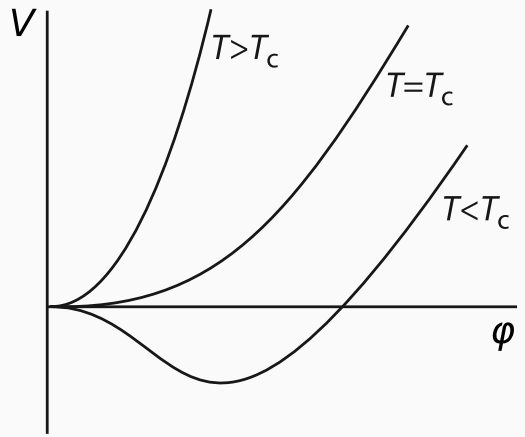

[Kinnunen, Baarsma, Martikainen, Törmä: 1706.07076]

GWs from strong first-order phase transitions (SFOPTs)

- Barrier in the effective potential of the order parameter (scalar field)
- Thermal jump or quantum tunneling $\rightarrow$ bubble nucleation in position space
- Bubbles expand, accelerate, transfer energy to the surrounding plasma, and collide

Three sources of GWs

- Ω_{b}: Bubble collisions, gradient energy in the scalar field
- Ω_{s}: Sound waves, compression and rarefaction waves in the bulk plasma
- Ω_{t}: Magnetohydrodynamic turbulence, vortical motion in the bulk plasma

LISA sensitivity to GWs from sound waves

[**KS**: 2005.10789]

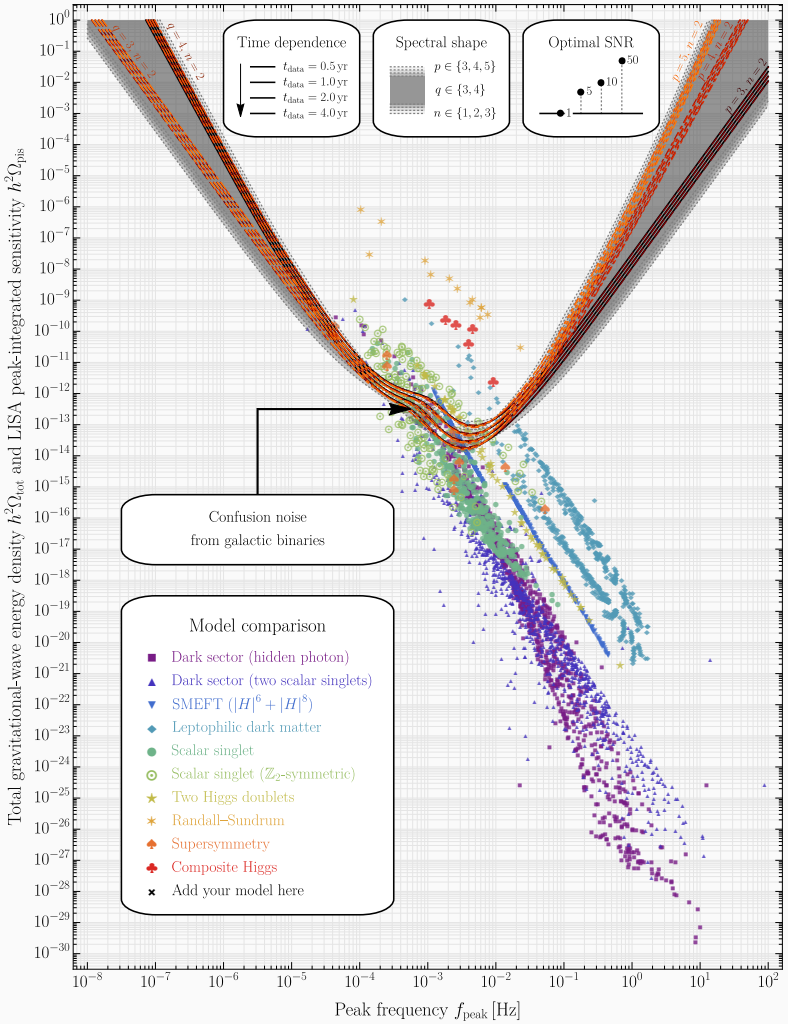

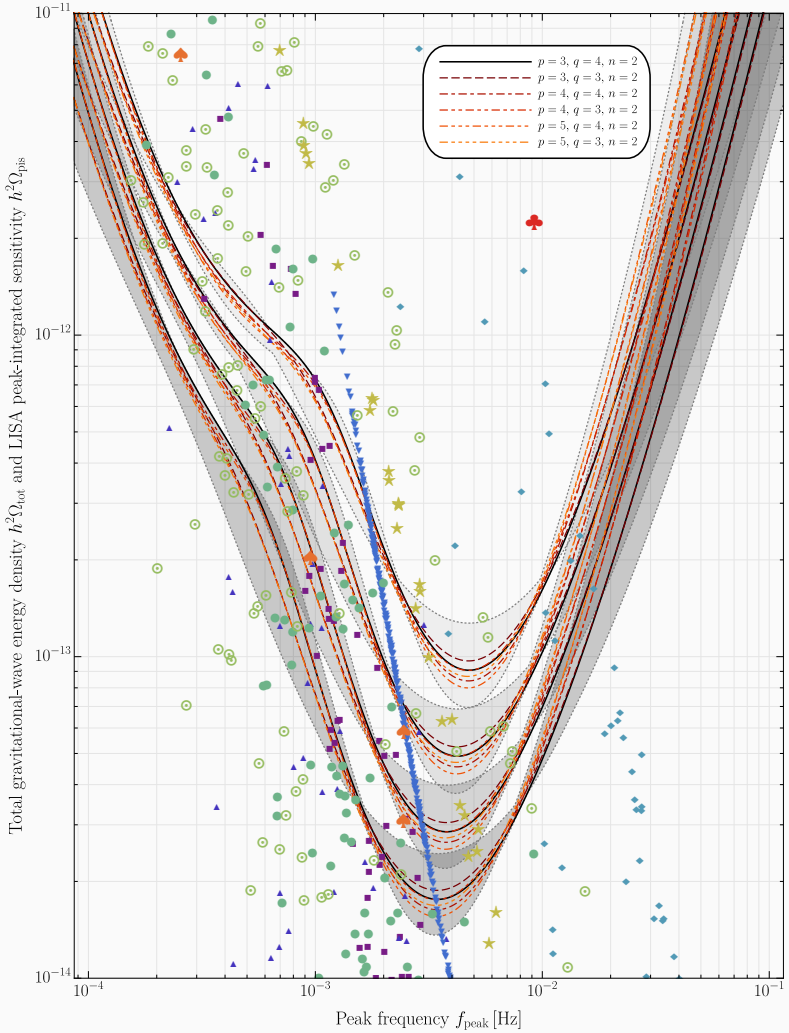

Peak-integrated sensitivity: LISA sensitivity projected onto $f_{\rm peak} - h^2\Omega_{\rm tot}$ plane

Peak amplitude and frequency

$$\Omega_{\mathrm{GW}}^{\mathrm{peak}} \propto (H_* R_*)^2 \left(\frac{\alpha_*}{1+\alpha_*}\right)^2$$

$$f_{\mathrm{peak}} \propto \frac{T_*}{H_* R_*}$$

Parameters

T_*	Percolation temperature
α_*	Transition strength
$H_* R_*$	Bubble separation

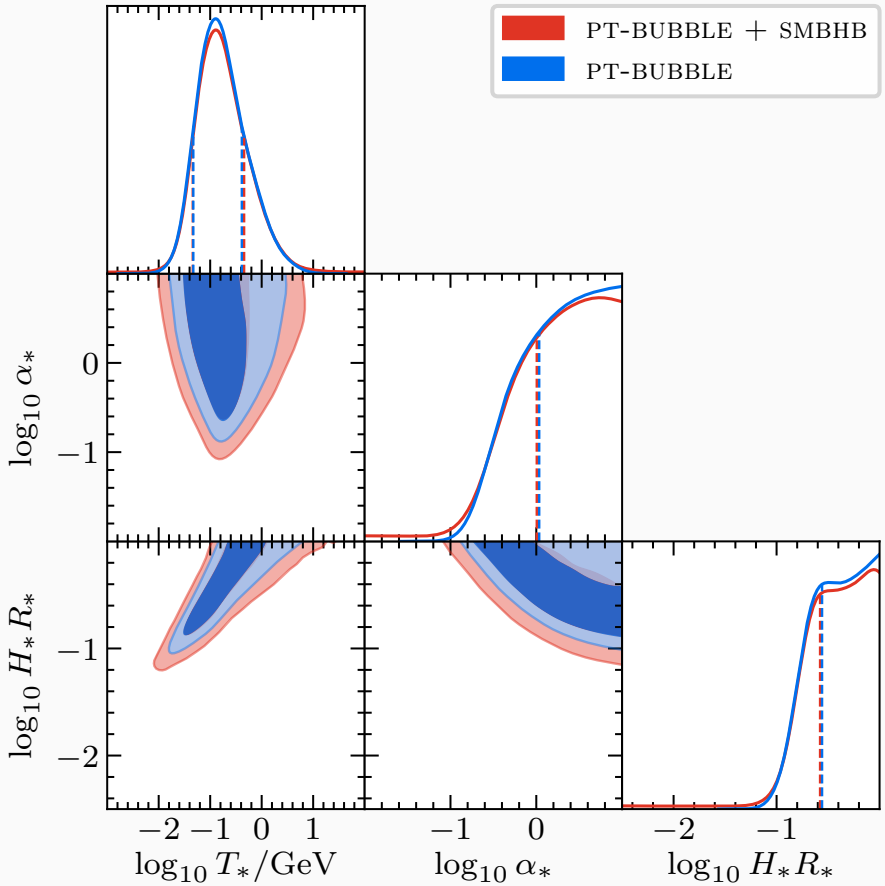

Lessons

- Strong ($\alpha_* \sim 1$) and slow ($H_* R_* \sim 1$) transition at a temperature $T_* \sim 100\,\mathrm{MeV}$
- Just the right ballpark for BSM modifications of the **QCD phase transition**
- Alternatively, phase transition in a **dark sector** $\rightarrow$ complementary to lab searches

Sound wave model

Phase transition, sound waves (PT-SOUND)

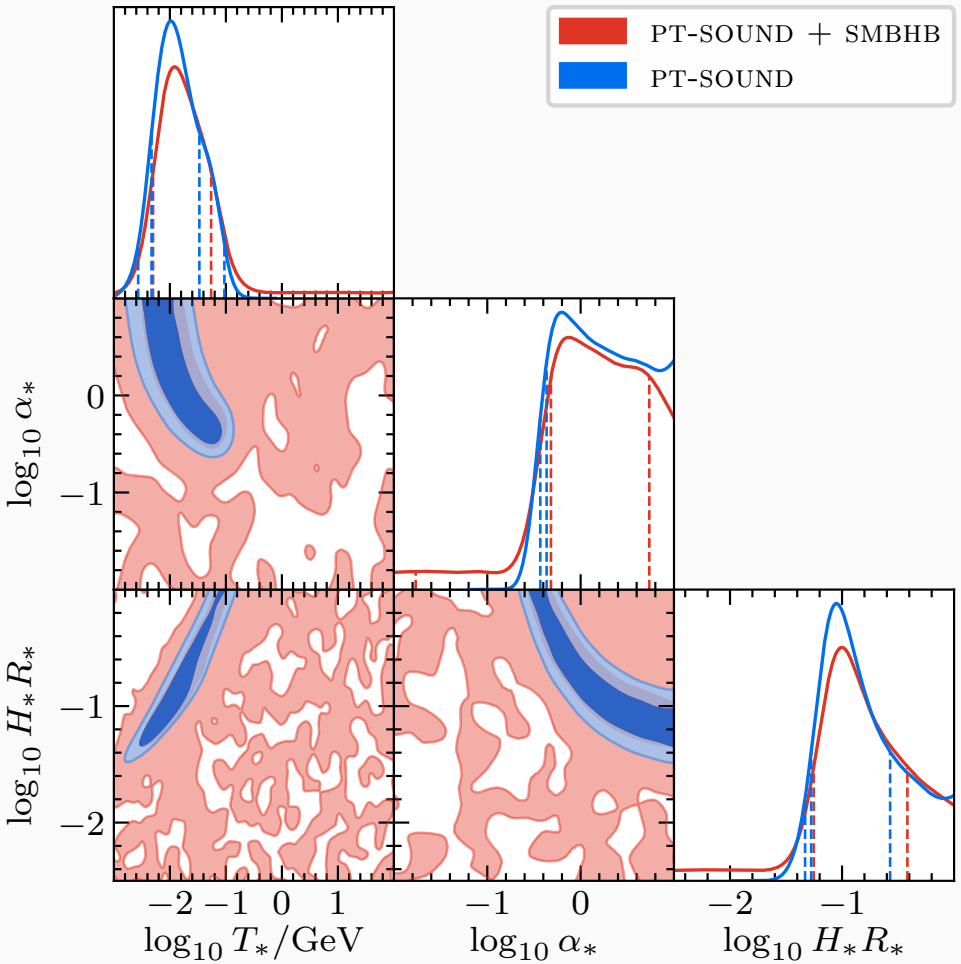

❹ BSM scenario: Cosmic defects

Big questions: How are the tiny SM neutrino masses generated? What is the origin of the matter–antimatter asymmetry? Is the SM embedded in a grand unified theory?

❹ BSM scenario: Cosmic defects

Big questions: How are the tiny SM neutrino masses generated? What is the origin of the matter–antimatter asymmetry? Is the SM embedded in a grand unified theory?

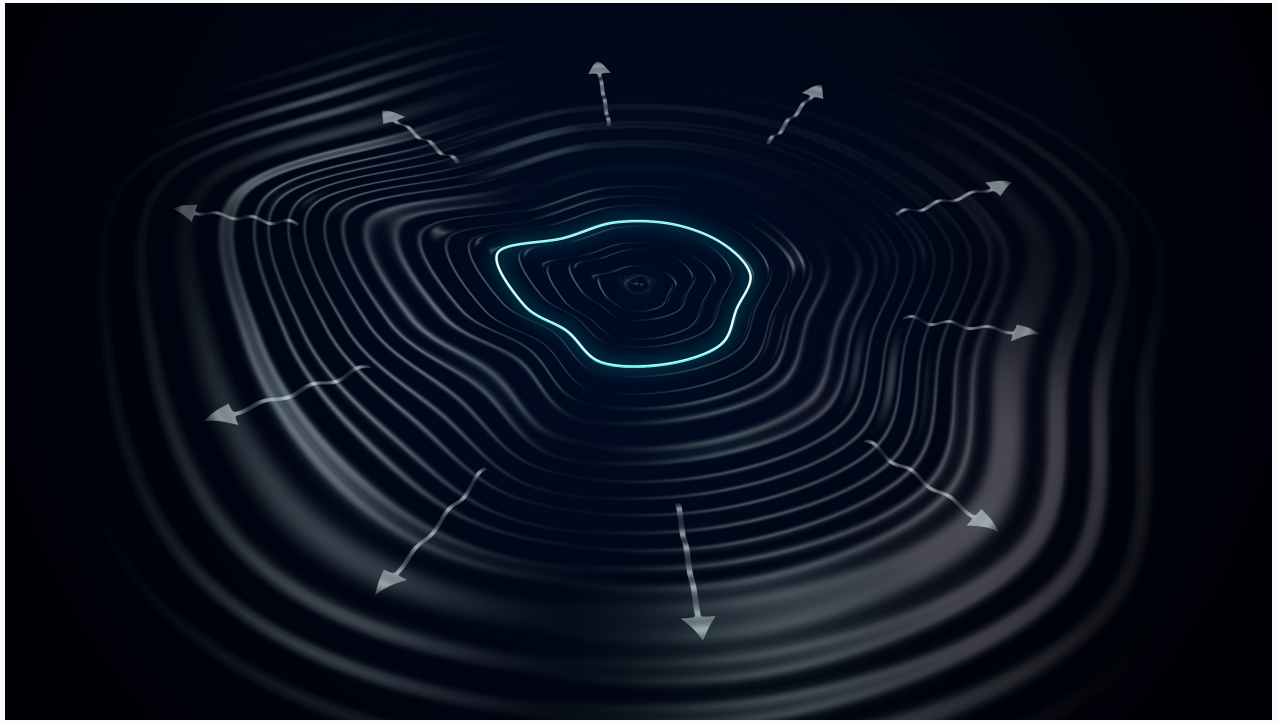

Cosmic strings / domain walls: Defects after spontaneous breaking of GUT symmetries

- Typical scenario: $U(1)_{B-L}$ breaking $\rightarrow$ neutrino masses, leptogenesis, and strings
- Dynamics and decay of defect networks yield anisotropic stress and hence GWs

Magnetic domains in a ferromagnet

[wikimedia.org]

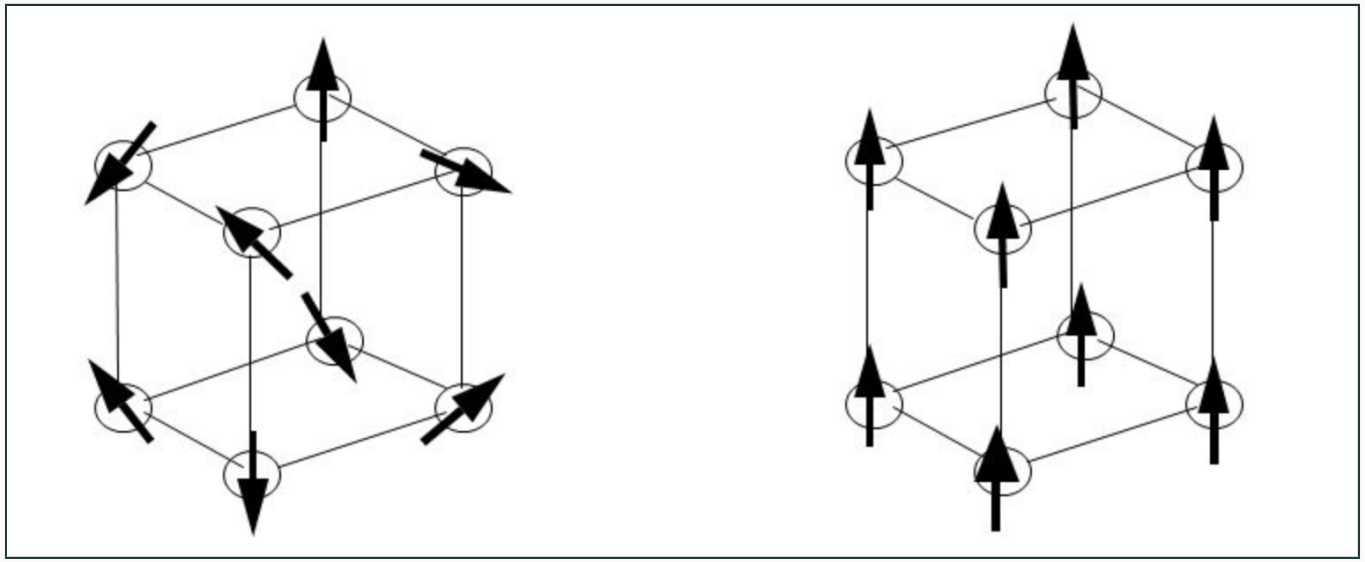

Magnetization in a ferromagnet

- Phase transition at the Curie temperature: paramagnet $\rightarrow$ ferromagnet
- Magnetic dipoles align spontaneously due to exchange interaction
- Translation and rotation invariance spontaneously broken
- Magnetic domains, regions of uniform magnetization, separated by domain walls
- Domain walls are stable, unless an external force (magnetic field) is applied

Magnetic domains in a ferromagnet

[wikimedia.org]

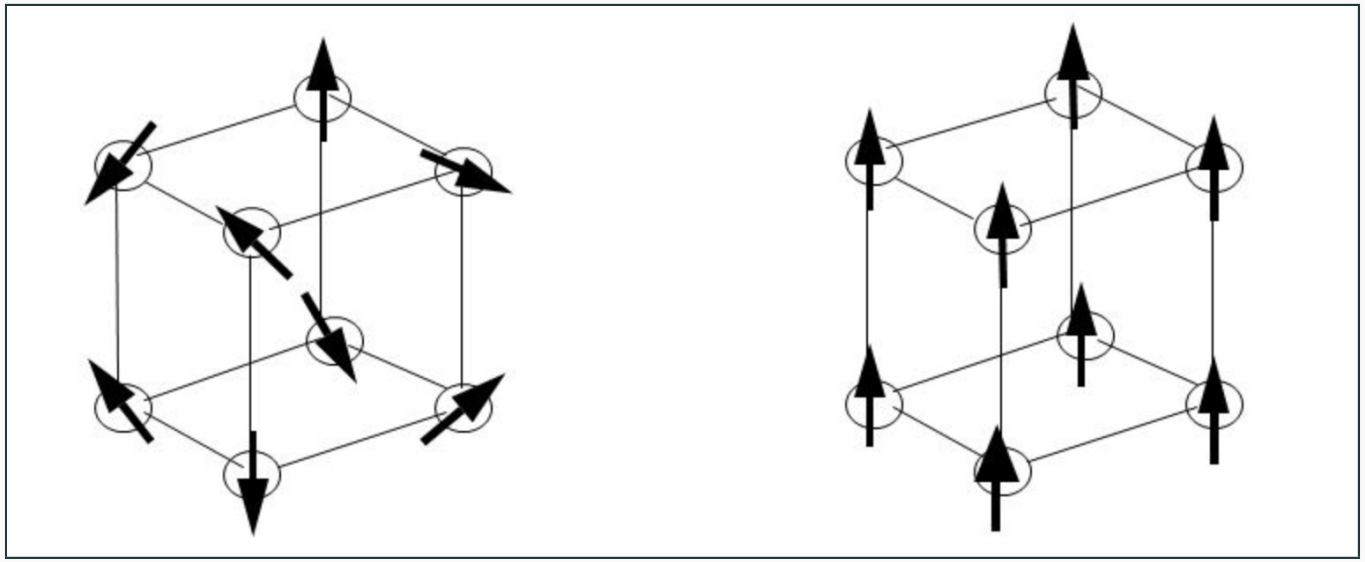

Magnetization in a ferromagnet

- Phase transition at the Curie temperature: paramagnet $\rightarrow$ ferromagnet
- Magnetic dipoles align spontaneously due to exchange interaction
- Translation and rotation invariance spontaneously broken
- Magnetic domains, regions of uniform magnetization, separated by domain walls
- Domain walls are stable, unless an external force (magnetic field) is applied

Similar phenomenology after phase transitions in the early Universe!

Topological defects in the early Universe

[Viatcheslav Mukhanov: Physical Foundations of Cosmology, Cambridge University Press (2005)]

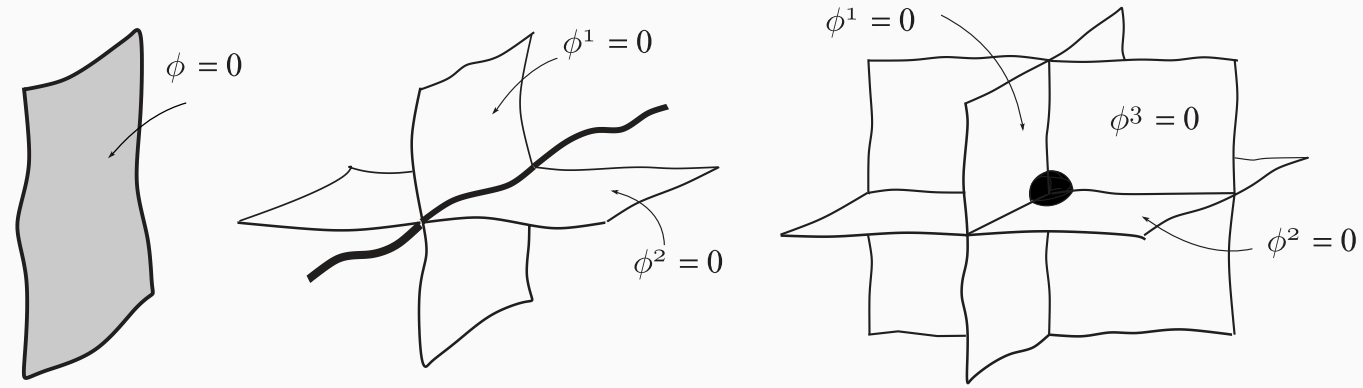

domain wall string monopole

Consider spontaneous symmetry breaking in an N-dimensional scalar field space:

$$V(\Phi) = \frac{\lambda}{4}\left(\Phi^2 - v^2\right)^2, \qquad \Phi = \frac{1}{\sqrt{N}}\left(\phi_1, \phi_2, \cdots, \phi_N\right)^T$$

Topological defects in the early Universe

[Viatcheslav Mukhanov: Physical Foundations of Cosmology, Cambridge University Press (2005)]

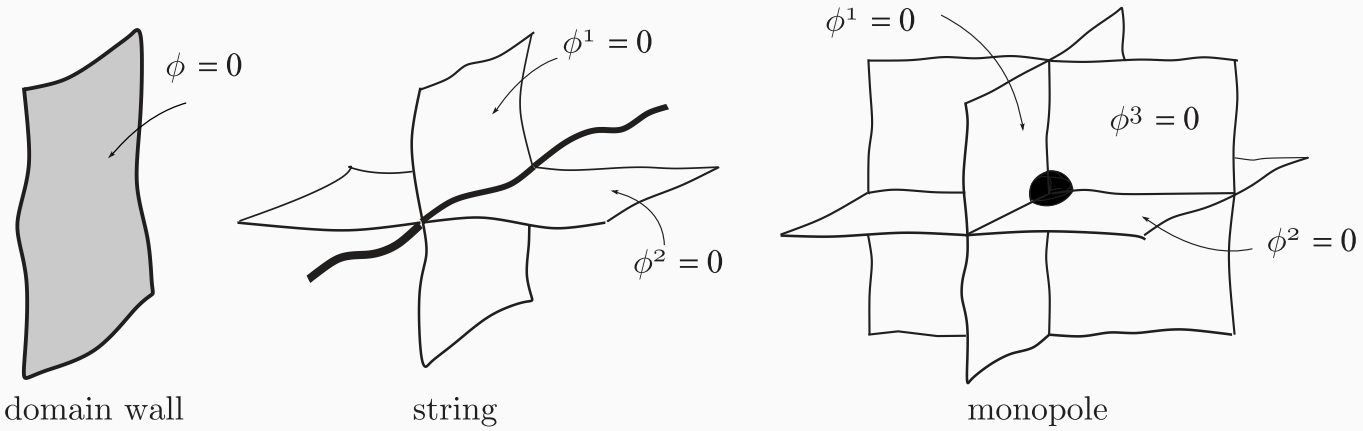

Consider spontaneous symmetry breaking in an N-dimensional scalar field space:

$$V(\Phi) = \frac{\lambda}{4}\left(\Phi^2 - v^2\right)^2, \qquad \Phi = \frac{1}{\sqrt{N}}\left(\phi_1, \phi_2, \cdots, \phi_N\right)^T$$

- Scalar fields transform under $SO(N)$ global or local gauge symmetry

Topological defects in the early Universe

[Viatcheslav Mukhanov: Physical Foundations of Cosmology, Cambridge University Press (2005)]

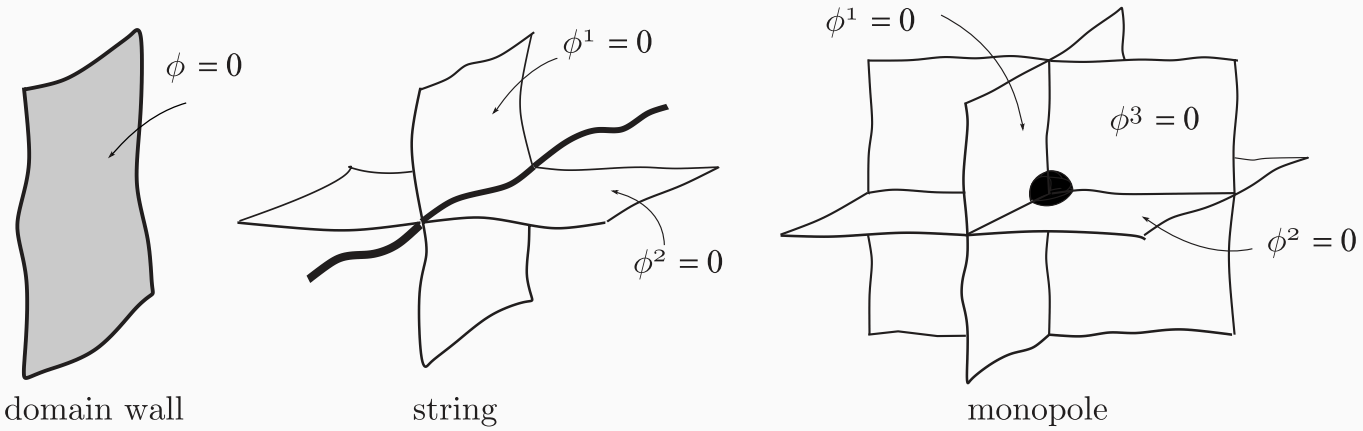

Consider spontaneous symmetry breaking in an N-dimensional scalar field space:

$$V(\Phi) = \frac{\lambda}{4}\left(\Phi^2 - v^2\right)^2, \qquad \Phi = \frac{1}{\sqrt{N}}\left(\phi_1, \phi_2, \cdots, \phi_N\right)^T$$

- Scalar fields transform under $SO(N)$ global or local gauge symmetry
- $\mathbb{Z}_2 \rightarrow$ domain walls; $U(1)$, $SO(2) \rightarrow$ cosmic strings; $SU(2)$, $SO(3) \rightarrow$ monopoles

Topological defects in the early Universe

[Viatcheslav Mukhanov: Physical Foundations of Cosmology, Cambridge University Press (2005)]

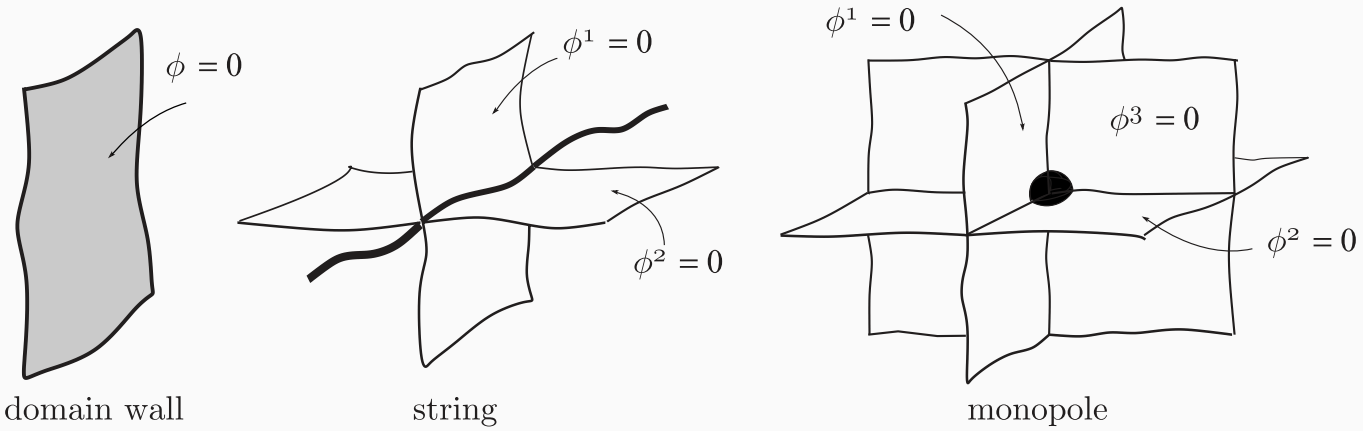

Consider spontaneous symmetry breaking in an N-dimensional scalar field space:

$$V(\Phi) = \frac{\lambda}{4}\left(\Phi^2 - v^2\right)^2, \qquad \Phi = \frac{1}{\sqrt{N}}\left(\phi_1, \phi_2, \cdots, \phi_N\right)^T$$

- Scalar fields transform under $SO(N)$ global or local gauge symmetry
- $\mathbb{Z}_2 \rightarrow$ domain walls; $U(1)$, $SO(2) \rightarrow$ cosmic strings; $SU(2)$, $SO(3) \rightarrow$ monopoles
- Solitonic solutions of classical equations of motion for the gauge and Higgs fields

Topological defects in the early Universe

[Viatcheslav Mukhanov: Physical Foundations of Cosmology, Cambridge University Press (2005)]

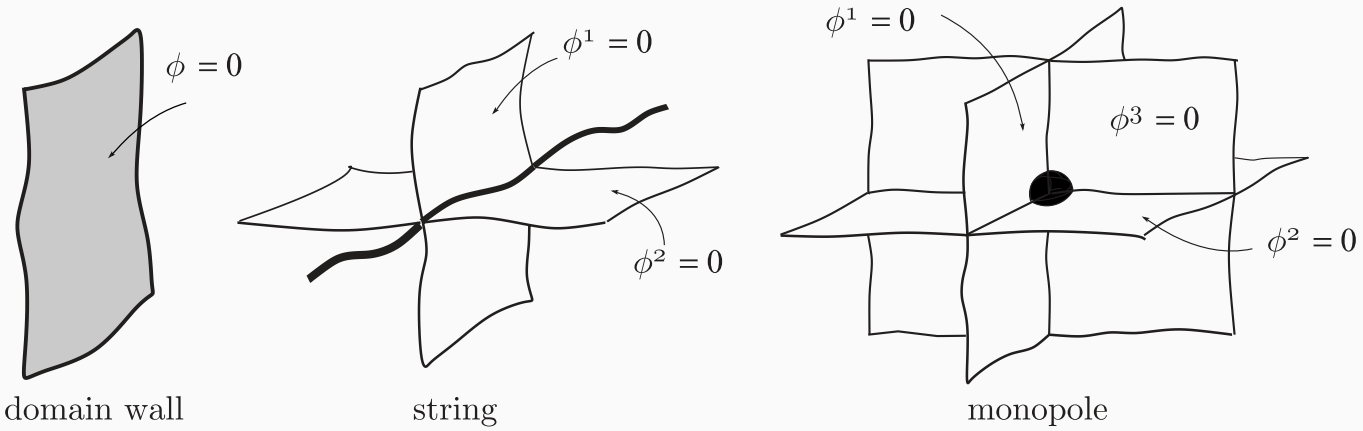

Consider spontaneous symmetry breaking in an N-dimensional scalar field space:

$$V(\Phi) = \frac{\lambda}{4}\left(\Phi^2 - v^2\right)^2, \qquad \Phi = \frac{1}{\sqrt{N}}\left(\phi_1, \phi_2, \cdots, \phi_N\right)^T$$

- Scalar fields transform under $SO(N)$ global or local gauge symmetry
- $\mathbb{Z}_2 \rightarrow$ domain walls; $U(1)$, $SO(2) \rightarrow$ cosmic strings; $SU(2)$, $SO(3) \rightarrow$ monopoles
- Solitonic solutions of classical equations of motion for the gauge and Higgs fields
- Formal description in terms of topology of vacuum manifold $\mathcal{M}(\Phi) \rightarrow$ stability

Topological defects in the early Universe

[Viatcheslav Mukhanov: Physical Foundations of Cosmology, Cambridge University Press (2005)]

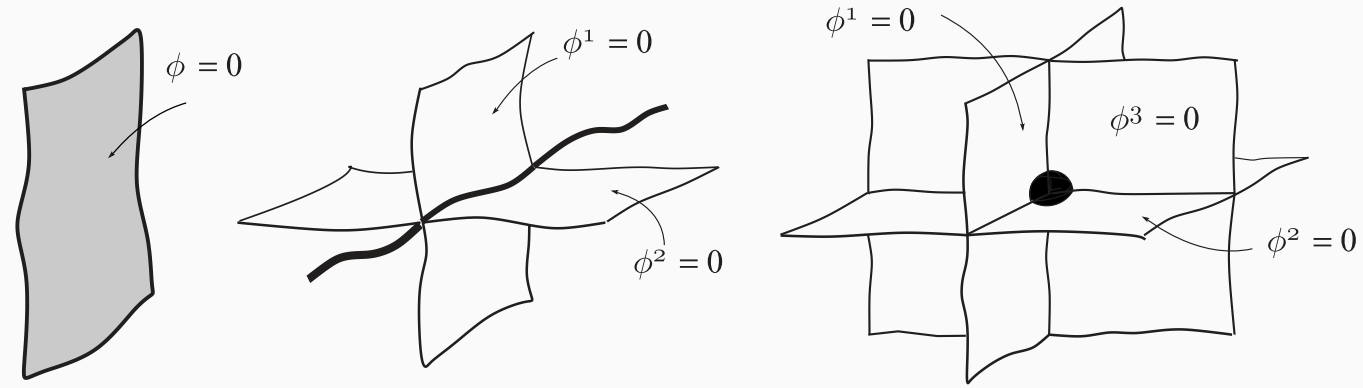

Consider spontaneous symmetry breaking in an N-dimensional scalar field space:

$$V(\Phi) = \frac{\lambda}{4}\left(\Phi^2 - v^2\right)^2, \qquad \Phi = \frac{1}{\sqrt{N}}\left(\phi_1, \phi_2, \cdots, \phi_N\right)^T$$

- Scalar fields transform under $SO(N)$ global or local gauge symmetry
- $\mathbb{Z}_2 \rightarrow$ domain walls; $U(1)$, $SO(2) \rightarrow$ cosmic strings; $SU(2)$, $SO(3) \rightarrow$ monopoles
- Solitonic solutions of classical equations of motion for the gauge and Higgs fields
- Formal description in terms of topology of vacuum manifold $\mathcal{M}(\Phi) \rightarrow$ stability
- In addition, whole zoo of composite defects, non-topological defects, etc.

Cosmic strings

[Ringeval: 1005.4842]

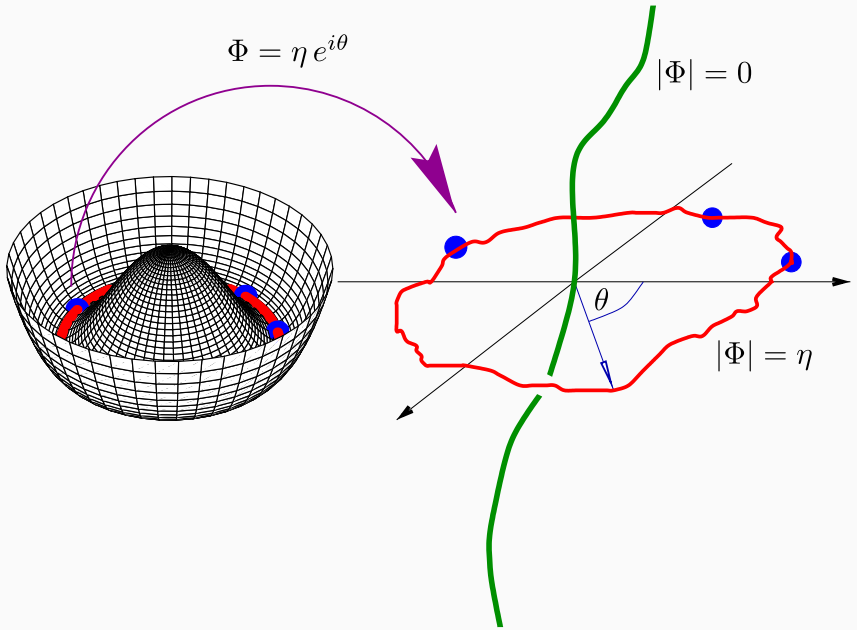

Properties

- Topological defects after spontaneous $U(1)$ breaking in the early Universe
- Global / local $U(1)$ symmetry restored (never broken) at the core of strings
- Condensed matter analog: magnetic field vortices in a superconductor

Cosmic strings

[Ringeval: 1005.4842]

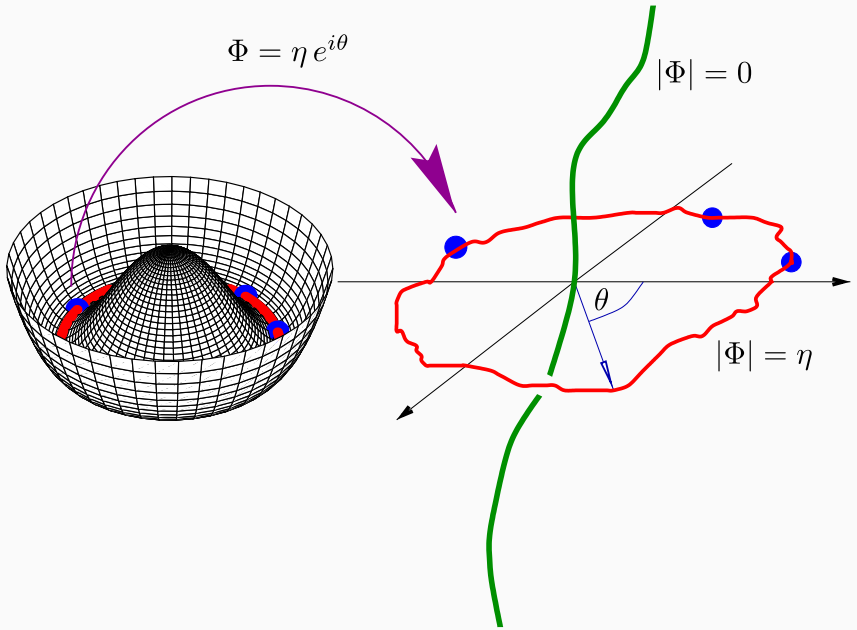

Properties

- Topological defects after spontaneous $U(1)$ breaking in the early Universe
- Global / local $U(1)$ symmetry restored (never broken) at the core of strings
- Condensed matter analog: magnetic field vortices in a superconductor

Relevant parameters

- $G\mu$: String tension = energy per unit length, in units of $G = 1/M_{\rm P}^2$
- α: Size of string loops at the time of formation, in units of H^{-1}

Embedding in grand unification

[Dror, Hiramatsu, Kohri, Murayama, White: 1908.03227]
[See also King, Pascoli, Turner, Zhou: 2005.13549, 2106.15634]

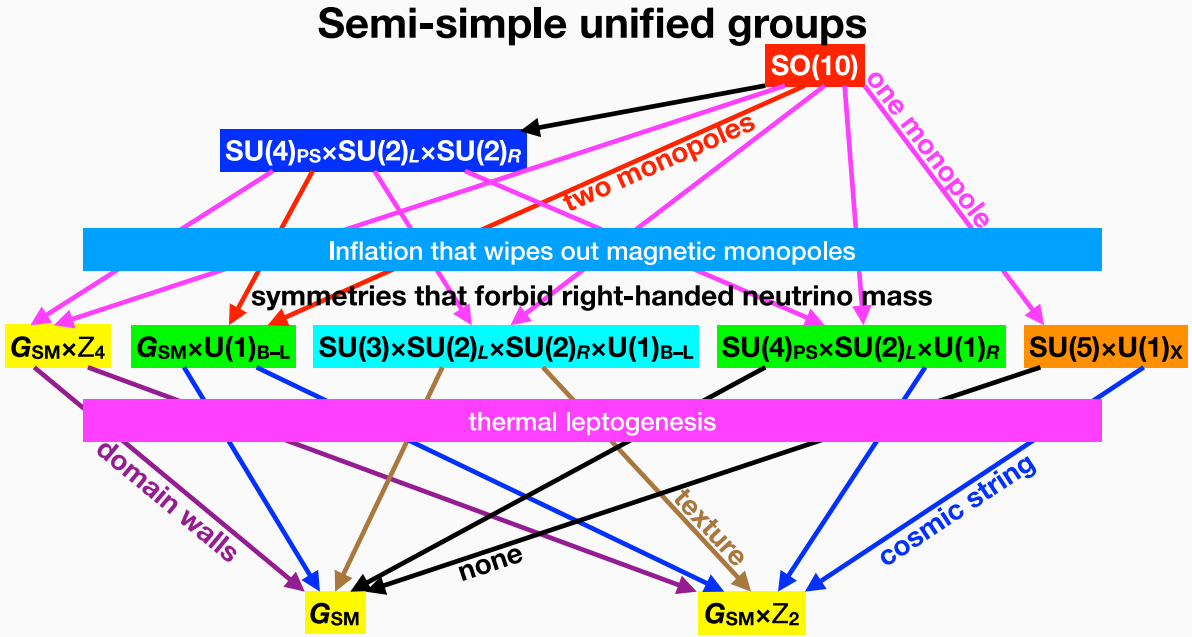

UV embedding of the seesaw mechanism in grand unified theories

- Right-handed neutrinos explain neutrino oscillations and baryon asymmetry
- Right-handed neutrino masses are consequence of symmetry breaking
- Symmetry breaking also results in cosmic strings and hence GWs

Gravitational waves from cosmic strings

[Allen, Martins, Shellard: ctc.cam.ac.uk/outreach]

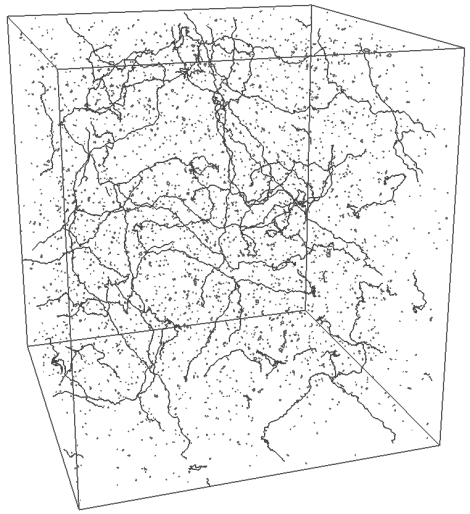

Infinite strings and string loops;
scaling regime: $\rho_{\rm cs} \propto \rho_{\rm crit} \propto H^2$

[Gouttenoire, Servant, Simakachorn: 1912.02569]

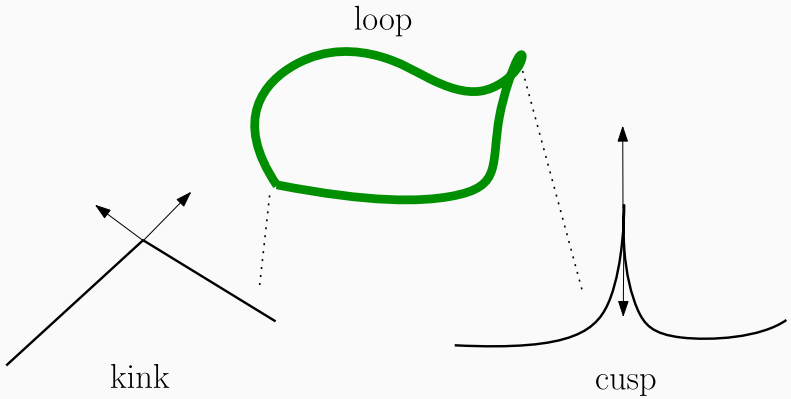

Gravitational waves from

- Cusps
- Kinks
- Kink–kink collisions

Gravitational waves from cosmic strings

[Allen, Martins, Shellard: ctc.cam.ac.uk/outreach]

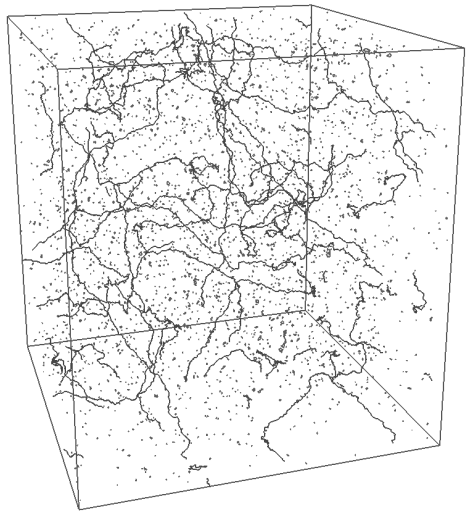

Infinite strings and string loops;
scaling regime: $\rho_{\mathrm{cs}} \propto \rho_{\mathrm{crit}} \propto H^2$

[Gouttenoire, Servant, Simakachorn: 1912.02569]

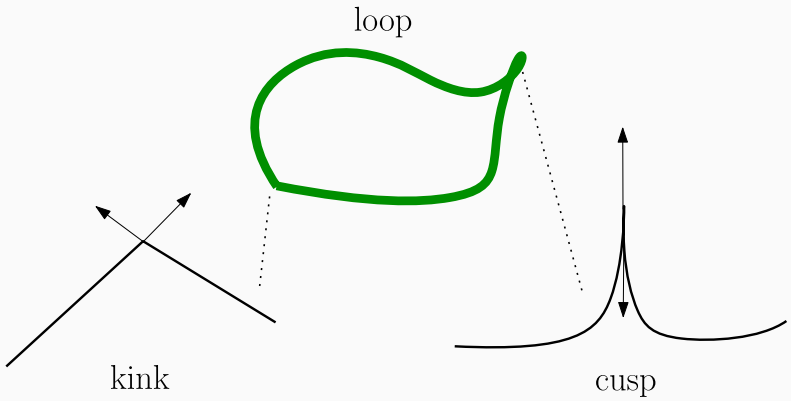

Gravitational waves from

- Cusps
- Kinks
- Kink–kink collisions

- Nambu–Goto action: infinitely thin strings, no particle emission
- Abelian-Higgs model: short-lived loops, decay into massive particles
- Nonminimal models: Metastable strings, current-carrying cosmic strings, ...

[Vachaspati, Vilenkin: PRD 31 (1985) 3052] [LISA Cosmology Working Group, Auclair et al.: 1909.00819]

Decay rate per length

$$\Gamma_d = \frac{\mu}{2\pi} e^{-\pi\kappa}$$

Parameters

- μ Tension (energy per length)
- κ Decay parameter

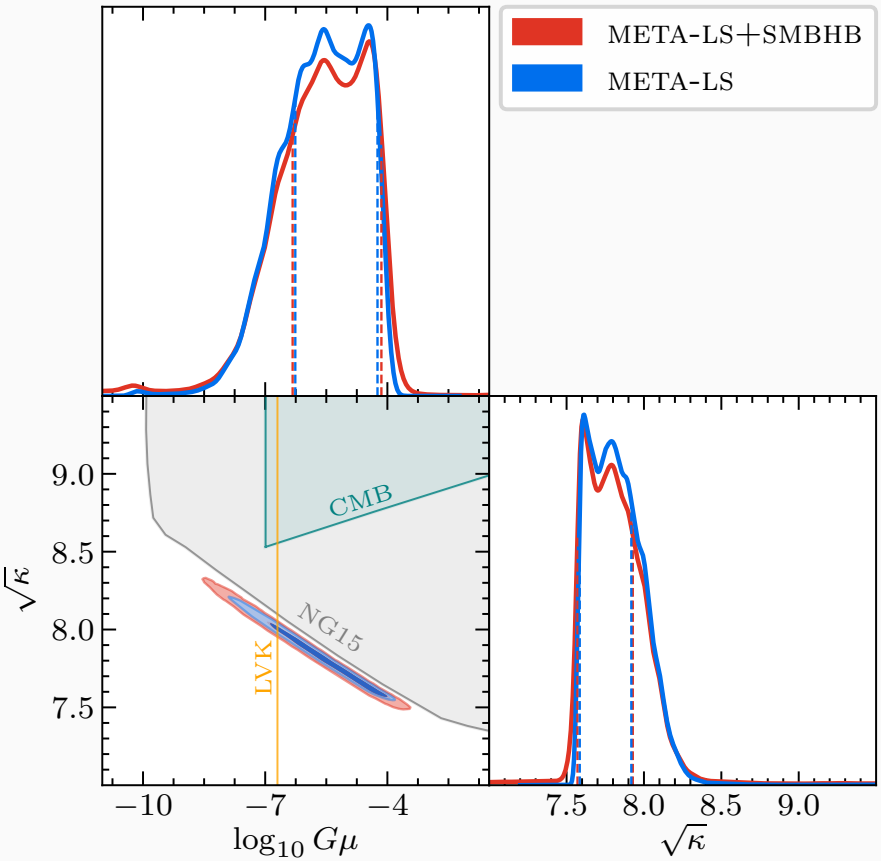

Lessons

- Prefered parameter values → input for **GUT model building** at $E \lesssim 10^{16}\,\mathrm{GeV}$
- Metastable strings yield a good fit; can be probed / excluded by **LVK observations**
- PTA bounds outperform **CMB bounds**, *irrespective of the origin of the signal (!)*

Alternative scenarios

Stable cosmic strings (STABLE)

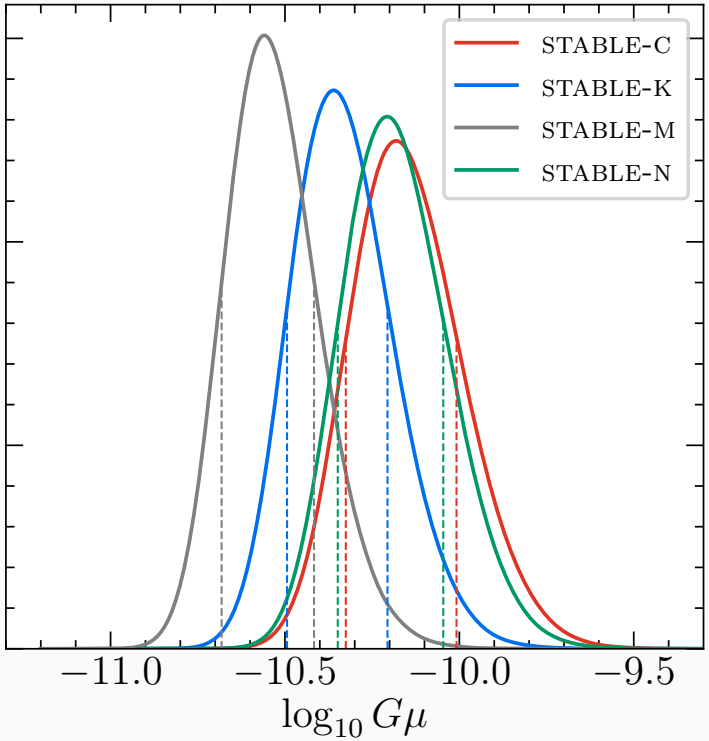

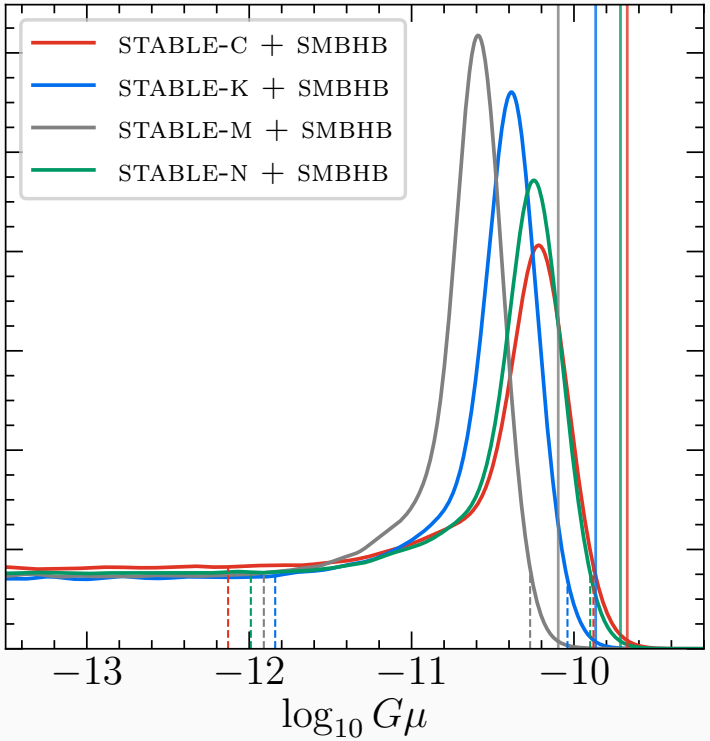

Alternative scenarios

Metastable cosmic strings, loops (META-L)

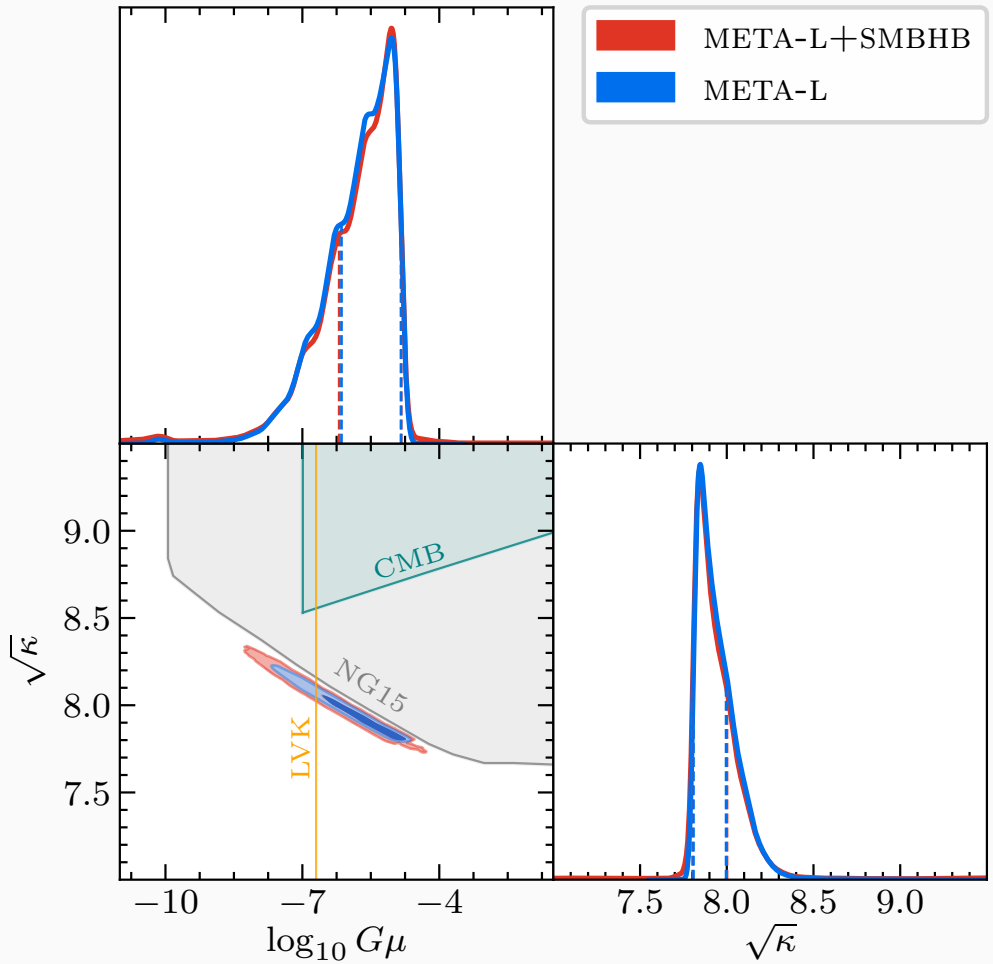

Alternative scenarios

Cosmic superstrings (SUPER)

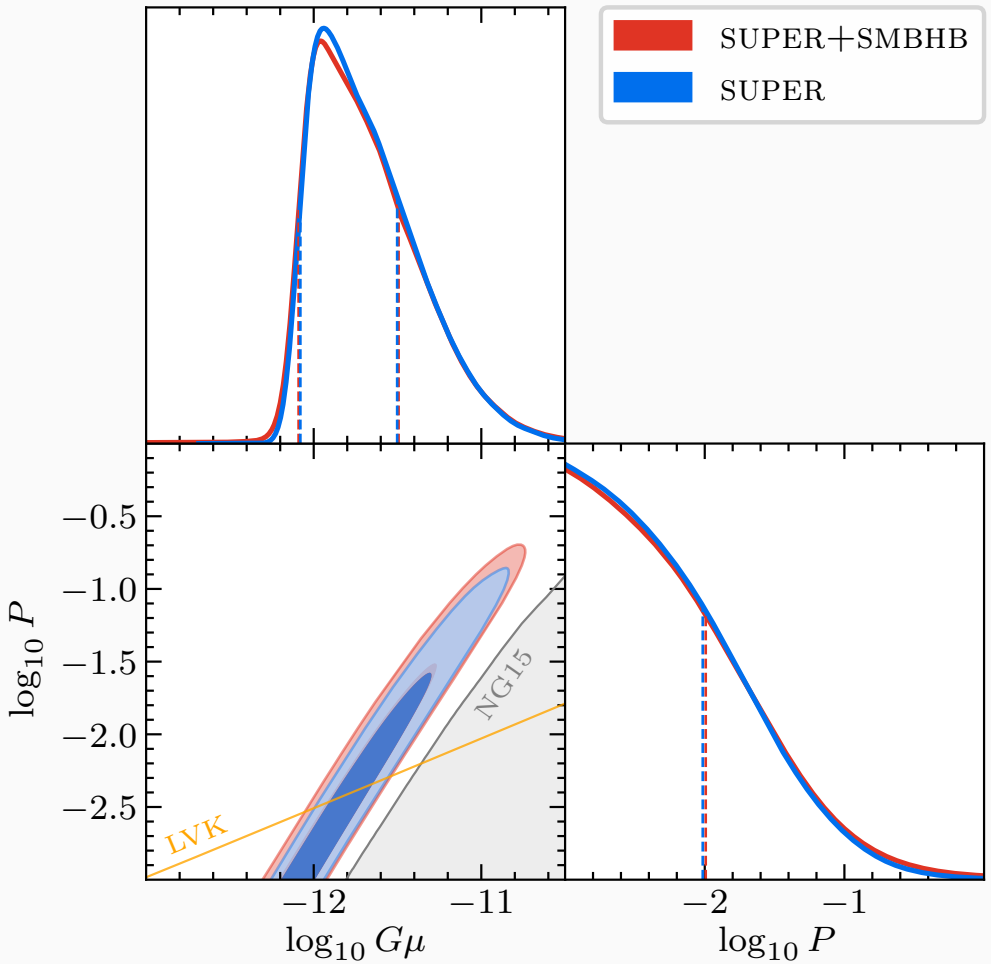

Alternative scenarios

Domain walls, decay into Standard Model particles (DW-SM)

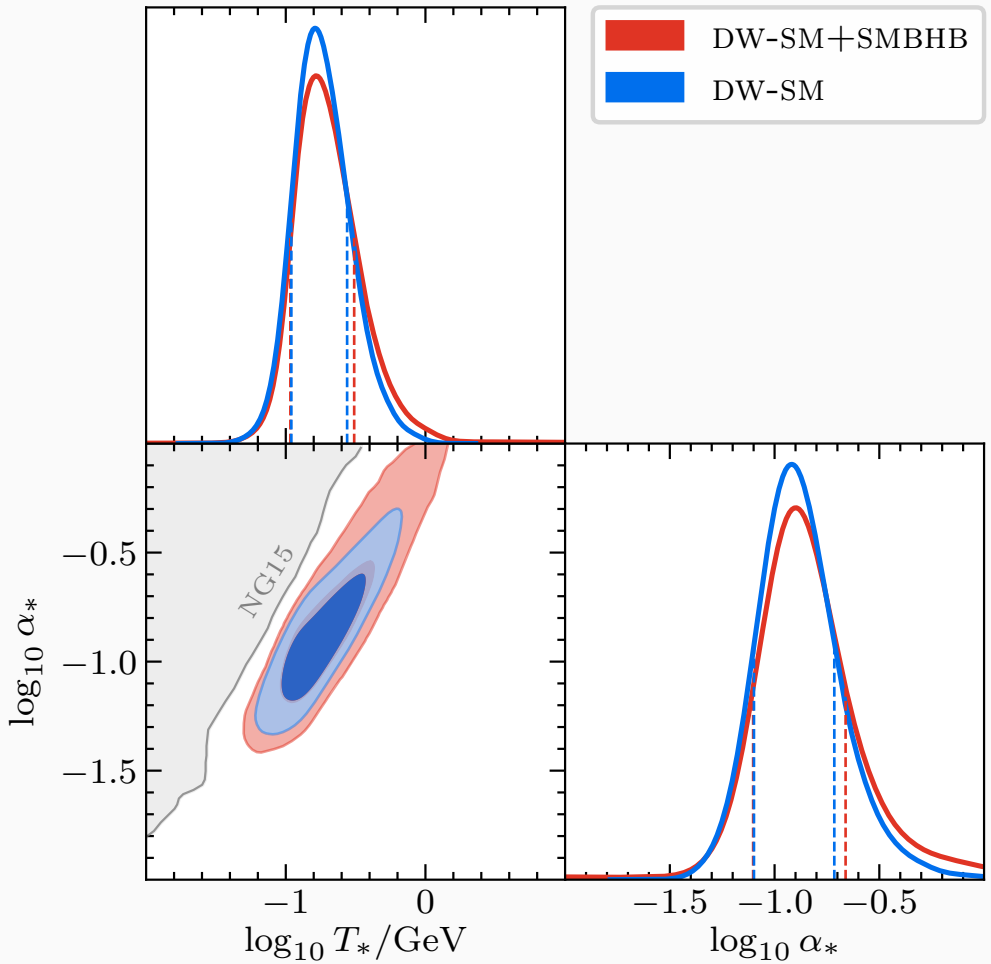

Alternative scenarios

Domain walls, decay into dark radiation (DW-DR)

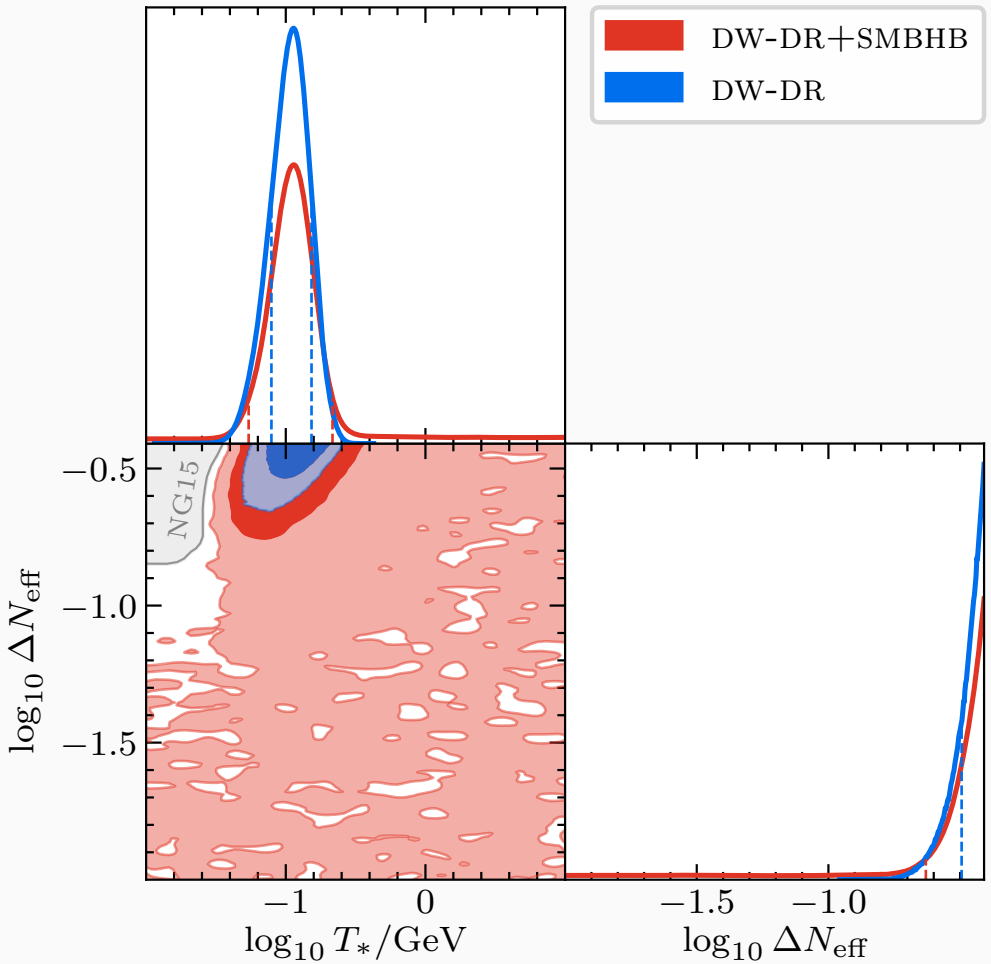

IV) Conclusions and outlook: Summary, dark matter, next steps

Point values and uncertainty estimates

Table 4. Bayesian Estimators, Maximum Posterior Values, and 68% Credible Intervals for the Parameters of the New-physics Models. Values annotated with * are at the boundary of the prior range used in the analysis.

Parameter	Bayes Estimator		Maximum Posterior		68% Credible Interval		K Bound
	NP	NP+SMBHB	NP	NP+SMBHB	NP	NP+SMBHB	
Inflationary Gravitational Waves (IGW)							
$\log_{10} T_{\rm rh}/{\rm GeV}$	0.02 ± 1.60	-0.07 ± 1.61	-0.53	-0.60	$[-1.51, 2.53]$	$[-1.89, 2.11]$	...
$\log_{10} r$	-14.06 ± 5.82	-15.97 ± 7.27	-10.14	-10.59	$[-22.16, -6.58]$	$[-23.03, -7.21]$	...
n_t	2.61 ± 0.85	2.68 ± 0.97	2.02	2.08	$[1.53, 3.92]$	$[1.56, 4.03]$	5.72
$\log_{10} A_{\rm BHB}$	...	-15.60 ± 0.56	...	-15.64	...	$[-16.20, -15.14]$	...
$\gamma_{\rm BHB}$	...	4.61 ± 0.37	...	4.64	...	$[4.26, 5.00]$	...
Scalar-induced Gravitational Waves (SIGW-DELTA)							
$\log_{10} A$	-0.69 ± 0.47	-0.71 ± 0.49	-0.14	-0.17	$[-1.00, -0.01]$	$[-1.03, -0.02]$	...
$\log_{10} f_*/{\rm Hz}$	-5.90 ± 0.60	-5.93 ± 0.67	-5^*	-5^*	$[-6.17, -5^*]$	$[-6.19, -5^*]$	...
$\log_{10} A_{\rm BHB}$	...	-15.77 ± 0.46	...	-15.71	...	$[-16.18, -15.29]$	...
$\gamma_{\rm BHB}$	...	4.65 ± 0.35	...	4.65	...	$[4.31, 4.99]$	...
Scalar-induced Gravitational Waves (SIGW-GAUSS)							
$\log_{10} A$	-0.38 ± 0.58	-0.36 ± 0.61	-0.34	-0.29	$[-1.03, 0.20]$	$[-1.04, 0.24]$	...
$\log_{10} f_*/{\rm Hz}$	-6.32 ± 0.71	-6.30 ± 0.73	-7.03	-6.85	$[-7.25, -5.65]$	$[-7.17, -5.57]$	...
Δ	1.35 ± 0.70	1.30 ± 0.70	1.60	1.54	$[0.51, 2.07]$	$[0.37, 1.92]$	...
$\log_{10} A_{\rm BHB}$	...	-15.72 ± 0.46	...	-15.65	...	$[-16.14, -15.22]$	...
$\gamma_{\rm BHB}$	...	4.65 ± 0.34	...	4.65	...	$[4.32, 5.00]$	...

Best-fit values and constraints for the parameters of all BSM models

New Physics in PTA data

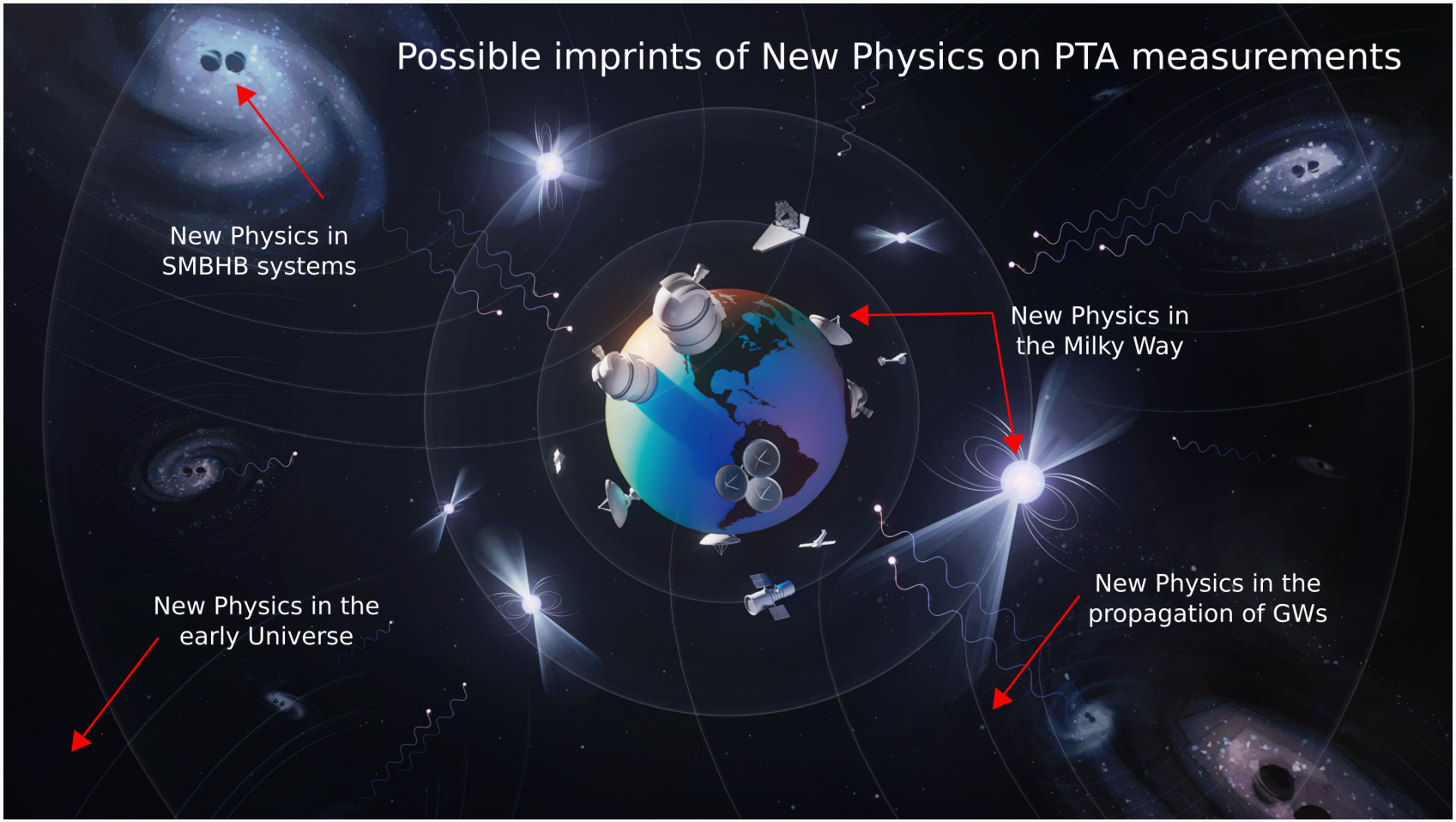

Deterministic signals

New physics in the early Universe $\rightarrow$ new physics in our Milky Way today

Additional, deterministic contributions to timing residuals on top of the GWB

Deterministic signals

New physics in the early Universe → new physics in our Milky Way today

Additional, deterministic contributions to timing residuals on top of the GWB

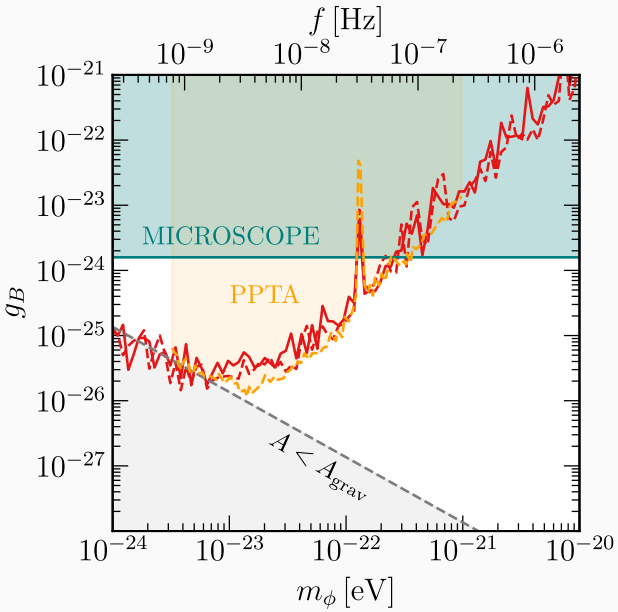

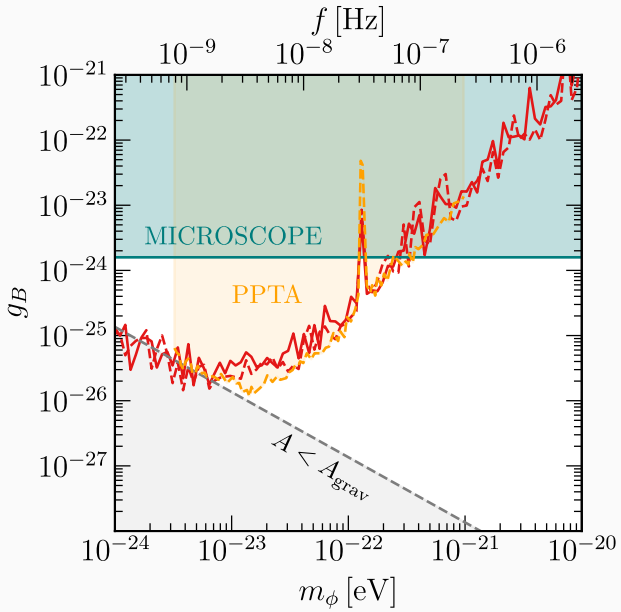

Search for signals from ultralight dark matter and dark-matter substructures

- Metric fluctuations, Doppler $U(1)$ forces, pulsar spin fluctuations, clock shifts
- Doppler and Shapiro signals because of passing primordial black holes

Deterministic signals

New physics in the early Universe → new physics in our Milky Way today

Additional, deterministic contributions to timing residuals on top of the GWB

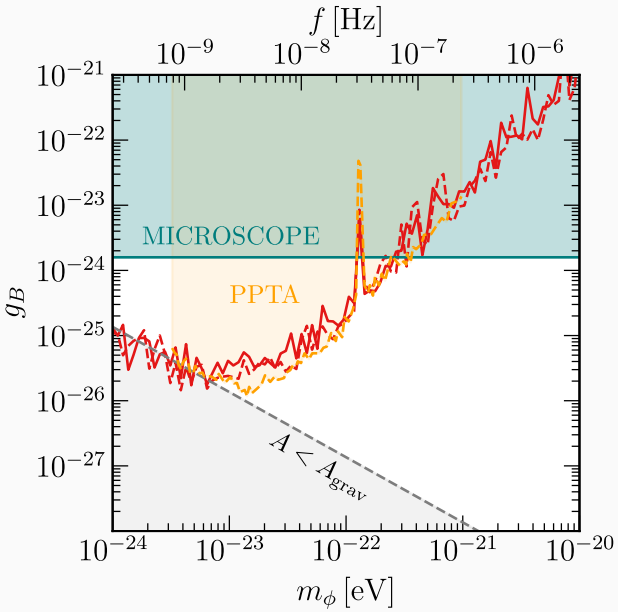

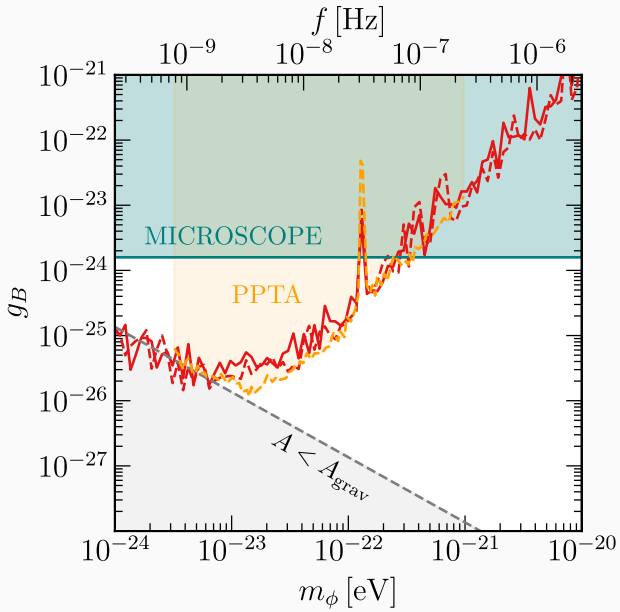

Search for signals from ultralight dark matter and dark-matter substructures

- Metric fluctuations, Doppler $U(1)$ forces, pulsar spin fluctuations, clock shifts
- Doppler and Shapiro signals because of passing primordial black holes

We find no signals → new bounds on parameter space (partially world-leading)

Complementary observables: Anisotropies

[NANOGrav 2306.16221]

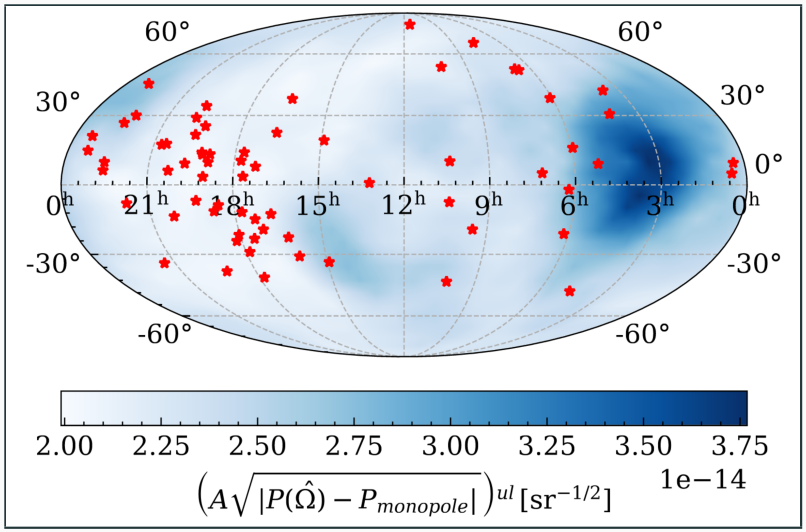

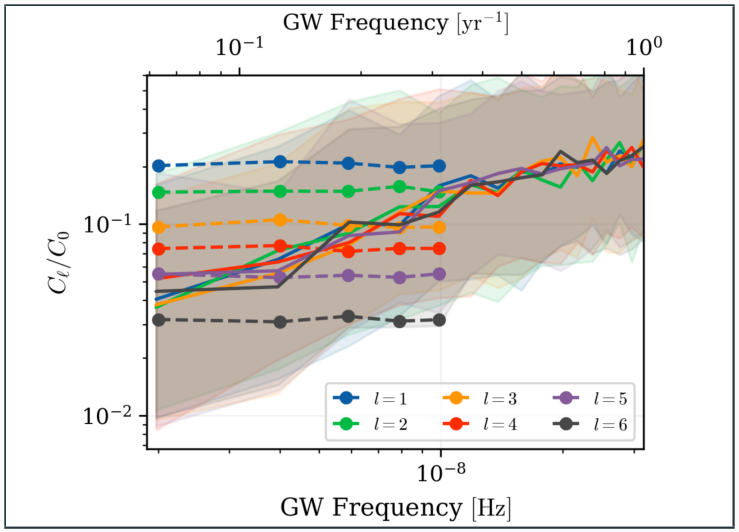

Search for anisotropies in the GWB signal in the sky

- Current sensitivity already at the level of expected anisotropies from SMBHBs
- No signal detected $\rightarrow$ sky-dependent upper limits on deviation from monopole

Complementary observables: Anisotropies

[NANOGrav 2306.16221]

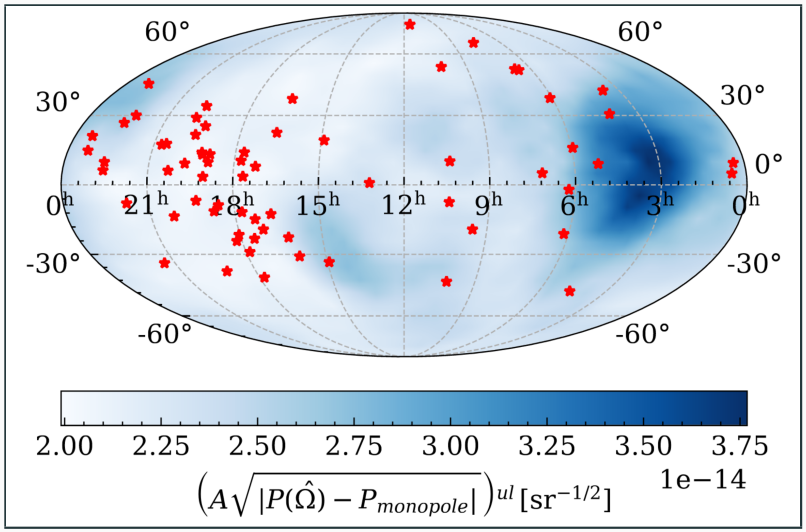

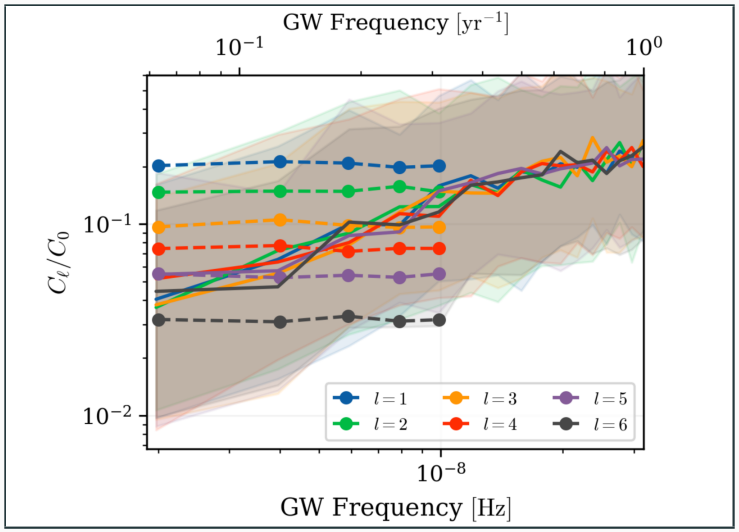

Search for anisotropies in the GWB signal in the sky

- Current sensitivity already at the level of expected anisotropies from SMBHBs
- No signal detected → sky-dependent upper limits on deviation from monopole

No detection of anisotropies with future data sets → hint of primordial origin?

Complementary observables: Continuous-wave signals

[NANOGrav 2306.16222]

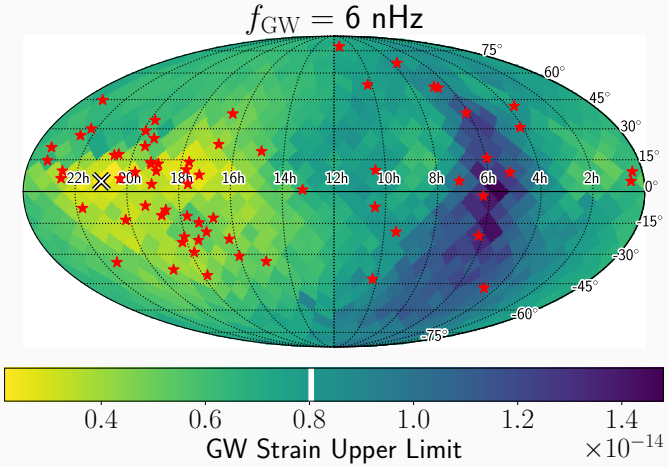

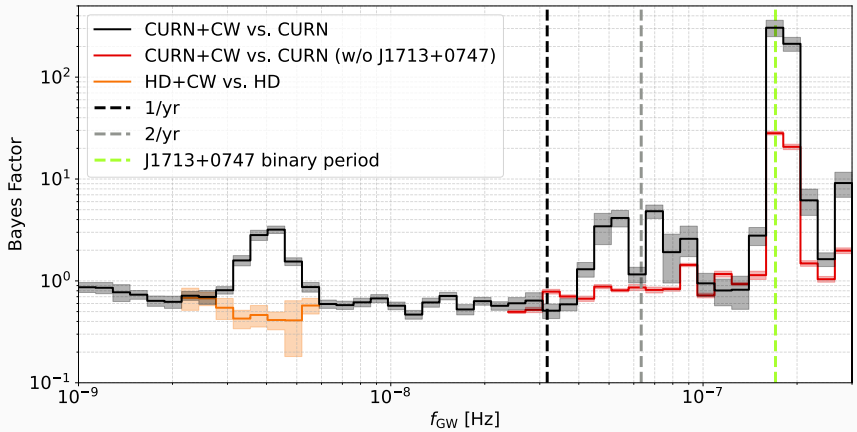

Search for continuous-wave signals from individual nearby SMBHB systems

- Interesting hints in the data, which, however, do not withstand further scrutiny
- Overall, no signal detected $\rightarrow$ sky-dependent upper limits on GW amplitude

Complementary observables: Continuous-wave signals

[NANOGrav 2306.16222]

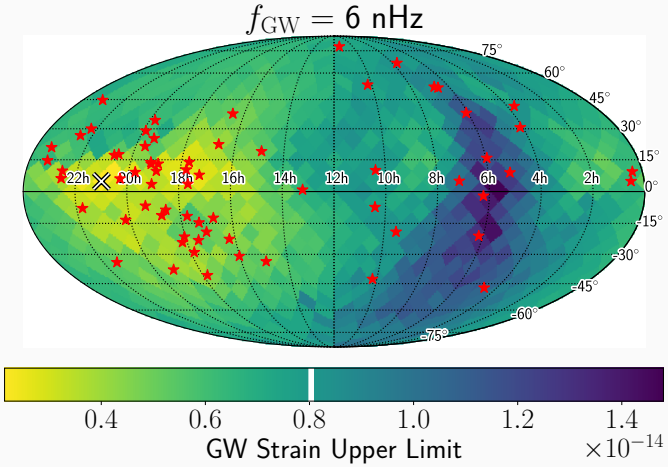

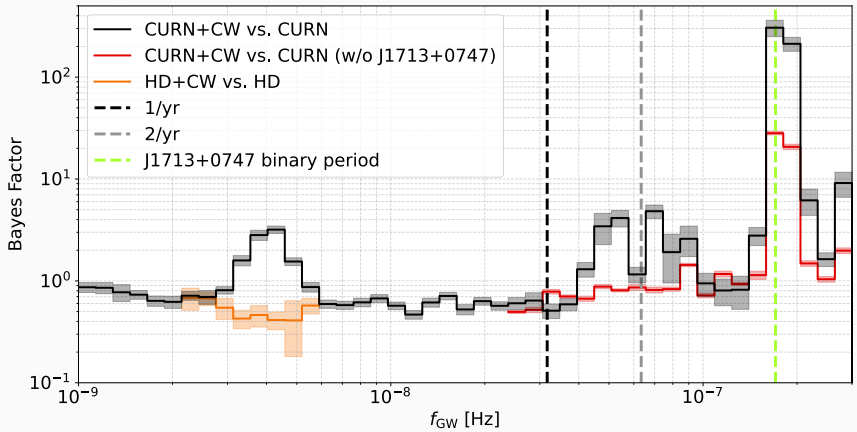

Search for continuous-wave signals from individual nearby SMBHB systems

- Interesting hints in the data, which, however, do not withstand further scrutiny
- Overall, no signal detected $\rightarrow$ sky-dependent upper limits on GW amplitude

---

Prospect: Combined information on GWB spectrum, anisotropies, continuous-wave signals (plus other GW searches, CMB observations, etc.) $\rightarrow$ origin of the PTA signal

A bright future for GW science with PTAs

- Status: Common-spectrum process; $3 \cdots 4\,\sigma$ evidence for HD correlations
- Next: HD correlations at $5\,\sigma$, spectral shape, anisotropies across the sky, ...
- Promise: Deep insights into galaxy and BH evolution and/or BSM physics

This is only the beginning!

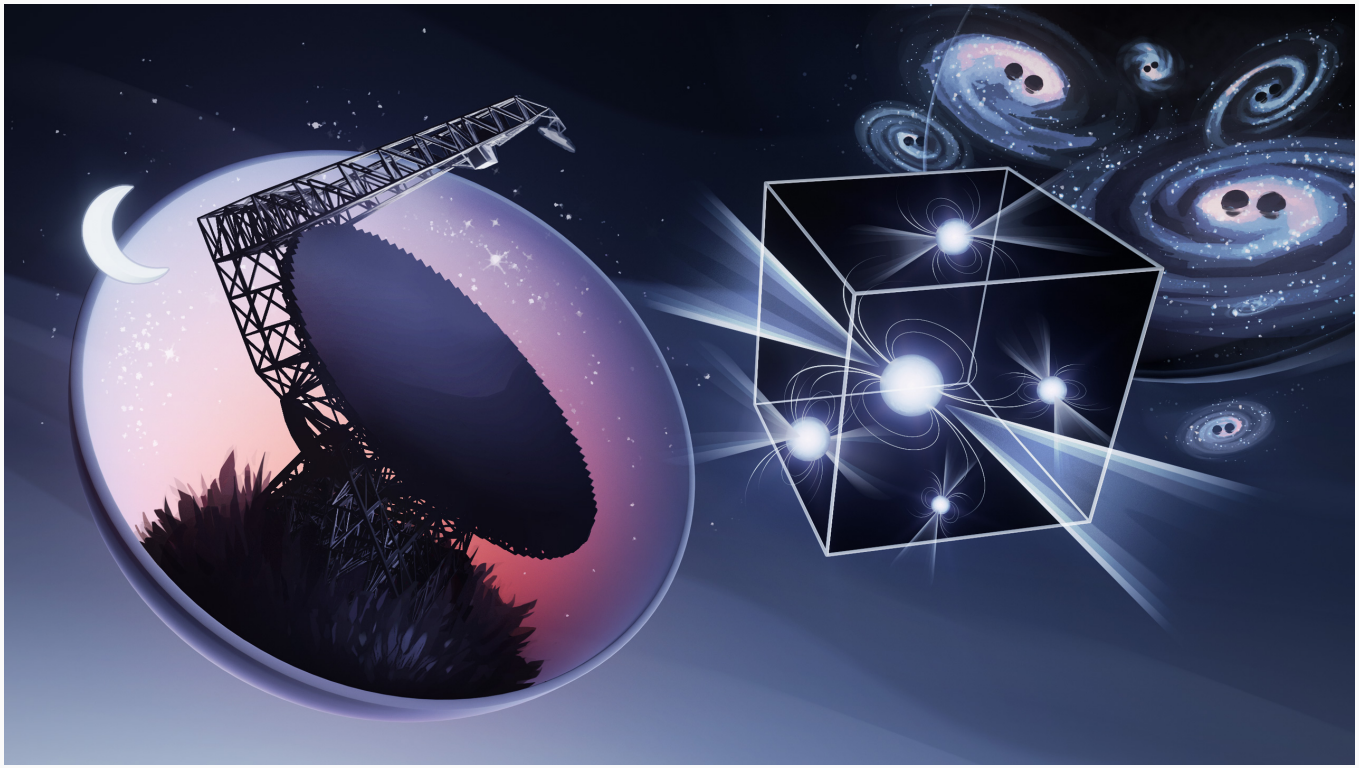

New Physics at the PTA Frontier

- Rich and exciting research program for many years and decades to come
- Build new models, improve theoretical modeling, develop better tools
- Streamline analysis pipelines for IPTA eDR3, IPTA DR3, and beyond

Stay tuned!

And thanks a lot for your attention